Investigations of cellular dynamics during bleaching in the symbiotic anemone, *Aiptasia pallida*

by

Shanna D. Hanes

A dissertation submitted to the Graduate Faculty of
Auburn University
in partial fulfillment of the
requirements for the Degree of
Doctor of Philosophy

Auburn, Alabama
August 3, 2013

Keywords: Coral bleaching, Heat stress, *Aiptasia,* Autophagy, *Symbiodinium*

Approved by

Stephen Kempf, Chair, Associate Professor, Dept. of Biological Sciences
Anthony Moss, Associate Professor, Dept. of Biological Sciences
Scott Santos, Associate Professor, Dept. of Biological Sciences
Richard C. Bird, Professor, Dept. of Pathobiology, College of Vet. Medicine
Bernhard Kaltenboeck, University Reader, Dept. of Pathobiology, College of Vet. Medicine

Abstract

The global decline of coral reefs continues at an increasing rate despite efforts to identify key cellular interactions responsible for the breakdown of these essential ecosystems. Coral bleaching involves the loss of essential, photosynthetic dinoflagellates (*Symbiodinium*) from host gastrodermal cells in response to temperature and/or light stress conditions. Although numerous potential cellular bleaching mechanisms have been proposed, few studies have investigated the early host stress response when symbiotic breakdown is initiated. In this investigation, both cellular and molecular techniques were employed in order to 1) carefully examine and characterize host anthozoan tissues at multiple stages of the symbiosis, including: i) healthy symbiotic, ii) several stages of active heat stress induced-bleaching, iii) aposymbiotic (symbiont-free); 2) document and describe all cellular bleaching mechanisms that occur during heat stress treatment; 3) quantify any observed cellular bleaching mechanisms in both symbiotic and aposymbiotic anemones to determine whether the response is host derived; 4) conduct a gene expression analysis on heat stressed symbiotic *A. pallida* anemones in order to quantify the response using RNA-Seq on an Illumina platform. First, histological and ultrastructural examinations were conducted using light and transmission electron microscopy on healthy symbiotic anemeone tentacle tissues in order to establish baseline information. A detailed ultrastructural analysis was conducted of numerous cellular regions and compared to previous cnidarian literature. This study provided an essential diagnostic analysis of normal healthy tissues that was used to assess the health condition of the anemones during the subsequent heat

stress treatments. Bleaching was induced by exposing both symbiotic and/or aposymbiotic *A. pallida* anemones, to ~32.5^{o}C at 120 μmols irradiance for 12 h followed by 12 h in the dark at 24 ^{o}C daily for 2 days. Samples were taken thoughout the 48 h period. Ultrastructural examination revealed numerous autophagic structures and associated cellular degradation in tentacle tissues after ~12 h of stress treatment and also after 12 h of exposure to the known autophagy inducer, rapamycin. Additionally, symbionts were observed detaching from highly degraded gastrodermal cells in an apocrine-like manner. The abundance of autophagic structures was quantified in gastrodermal and epidermal tissues of symbiotic and aposymbiotic tissues, and also in rapamycin treated tissues using ImagePro Plus 7.0 software. Results from the RNA-Seq analysis revealed the highest levels of differential gene expression in symbiotic *A. pallida* anemones after 3 h during a 48 h thermal stress treatment, suggesting that the gene expression profile changes in early stages of the host stress response. In addition, several key processes were identified that are involved in the host response, including stress response, protein degradation/synthesis, calcium homeostasis and others, which provides a better understanding of the genetic determinants of stress tolerance in a host anthozoan. This investigation provided the first ultrastructural evidence of host autophagic degradation during thermal stress in a cnidarian system and supports earlier suggestions that autophagy is an active cellular mechanism during early stages of bleaching.

Acknowledgements

I would like to thank my advisor, Dr. Stephen Kempf for the knowledge that he has bestowed on me over these years (I owe you a jerk mahi sandwich with mango chutney) as well as my entire committee for their contributions to my dissertation as well as their support. I would also like to thank my faithful lab members, Maria Mays and Ivey Ellis Holt, who have both served as my allies and great friends throughout all our lab adventures- Kempf Lab Unite! Mostly I would like to thank my family, who has shown me so much love, support, and acceptance over these years for following the beat of my own drum (despite how far marine biology may take from home). Mom and Dad, you are the greatest parents anyone could ever hope for, and Adam, Shari, and Emma, you are my inspiration! And I also must acknowledge Spyros Mourtzinis, who has stuck by my side through the darkest of days and served as my source of strength when I needed it most. He also contributed significantly to the development of this dissertation. Thank you so much for everything, Σ' αγαπώ! I would also like to thank Dr. Bill Fitt at UGA for allowing us access to collection our *Aiptasia* specimens and also several undergrads that have worked in the labs, especially Kristina Looney.

Table of Contents

List of Tables

List of Figures

List of Abbreviations

APS autophagic structure

Gv gastrovascular cavity

ROS reactive oxygen species

I. Coral bleaching: A cellular breakdown in symbiosis

Coral-dinoflagellate symbiosis

Coral reefs are highly diverse and productive ecosystems that provide sustenance and shelter to a multitude of reef organisms, as well as a wide variety of services to millions of people worldwide (NOAA, 2012). Hermatypic (reef building) corals precipitate a calcium carbonate skeleton, which contributes over time to the formation of coral reefs. Coral reefs can support more species per unit area than any other marine environment (NOAA, 2012). It is generally accepted that the productivity of reefs can be largely attributed to the establishment of close associations or 'symbioses' between coral hosts and photosynthetic dinoflagellates of the genus *Symbiodinium* (Freudenthal, 1962), which are often referred to as "zooxanthellae" (Hoegh-Guldberg, 1999). Most symbioses between dinoflagellates and their cnidarian hosts are obligate mutualisms that may have been selected for as a means to supplement nutrients in the oligotrophic tropical waters where most hermatypic corals are located (Muscatine and Porter, 1977).

The coral-dinoflagellate symbiosis has been a subject of interest since each symbiotic member was individually classified in the late 19th century (Brandt, 1881). Members of *Symbiodinium* spp. have been divided into 11 species that comprise at least eight groupings or 'clades' (A-H). The clades, in turn, contain multiple subclade types (Stat et al., 2006) that can be identified at the molecular level. Members of at least five invertebrate phyla are known to live symbiotically with *Symbiodinium* spp. These include Protista, Porifera, Cnidaria,

Platyhelminthes and Mollusca (Hoegh-Guldberg, 1999; Stat, 2006). The variety of hosts harboring these symbionts is greatest in Cnidarians with many examples, such as hermatypic corals, found in the class Anthozoa, subclass Hexacorallia (=Zoantharia). Such hosts maintain symbiotic relationships with a variety of *Symbiodinium* types (Weis et al., 2008; Sunagawa et al., 2009; Lenhart et al., 2012). Symbionts can be gained through two basic methods of acquisition by their cnidarian hosts, which include taking them up from the surrounding environment through horizontal transfer or gaining them directly from their parent through vertical transmission (Stat et al., 2006).

Symbiont maintenance and nutrient exchange

At the tissue level, the cnidarian bauplan consists of two cellular layers, the external epidermis and internal gastrodermis, lying on either side of an acellular collagenous mesoglea. Symbionts reside intracellularly within nutritive-muscular cells of the gastrodermis, each present within a specialized host vacuole called the 'symbiosome' (Wakefield and Kempf, 2001). The symbiosome membrane and the underlying symbiont secretions serve as the interface between host and symbiont, where essential nutrients are transferred between both members of the association. While harbored within host tissues, symbionts are sheltered from the external environment and receive host inorganic metabolic products, including ammonia, phosphates, and CO_2 (Trench, 1979). In turn, symbionts may transfer as much as 95% of their photosynthetic products, including sugars, amino acids, and carbohydrates to their coral hosts (Trench, 1979). These essential nutrients provide the coral with the necessary energy for growth and calcium carbonate deposition (Muscatine, 1990), which contributes greatly to the fitness of the coral (D'Elia and Wiebe, 1990; Muscatine, 1990). Any factor that reduces the efficiency of this

relationship will have a major effect on the ecological success of these obligate members of the symbiosis (Glynn, 1996).

Bleaching response

Throughout time, corals have adapted to survive despite a variety of naturally occurring disturbances, including fluctuations in salinity (Coles and Jokiel, 1992), sedimentation (Rogers, 1990), and predation (Porter, 1972). However, the past several decades have produced a surge of anthropogenic impacts that have introduced new challenges for corals and that threaten their future survival (Wilkinson, 1993; Donner et al., 2007). The danger for coral reefs is complex. Although corals have historically demonstrated an ability to recover from natural disturbances, the anthropogenic-driven increase in frequency and severity of environmental stressors have contributed to the loss of over 19% loss of coral reefs globally in recent years (Wilkinson, 2008).

Although a wide variety of environmental stressors currently threaten corals, including disease outbreaks (Kushmaro et al., 1997; Harvell et al., 1999) and ocean acidification (Hoegh-Guldberg et al., 2007), one of the major factors currently responsible for large-scale coral reef mortality is elevated sea temperature and/or high solar irradiance (particularly UV wavelengths) (Glynn, 1996; Hughes, 2003; Hoegh-Guldberg et al., 2007). When the thermal threshold of the host, symbiont, or both is exceeded, the symbiont cells and/or associated symbiont photosynthetic pigments can be lost from host gastrodermal cells (Hoegh-Guldberg, 1999; Fitt et al., 2001). This process, known as 'bleaching', results in a lightening of the host coral as the underlying white calcareous skeleton is exposed through translucent coral tissue. Although corals can survive for a short period of time without their symbiotic partners, longer periods of time result in reduced reproductive capability (Szmant and Gassman, 1990), decreased growth and

calcification rates (Glynn, 1993), and death of the coral host (Brown, 1997; Hoegh-Guldberg, 1999).

Breakdown of the symbiosis

Collapse of the coral-dinoflagellate symbiosis is tightly regulated by stress responses of both members of the symbiosis. However, many studies have identified the photosynthetic apparatus of the symbiont as the first structure to be affected by temperature or light stress conditions (Lesser et al., 1990; Iglesias-Prieto et al., 1992; Warner et al., 1999). During elevated temperature conditions, symbionts absorb more light energy than can be utilized for photosynthesis, thus reducing the available excitation energy for the electron transport chain (Smith et al., 2005). These events set in motion a state known as 'photoinhibition', which involves photodamage to the photosynthetic apparatus of the symbiont (Warner et al., 1999; Lesser, 2006). The damage is primarily targeted to the D1 protein located within the PSII reaction center (Warner et al., 1999; Smith et al., 2005). When the extent of D1 damage exceeds the rate of repair a loss of functional PSII reaction centers occurs, photosynthesis declines (Smith et al., 2005) and the production of damaging reactive oxygen species (ROS) occurs (Franklin et al., 2004; Lesser, 1996).

Alternatively, symbiotic breakdown has also been shown to originate in the host as a result of mitochondrial membrane damage (Dykens et al., 1992; Nii and Muscatine, 1997; Dunn et al., 2012). The cellular mechanisms involved with the initial heat and/or light stress response have not been as well characterized in host cells as they have in symbionts. However, as is the case for chloroplast thylakoid membranes, damage to mitochondrial membranes can also produce high levels of ROS that will inevitably diffuse into host tissues (Dykens et al., 1992; Nii

and Muscatine, 1997; Dunn et al., 2012). If the rate of ROS generation exceeds the rate of ROS detoxification, then accumulation of ROS may result in oxidative damage to cellular structure (Lesser and Farrell, 2004; Richier et al., 2005), loss of cell function, and ultimately death of the affected cell (Chen and Gibson, 2008; Lesser, 1997; Perez and Weis, 2006; Sherz-Shouval et al., 2007). Recent investigations suggest that such ROS-mediated stress is the underlying cause of symbiont loss during bleaching (Franklin et al., 2004; Lesser, 2007; Perez and Weis, 2006).

Reactive Oxygen Species

Reactive oxygen species (ROS) such as superoxide ($O_2^{\cdot-}$), singlet oxygen (O_2^{-}), hydrogen peroxide (H_2O_2), hydroxyl radical ($^{\cdot}OH$), nitric oxide (NO), and peroxynitrite (ONOO-) are an inevitable by-product of photosynthesis due to the difference in redox potential between the products and reactants of photosynthetic pathways (Niyogi, 1999). These molecules can directly damage lysosomal membranes, which serve a vital function by isolating potent degradative enzymes from other intracellular components (Kiffin et al., 2006). ROS are normally detoxified by antioxidants, such as catalase, superoxide dismutase and ascorbate peroxidase; however, when ROS production exceeds the detoxification capability of a cell, membrane damage often results in leakage of potent lysosomal hydrolases that can significantly disrupt intracellular organization (Kiffin et al., 2006) and lead to cell death.

Mechanisms of Symbiont loss

As a response to the various stimuli that trigger the bleaching process, symbiont loss can occur via a number of potential cellular mechanisms. These have been covered in several reviews (Gates et al., 1992; Douglas, 2003; Lesser, 2004; Weis, 2008).

Exocytosis

The first cellular bleaching mechanisms suggested to result in loss of symbionts from host tissues was exocytosis. This process has been implicated as a mechanism of bleaching in several studies (Yonge and Nichols, 1931; Steen and Muscatine, 1987; Brown et al., 1995). Steen and Muscatine (1987) exposed *Aiptasia pulchella* anemones to a low temperature of 4^{o}C, which induced bleaching after 8 hours. Scanning electron microscopy revealed that symbionts migrated to the apical ends of host gastrodermal cells, causing them to bulge into the gastrovascular cavity into which they were eventually exocytosed. The released symbionts were expelled from the gastrovascular cavity in various stages of disintegration. They concluded that low temperature either increased the rate of microtubule depolymerization or increased cytosolic Ca^{2+}, both of which could potentially induce exocytosis. Fang *et al.* (1997) found that intracellular calcium steadily increased in coral cells undergoing hyperthermic stress. A subsequent study by Fang *et al*. (1998), also suggested that coral bleaching requires motor proteins in order to transport symbiont-containing vesicles via the cytoskeletal track to the cell membrane.

Budding/Pinching off

Glider (1983) first described this cellular mechanism in his doctoral dissertation while examining transmission electron micrographs of healthy *Aiptasia pallida* anemone tissues. The micrographs suggested that during this process, initially termed 'budding,' the cell membrane of host gastrodermal cells pinched inward, and symbionts along with surrounding host cell membrane and cytoplasm were released into the GVC. Observations of later stages revealed that

expelled symbionts were photosynthetically intact after release. The author hypothesized that this cellular mechanism was a method of symbiont population control in non-stressed members of *A. pallida*. Gates et al (1992) later renamed this mechanism as "pinching off" and suggested that it could be a potential cellular bleaching mechanism.

Host cell detachment

This mechanism whereby bleaching occurred when gastrodermal cells containing intact symbionts were released from the mesoglea and expelled into the GVC, was initially proposed by Gates *et al.* (1992). This response was observed after exposing the anemone *Aiptasia pulchella* and the coral *Pocillopora damicornis* to extreme temperatures of either 12^{o}C or 32 ^{o}C (10^{o}C above and below ambient temperature), both of which were beyond the temperature extremes recorded in the natural habitat from which these species were collected. Thus, it has been argued that this bleaching method only occurs as an extreme stress response, which is often followed by death of the host (Brown et al., 1995). The authors proposed that host cell release may occur as a result of cell adhesion dysfunction and calcium ion influx, however efforts to test this hypothesis were unsuccessful (Sawyer and Muscatine, 2001).

In situ degradation

This process was first described by Brown *et al.* (1995) in corals that were collected from a bleaching event. Histological examinations of bleached tissues revealed numerous symbionts that appeared "disrupted" and "misshapen" within host gastrodermal cells. Degraded symbionts were observed being exocytosed from host cells. However, within tissues that had been subjected to an advanced state of thermal stress, host cells containing symbionts appeared to be released

from the gastrodermis (see host cell detachment). Symbionts showed a spectrum of morphologies from normal to completely degraded, which suggested that progressive degradation was occurring *in situ* prior to the actual loss of symbionts from host tissues. Several other reports of *in situ* degradation of symbionts have been described in both naturally bleaching corals (Le Tissier and Brown, 1996; Ainsworth and Hoegh-Guldberg, 2008) and experimentally heat stressed corals, as well as in anemones (Dunn et al., 2004; Franklin et al., 2004; Strychar et al., 2004). However, most observations of *in situ* symbiont degradation were claimed to be the result of other degradative events, such as apoptosis or necrosis, rather than as an independent bleaching mechanism (Dunn et al., 2004; Franklin et al., 2004; Strychar et al., 2004; Ainsworth and Hoegh-Guldberg, 2008). There still remains much uncertainty over whether the appearance of degraded symbionts *in situ* is a result of ROS-mediated cell death activity or if the process functions as a host-controlled independent bleaching mechanism.

Cell death mechanisms

Cell death is an important function for proper development, controlling cell numbers and eliminating abnormal or damaged cells or invasive pathogens (Kourtis and Tavernarakis, 2009). Three major types of cell death have been defined, based on morphological criteria (Edinger and Thompson, 2004), apoptosis, autophagy, and necrosis, all of which have been implicated in cnidarian bleaching. Although these forms of cell death are morphologically independent processes, there is growing evidence that some may be interrelated (Xue et al.,1999; Klionsky and Emr, 2000; Dunn et al., 2002; 2004; 2007; Abraham and Shaham, 2004; Kourtis and Tavernarakis, 2009).

Apoptosis: Type I cell death

Apoptosis is a type of programmed cell death (PCD) that is a critical process in cell homeostasis and the deletion of damaged or unwanted cells. In vertebrates, apoptosis is highly complex and involves multiple interacting pathways that eventually lead to death of the cell. This process is characterized by distinctive morphological features, including cell shrinkage, chromatin condensation, and nucleosomal DNA fragmentation (Edinger and Thompson, 2004). During the final stages of apoptosis, the entire cell is packaged into "apoptotic bodies" which are ingested by phagocytes. The remnants of the cell are removed by phagocytic or neighboring cells (Gozuacik and Kimchi, 2004), thus no inflammation of surrounding tissues occurs (Edinger and Thompson, 2004).

Genetic regulation of apoptosis

Apoptosis is regulated by the activation of caspases, which are a family of cysteine proteases that undergo proteolysis and activation by other proteins and/or transcription factors (Earnshaw, 1999). Apoptotic activation can be induced by either the receptor-mediated, "extrinsic" pathway or the mitochondrial, "intrinsic" pathway (Lawen, 2003). The extrinsic pathway is executed when receptors such as tumor necrosis factor receptor (TNF-R), located on the plasma membrane of the cell, are activated by extracellular ligands (Lawen, 2003). This leads to the activation of initiator caspases (Caspase-8 or -10) that initiate executioner caspases (Caspase-3, -6, -7) that degrade cellular targets (Lawen, 2003). Alternatively, intrinsic-mediated apoptosis is often activated by a variety of intracellular ROS, NOS, or cytotoxic stress/damage to the outer mitochondrial membrane (Brune et al., 1999). These stressors activate regulatory proteins, such as bcl-2, which are also embedded in the outer mitochondrial membrane. These

factors all initiate the release of pro-apoptotic molecules, such as cytochrome *c,* from the mitochondrial intermembrane space into the cytosol (Lawen, 2003), where it binds to Apoptotic Protease Activating Factor (Apaf-1)/Caspase-9 complex that initiates executioner caspase, Caspase-3.

Apoptosis during bleaching

Caspases and other apoptosis genes are highly conserved among taxa and have been connected to the bleaching process in cnidarians. It has been suggested that during bleaching apoptosis acts to mitigate tissue damage from ROS by eliminating damaged cells (Dunn et al., 2004). A similar process occurs in higher taxa where apoptosis is utilized to remove invading microbes if they manage to evade host innate immune defenses (James and Green, 2004). It's also an essestial cellular process that plays an important in regulating developmental processes.

Autophagy

Although primarily a homeostatic response, the presence of autophagic structures in dying cells has recently implicated autophagy as a Type II cell death process (Kourtis and Tavernarakis, 2009). Autophagy is a process of cell recycling through lysosomal degradation that is essential for cell survival, differentiation, development, and homeostasis through cytoplasmic, protein, and organelle turnover (Holtzman, 1989). The autophagic process is generally accepted as a ubiquitous activity in eukaryotic cells (Ohsumi and Mizushima, 2004), and both protective and destructive contributions have been reported, largely from morphological observations of cell activities. Using autophagy, cells dispose of obsolete, excess or damaged parts, such as mitochondria, peroxisomes and regions of the Golgi, but the process can also result in cell death

(Cuervo, 2004). Autophagy is primarily characterized by the increased appearance of double membrane-bound cytoplasmic vesicles (autophagosomes) that engulf bulk cytoplasm and/or cytoplasmic organelles. These autophagic vesicles and their contents are then destroyed by the lysosomal system of the same cell.

Stages of the autophagic degradative process

The process of autophagic lysosomal degradation consists of several sequential steps involving sequestration, transport of lysosomes, degradation, and utilization of degradation products (Holtzman, 1989). First, various components of the cytoplasm, long-lived proteins, and intracellular organelles are sequestered within cytoplasmic double-membrane vesicles called autophagosomes or autophagic vacuoles (Kourtis and Tavernarakis, 2009). Young autophagosomes arise as regions of cytoplasm surrounded by a cup-shaped 'pre-autophagosomal structure' that eventually fuses with itself to seal off or "sequester" the vacuole's contents from the rest of the cytoplasm and form the actual 'autophagosome' (Holtzman, 1989). These structures are generally termed 'autophagolysosomes' after they fuse with primary lysosomes, which contain acid hydrolases that degrade the sequestered materials (Fawcett, 1981; Jing and Tang, 1999). The apparent continued sequestration of cytoplasmic contents by autophago(lyso)somal structures prior to or after fusion with the primary lysosome has been observed in the anemone, *Aiptasia pallida,* during heat stress induced-autophagy (Chapter 3); however, whether this is a common occurrence in other cnidarians is unknown. Breakdown of sequestered materials by lysosomal hydrolases results in release of the digested materials back into the cytoplasm to be recycled for macromolecular synthesis and/or ATP generation (Wang and Klionsky, 2003). As digestion proceeds, the autophagolysosomes eventually condense into

electron dense, heterogeneous, indigestible materials within the autophagosome membrane (Fawcett 1981; Holtzman 1989). These end products of autophagy are called residual bodies.

Role of autophagy during stress or injury

Although autophagy is regularly seen under normal, non-pathological circumstances in many cell types, it may be induced under conditions of stress such as hyperthermia, which often results in cell damage or death (Schwartz et al., 1992; Swanlund et al., 2008). However, autophagy has also been implicated as a pro-survival process for its response to intracellular stress conditions, whereby free amino and fatty acids are produced as metabolic substrates for adaptation to stress. In the absence of autophagy, the turnover of cytoplasmic proteins is impaired, which increases the likelihood they will become damaged, misfolded, ubiquitinated and removed (Hara et al., 2006; Komatsu et al., 2006). Defective autophagic activity contributes to a number of diseases, including myopathies, neurodegenerative diseases (e.g. Parkinson's and Alzheimer's), and some forms of cancers (Kelekar, 2006). Recent studies have indicated that ROS production induces autophagy (Sherz-Shouval and Elazar, 2007), which plays a role in eliminating proteins damaged during oxidative stress (Xiong et al., 2007).

Co-involvement of autophagy and apoptosis

Based on the fact that both autophagy and apoptosis share several key genes and transcription factors in their respective molecular pathways, there is growing evidence that the two processes are interrelated (Xue et al., 1999; Klionsky and Emr, 2000; Abraham and Shaham, 2004; Dunn et al., 2007; Kourtis and Tavernarakis, 2009). Several pro-apoptotic signals induce

autophagy, whereas signals that inhibit apoptosis also inhibit autophagy; however, the exact nature of the relationship between autophagy and apoptosis is complex and not fully understood (Kourtis and Tavernarakis, 2009). Since autophagic activity is often detectable in regions where apoptosis is occurring, it has been suggested that autophagy is a type of non-apoptotic PCD (Tsujimoto and Shimizu, 2005). Alternatively, autophagy may also precede apoptosis as a defense mechanism (Lockshin and Zakeri, 2004) or function to ensure cell death in the event of inhibition of other death pathways (Kosta et al., 2004).

Autophagy during bleaching

Recent investigations of cnidarian bleaching corroborate this idea by providing evidence that autophagy is interlinked with apoptosis during hyperthermic stress (Dunn et al., 2007). In *A. pallida*, Dunn *et al.* (2007) demonstrated that chemical induction of autophagy by rapamycin caused massive bleaching at ambient temperature (24^{o}C) suggesting that autophagy can play a role in symbiont regulation. However, elevated temperature-induced bleaching was repressed only when both apoptosis and autophagy were inhibited simultaneously. Thus, it was hypothesized that the two forms of cell death were interconnected, such that when one is inhibited, the other is induced. A more recent investigation (see Chapter 3) documented autophagic activity in *A. pallida* tissues exposed to heat stress conditions. In this study, anemones treated with rapamycin, a known autophagy inducer (Noda and Ohsumi, 1998), exhibited the same ultrastructural characteristics as heat stressed tissues, confirming that the structures observed during heat stress treatment were autophagic. Rapamycin-induced (and heat-induced) autophagic structures contained sequestered host cellular material and were often found within highly degraded regions of the cell that exhibited an abnormally sparse cytoplasm.

In addition, a novel bleaching mechanism termed as 'apical detachment' was observed in the same thermally stressed tissues undergoing active autophagy. This bleaching mechanism was characterized by a series of cellular events that occurred in autophagic host cells. These steps involved the i) gradual movement of the healthy symbiont within its symbiosome toward the apical region of host cells ii) bulging of symbiont/symbiosome with associated host cell plasma membrane and cytoplasm into gastrovascular cavity, iii) detachment of apical portion of host cell along with healthy symbiont/symbiosome in an apocrine-like manner into the gastrovascular cavity. The authors suggested that heat stress induced autophagic degradation led to reduced cellular stability, eventually resulting in the loss of symbionts via this apical detachment mechanism.

Symbiophagy:

One recent study measured elevated autophagic activity in the heat stressed coral *Pocillopora damicornis* using markers of autophagy (Rab 7 and LAS) (Downs et al., 2009). Histological examinations of bleaching tissues revealed an increase in the vacuolar space between the symbiont and host tissues with length of thermal treatment. Downs *et al*. (2009) hypothesized that symbionts were digested by the host through an innate intracellular protective pathway termed "symbiophagy". This term was modified from the process known as "xenophagy", which involves the digestion of potential intracellular pathogens. The authors suggested that during symbiophagy, the vacuolar membrane (or symbiosome) that envelopes the symbiont is transformed from a conduit of nutrient exchange to that of a phagolysosome that is then recognized by the lysosomal system. As a result lysosomes fuse with the former

symbiosome leading to the digestion of the symbiont. Experimental data supporting this hypothesis remains to be provided.

Molecular studies of autophagy

Autophagy was discovered in mammalian cells but has been extensively studied in yeast (Huang and Klionsky, 2002), where over 20 genes encoding proteins involved in autophagy (designated as AuTophaGy related - ATG) have been identified (Klionsky et al., 2003). The basic mechanism of autophagy has been well conserved among taxa and all share a similar set of ATG genes (Tsujimoto and Shimizu, 2005). Autophagy is controlled by several proteins, including the PI3IK/Akt complex which regulates another major protein kinase, mammalian Target Of Rapamycin (mTOR), which negatively regulates the pathway (Kamada et al., 2000). After the induction of autophagy, several regulatory stages mediated by various proteins and/or transcription factors must occur in order to complete the process. Downstream of mTOR kinase, membrane nucleation occurs by the joining of Beclin 1, a human homolog of the yeast autophagy gene ATG 6, the vacuolar protein sorting protein (VPS 15), and the kinase PI3K III. These subunits are regulated by the anti-apoptotic/anti-autophagic protein, Bcl-2, which also has a nuclear export signal (Kang et al., 2011). Numerous ATG proteins are essential for the later stages of autophagy (Levine and Klionsky, 2004), whereby cellular contents are sequestered into autophagosomes, which then fuse with lysosomes and degrade cellular contents.

Cell Necrosis: Type III cell death

Lastly, necrotic cell death is defined as non-lysosomal vesiculate degradation, which is characterized by the dilation of intracellular organelles and breakdown of the plasma membrane

that often causes inflammation of surrounding tissues (Edinger and Thompson, 2004). Cell necrosis is most often triggered by extrinsic factors, such as physical injury, that cause the cell and its organelles to swell and eventually rupture (Wyllie et al., 1980). In contrast to apoptosis and autophagy, necrosis has been classified as uncontrolled cell death; however, recent investigations suggest that programmed cell necrosis may occur (Edinger and Thompson, 2004). Several genes have been proposed to regulate programmed necrosis, such as the protein kinase RIP (receptor interacting protein) and poly (ADP-ribose) polymerase (PARP), which negatively regulate the caspase-independent pathway (Proskuryakov et al., 2003; Edinger and Thompson, 2004).

Cell necrosis during bleaching

Both cell necrosis and apoptosis were documented in host tissues and in the symbiont according to morphological appearance of cells in thermally stressed *A. pallida* (Dunn et al., 2002; 2004). In these studies, Dunn and colleagues subjected anemones to a range of elevated temperatures for varying lengths of time. These studies revealed a shift from apoptosis at the lower stress levels, i.e. moderate temperature stress and shorter duration, to necrosis at the more severe stress levels. This led to the hypothesis that apoptosis acts to mitigate tissue damage from ROS at moderate stress levels, thereby maintaining tissue homeostasis by eliminating damaged cells. However, this control is lost under severe stress, where necrosis predominates.

Summary of potential methods of symbiont loss

All the previously described cellular bleaching methods (cell death and non-cell death-related) were observed in a variety of cnidarian species under a range of thermal stress conditions. Thus, there is still no agreement on which method primarily occurs in nature, if any (Weis, 2008). The cellular mechanisms involved in the cnidarian bleaching process are a complex set of interactions between two symbiotic members that are affected by many environmental factors. Contrasting descriptions of bleaching (mechanisms of symbiont loss and relative contribution of zooxanthellae versus pigment loss) may reflect differences between species, the nature of the stressor and/or the amount of time lapsed between the onset of bleaching and collection of samples (Brown et al., 1995; Chapter 3). While some of these experiments have been successful in simulating "natural" bleaching conditions in the field, others have used conditions that are not typically experienced during natural conditions. Thus, extrapolation of potential methods of bleaching to those recorded during natural bleaching conditions in the field should be conducted with caution (Brown et al., 1995; Chapter 3). To further complicate matters, the majority of evidence for the proposed methods largely comes from histological snapshots of bleaching tissues. Therefore, the cellular dynamics underlying these events remain unresolved (Weis, 2008).

Conclusions

The earliest reports of bleaching events occurred in the late 19th century (Glynn, 1993). Over the past few decades, an increasing frequency of bleaching episodes has been documented (Gates et al., 1992, Hughes, 2003; Hoegh-Guldberg et al., 2007), and these have impacted reefs on a more global scale (Hoegh-Guldberg, 1999). Recent evidence suggests that since 18,000 years ago, tropical oceans have fluctuated in temperature by less than 2 ^{o}C (Thunnell et al., 1994). Thus, the cnidarian-dinoflagellate symbiosis has evolved to remain stable within a narrow temperature range. However, in the past 100 years sea surface temperatures have increased by almost 1 ^{o}C and are currently increasing at the rate of approximately 1-2^{o}C per century (Hoegh-Guldberg, 1999). Since corals are currently living close to their thermal maxima, even small increases in temperature (1-2^{o}C) can disrupt their symbiosis with *Symbiodinium* (Glynn, 1990; Hoegh-Guldberg, 1999). As a result, corals will continue to be threatened by increasing frequency and severity of bleaching events in combination with other anthropogenic-driven disturbances, such as coral disease and ocean acidification that often co-occur (Brown, 1997). If allowed to continue unchecked, these environmental impacts will have grave negative consequences on the health of reef ecosystems.

II. Histological and ultrastructural analysis of cell types within the tentacle tissues of the symbiotic anemone, *Aiptasia pallida*

Abstract

Coral bleaching involves the loss of essential, photosynthetic dinoflagellates (*Symbiodinium* sp.) from host gastrodermal cells and occurs as a stress response of both members of the symbiosis. Although this phenomenon has been thoroughly investigated for several decades, the complex set of cellular interactions involved in the breakdown of the symbiosis are only beginning to be unveiled. Thus, a detailed ultrastructural analysis of a commonly used model symbiotic cnidarian is critical in order to provide essential baseline information for future bleaching investigations to assess cellular changes in response to stress conditions. In this study, a detailed ultrastructural overview of the cellular and sub-cellular structures that underlie a healthy stable cnidarian-dinoflagellate symbiosis was carried out using the *Aiptasia –Symbiodinium* system. Both light and transmission electron microscopy (TEM) were used to examine multiple regions throughout the tentacles of *A. pallida*. Ultrastructural investigations revealed various cellular structures, some of which were similar in appearance to those previously described in other cnidarians while other structures appeared different from those in other cnidarians in the ultrastructural literature. Numerous cell processes were observed penetrating the mesoglea, which serves as acellular substrate for the attachment of all epithelial cells. Longitudinal sectioning revealed finger-like projections of mesoglea extending between adjacent gastrodermal cells and cell processes. These observations suggest that in *A. pallida*, the mesoglea is a complex matrix that extends amongst the entangled processes of adjacent epithelial

cells rather than forming a simple attachment along the bases of these cells. This complex structure has direct implications for a suggested cellular bleaching mechanism known as 'host cell detachment.' This study represents the first detailed and systematic analysis of the *Aiptasia* model system or any other symbiotic cnidarian. Futhermore, the ultrastructural information gained from this analysis can be used as an informative health assessment tool as they are manipulated in the lab or during field-mediated conditions.

Introduction

Coral reefs serve as the trophic and structural foundation of the reef ecosystem, a tropical oasis that boasts the highest diversity of marine organisms on the planet (Hoegh-Guldberg, 1999; Stat et al., 2006). Corals and other cnidarians belonging to the class Anthozoa, subclass Hexacorallia (= Zoantharia) are exclusively marine (Fautin and Romano, 1997). This group includes scleractinian corals as well as sea anemones that form symbioses with photosynthetic dinoflagellates from the genus *Symbiodinium* (Freudenthal, 1962). The intracellular symbionts comprise at least eight clades (A-H), which contain multiple subclade types (Stat et al., 2006) that can be identified at the molecular level.

Although hosts from five invertebrate phyla are currently known to harbor these intracellular symbionts, cnidarian-algal symbioses have gained the most attention in recent years (Stat et al., 2006). This primarily results from the rapid decline in coral abundance and diversity that has resulted from anthropogenic-linked environmental stressors (Hoegh-Guldberg et al., 1999, 2007). During stressful conditions, such as elevated temperature and light, the symbiotic relationship between the cnidarian host and the symbiotic cells breaks down through a series of

cellular events known as 'bleaching'. Cnidarian bleaching has been extensively studied for the past few decades. However there is still much uncertainty surrounding the cellular events that are involved during a natural bleaching episode (Weis, 2008).

Previous investigations have described a wide variety of cellular bleaching mechanisms resulting from examinations of temperature or light stressed cnidarian tissues (Taylor, 1973; Glynn et al., 1985; Steen & Muscatine, 1987; Gates et al., 1992; Brown et al., 1995; Dunn et al., 2002; 2007; Franklin et al., 2004; Strychar et al., 2004; Richier et al., 2006; Downs et al., 2009; Chapter 3). Yet one of the major impediments to these studies was that many of them were based on histological or ultrastructural 'snapshots' of the stressed tissues rather than conducting a proper comparison to control unstressed tissues over the time course of the bleaching episode. Such a comparison is critical when conducting ultrastructural analyses of cnidarian tissues, which can be quite complex and difficult to interpret after experimental manipulations without a thorough understanding of control tissues beforehand (Hanes, personal observation). In addition, it has been suggested that the utilization of an experimentally tractable model organism, such as the anemone symbiosis model, *Aiptasia* spp. (Order Actiniaria) would greatly aid future cellular investigations (Weis et al., 2008). For example, *Aiptasia* spp. maintain symbioses with a variety of *Symbiodinium* spp. types in a manner similar to what is seen in many corals (Weis et al., 2008; Sunagawa et al., 2010; Lenhart et al., 2012). The absence of a calcareous skeleton in anemones also enables most cellular and microscopical manipulations to be conducted with much less effort than if using scleractinian corals (Sunagawa et al., 2010; Lenhart et al., 2012). Thus, a detailed ultrastructural analysis of this commonly used model symbiotic cnidarian is critical in order to provide essential baseline information for future bleaching investigations to use to assess cellular changes in response to stress conditions.

Numerous early studies provided a detailed look at the histology and ultrastructure of cnidarians using *Hydra* as their model (Hess et al., 1957; Slautterback and Fawcett, 1959; Wood, 1961; Gauthier, 1963; Slautterback, 1967; Davis and Haynes, 1968; Haynes et al., 1968; Haynes and Davis, 1969; Rose and Burnett, 1968; Weis, 1971; Haynes, 1973; Weber and Schmid, 1985). More recent investigations have aimed to describe the ultrastructure of a wide variety of anthozoans (Westfall et al., 1973, 1997, 1998; 2002a; Fautin and Mariscal, 1991; Westfall and Elliot, 2002), including *A. pallida* (Westfall et al, 1997, 1998, 1999, 2001, 2002; Westfall and Elliot, 2002). However, most of the ultrastructural studies conducted by Westfall and colleagues have focused on identifying neural synapses with various cells types (Westfall et al, 1998, 1999, 2001) along with describing neural pathways (Westfall et al., 2002; Westfall and Elliot, 2002). Therefore, there are numerous aspects of the cellular ultrastructure of *A. pallida* that have yet to be described.

In this study, a detailed ultrastructural analysis of the tentacular tissues of healthy, unstressed *Aiptasia pallida* provide an overview of the cellular and sub-cellular structure that underlies a healthy cnidarian-dinoflagellate symbiosis.

Materials and Methods

Culture conditions

Aiptasia pallida harboring symbionts typed as Clade A4 *Symbiodinium* (Santos et al. 2002; Scott Santos, pers. comm.) were collected in the Florida Keys and maintained in artificial seawater (Reef Crystals) at 28-30 ppt salinity. Anemones were kept in two 150 gal tanks maintained at an average temperature of 24±1°C (such notation indicates mean ± standard deviation). The bottom of each tank, where most anemones were located, was ~1 m below a light

source that covered the length of each tank. The light source consisted of two fluorescent light fixtures per tank that were each equipped with two 32W bulbs (Phillips F32T8/TL841) producing a 50±4 µmol photons $m^{-2}s^{-1}$ irradiance at the bottoms of the tanks. Lights were set on a 12:12 h light/dark regime. The anemones were fed freshly hatched nauplii of *Artemia* three times per week.

Anemone preparation for light (LM) and transmission electron (TEM) microscopy

Twelve medium sized anemones were placed in identical, individual dishes that each contained ~200 mL 0.45 µm Millipore-filtered artificial aquarium sea water (MFAW) and were allowed to acclimate for ~5 d to the ambient lab temperature of 24±1° C with 50±4 µmol photons $m^{-2}s^{-1}$ ambient light intensity. Water in the dishes was changed daily, and the anemones were fed once during the first 3 d. They were then held unfed for 48 h prior to excision and fixation of tissues.

Anemones were all prepared for fixation by removing the seawater from each anemone container and replacing it with ~300 mL high Mg/low Ca seawater (Audesirk & Audesirk, 1980) for 30 min, followed by the addition of ~2 mL chloretone saturated seawater for an additional incubation time of 30 min. Next, a subset of tentacles was clipped from each of 6 randomly selected anemones. Tissues were fixed using methods similar to the protocol of Carroll & Kempf (1994) in a primary fixative solution of Millonig's phosphate-buffered 2.5% glutaraldehyde containing 0.14M NaCl for 1 h, followed by rinses with a 1:1 mixture of 0.34M NaCl and Millonig's phosphate buffer solution. The tentacles were secondarily fixed in a 1.25% $NaHCO_3$ buffered 2% OsO_4 solution for 1 h. Following secondary fixation, tentacles were rinsed three times in 1.25% $NaHCO_3$ buffer, dehydrated through an ethanol series to 100% ethanol,

transferred through three changes of propylene oxide, and infiltrated and embedded using EMbed 812 resin (Electron Microscopy Sciences). Embedded tentacles were sectioned at either 0.5 - 1 μm or ~60 nm thickness using a diamond knife (Diatome) on a Reichert-Jung Ultracut E microtome. Sections cut at 0.5 – 1 μm were stained with Richardson's stain for LM. Sections cut at 60 nm for TEM were stained with uranyl acetate and lead citrate. Tissues were visualized and photographed in sections from mid-tentacle length and around the circumference of each tentacle using a Zeiss EM 10C 10CR transmission electron microscope. Negatives from TEM were scanned as positives on an Epson Perfection 3200 Photo flatbed scanner at 1200 dpi, and contrast and levels were adjusted using Adobe Photoshop 8.0.

Results and Discussion

A. pallida exists as a solitary polyp that attaches to the substrate at the basal disk, extends upward along a column that terminates as the oral disk surrounded by numerous radiating tentacles (Fig. 1A). As is the case with all anemones, the column and tentacles (Fig. 1 A & B) consist of an epidermal and gastrodermal tissue layer separated by an acellular collagenous layer called the mesoglea (Fig. 1 C & D). The mouth at the center of the oral disk (Fig. 1B) opens into the gastrovascular cavity (Gv) that extends throughout the column and into the tentacles (Fig. 1C). *A. pallida* and many other diploblastic cnidarians harbor their symbionts within the cells of the digestive tissue (gastrodermis) (Fig. 1C, D and 2).

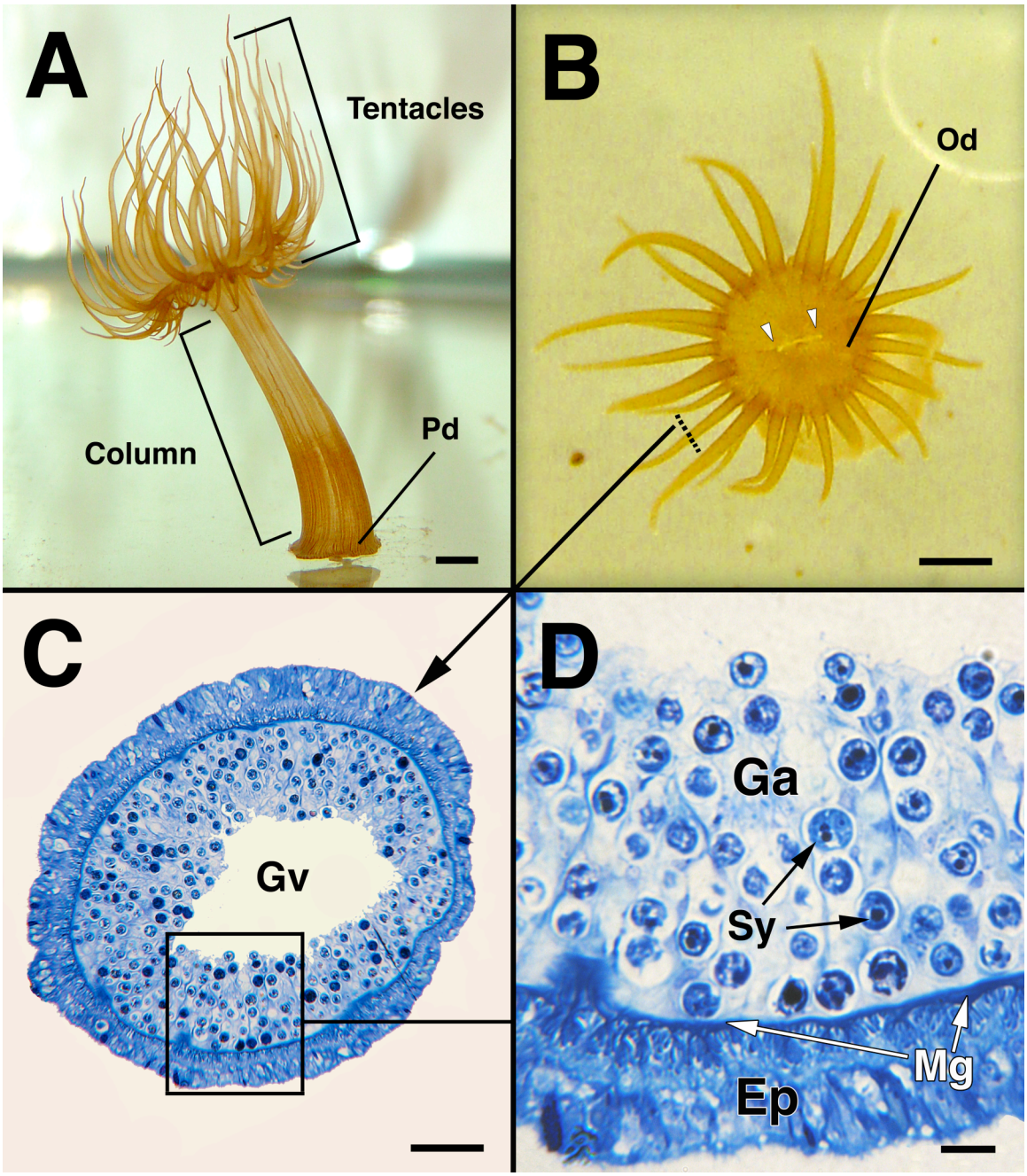

Figure 1. Morphology of *Aiptasia pallida* and histology of symbiotic tentacle tissues. A. From the side view, the anemone is attached to the substrate by the pedal disk (Pd), extends upward along the column and terminates at the oral disk (Od), from which numerous tentacles radiate. B. From the top view, the mouth appears as a slit, which serves as the solitary opening to the gastrovascular cavity (Gv). Note: The siphonoglyphs extend from either end of the mouth (arrowheads). C. Light micrograph of a transverse section of fixed and stained anemone tentacle taken from the approximate location of the dotted line in frame B. The tentacle exhibits the hollow Gv that extends from the column into each tentacle. D. High magnification of the gastrodermis (Ga) and epidermis (Ep), which are separated by the acellular mesoglea (Mg) (dark blue region indicated by white arrows). Healthy symbionts (Sy) can be seen within symbiosomes in the gastrodermal cells. Scale bars A-B=10mm; C=60 μm; D=10μm.

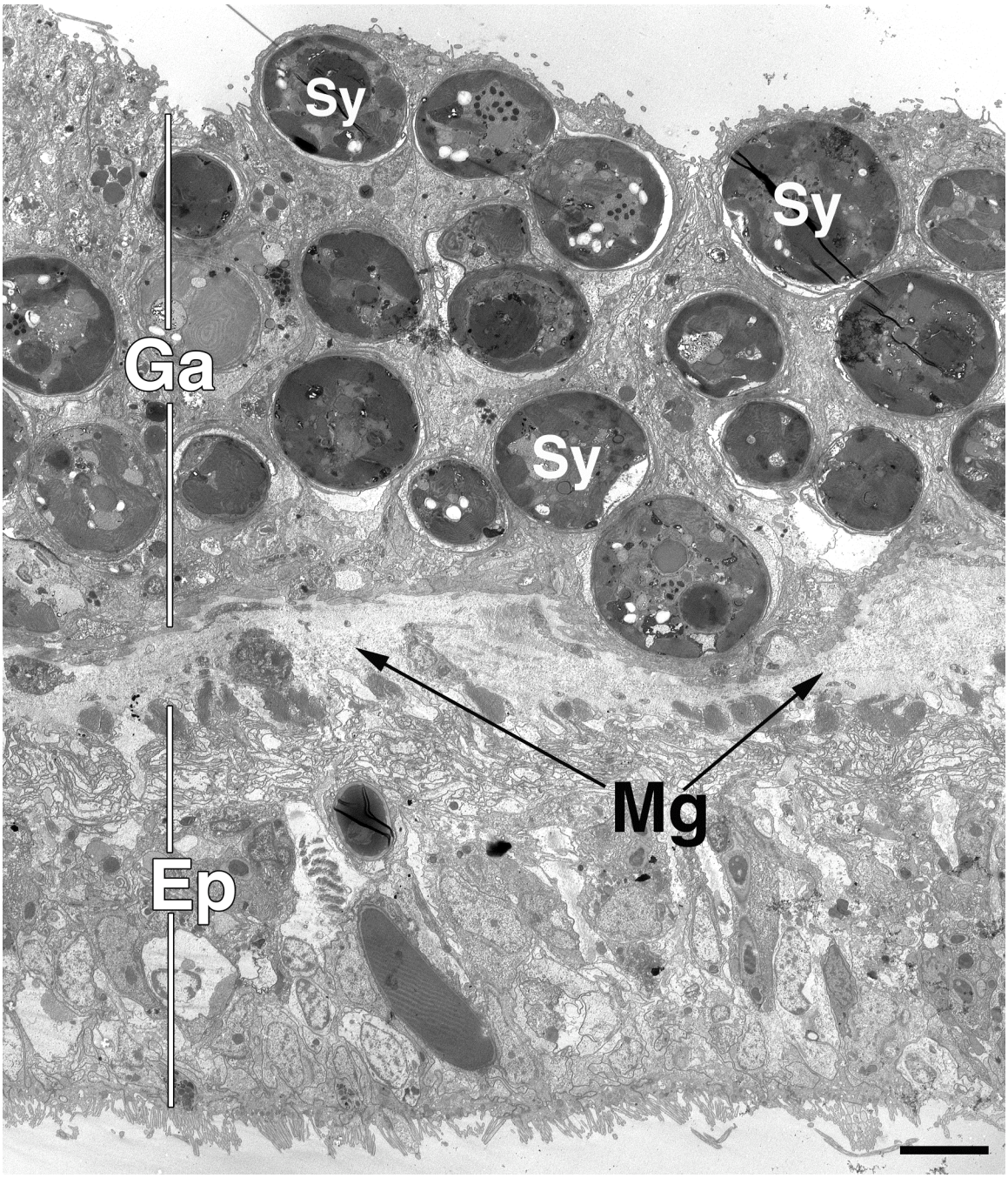

Figure 2. TEM: Transverse sections of symbiotic *Aiptasia pallida* tentacle tissues. Both tissue layers, the gastrodermis (Ga) and epidermis (Ep), are separated by the acellular mesoglea (Mg). The epidermis and gastrodermis each consist of an irregular epithelium of columnar cells and basal cells. Numerous intact symbionts (Sy) are located within cells of the host gastrodermis. Scale bar=5μm.

Gastrodermis

Within symbiotic *A. pallida* tissues, columnar gastrodermal cells extend from the mesoglea to the gastrovascular cavity (Fig. 2 and 3), where numerous microvilli project from the apical plasma membranes of the cells (Fig. 3, also see Figure 12 and associated text below). Symbiont cells are located intracellularly within a highly specialized host vacuole called the 'symbiosome' (Wakefield and Kempf, 2001) (Fig. 3). The host derived membrane of this vacuole and underlying symbiont secretions function as the interface between host and symbiont.

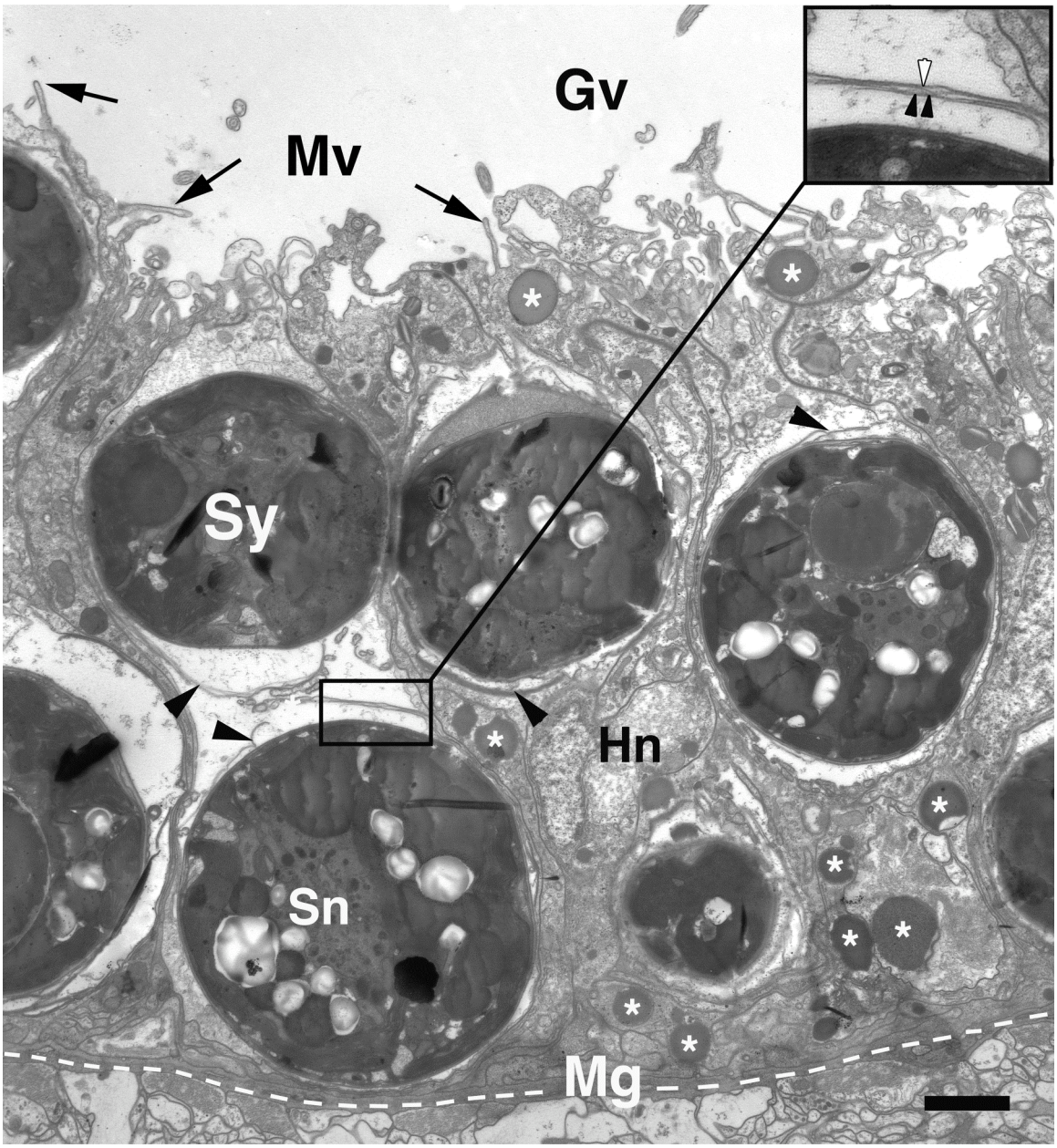

Figure 3. TEM: Transverse sections of symbiotic gastrodermal tentacle tissues of *A. pallida.* The gastrodermal tissue layer (Ga), extends from the mesoglea to the gastrovascular cavity (Gv). The host cells exhibit a healthy condition with dense cytoplasm and intact nuclei (Hn). Numerous symbiont cells (Sy) displaying healthy appearances and intact nuclei (Sn) were observed within host-derived symbiosomes (black arrowheads). The inset provides higher magnification of the boxed region allowing the symbiosome membrane (double black arrowheads) to be distinguished from the adjacent plasma membrane of the host cell (white arrowhead). Mg, mesoglea; Mv, microvilli. Scale bar=2μm.

Secretory-gland cells

Secretory gland cells were observed in the gastrodermis of *A.pallida* (Fig. 4). Putative mucus secreting cells are typically identified based on the abundant clear or pale inclusions (= vesicles/granules) present in their cytoplasm (Hyman, 1940; Hess et al., 1957; Rose and Burnett, 1968; Westfall et al., 2001). Numerous large pale inclusions were observed in abundance in *A. pallida* throughout the gastrodermis (Fig. 4A, B). These pale inclusions were observed frequently in regions surrounding symbionts and on occasion appeared to be secretions of symbiont cells (Fig. 4A, B). The overall density and composition of the inclusions being exuded by the symbionts (Fig. 4A, B) was strikingly similar to the numerous other inclusions located within putative gland cells of the gastrodermis (Fig. 4A). Other secretory gland cells were commonly observed throughout the gastrodermis, some of which contained small irregular electron dense inclusions (Fig. 4A).

Mucus-secreting gland cells have been previously described in a variety of cnidarians (Hyman, 1940; Hess et al., 1957; Rose and Burnett, 1968; Westfall et al., 2001), including *A. pallida* (Westfall et al., 2001) and have a similar appearance to those observed in host gastrodermal cells in this study (Fig. 4A).The pale inclusions (Fig. 4A) observed within putative gland cells of the gastrodermis have the same appearance as the substance that appears to be secreted by some symbionts (Fig. 4A, B). Thus, it is possible that the substance is either translocated from the symbiont cells or synthesized by the host gland cells. However, further investigation is necessary in order to confirm the identity of this substance and its origin.

Another type of gland cell that was frequently observed in the gastrodermis contained aggregations of large (~1.5um), round, electron-dense inclusions (Fig. 5). Such granules were first described as ‘zymogenic’ in a cnidarian gastrodermis by Gauthier (1963) based on their

morphological similarity to pancreatic zymogenic granules and their positive enzymatic reactivity. Since then, similar-appearing zymogenic granules have been described in a wide variety of cnidarians (Slautterback and Fawcett; 1959; Haynes and Davis, 69; Vader and Lonning, 1975; Westfall et al., 1997; 2001; Goldberg, 2002; Dandar-Roh et al., 2004) including *A. pallida* (Westfall et al., 1997; 2001). Their general characteristics include that they comprise two-thirds of the volume of a cnidarian gland cell and that they are membrane-bound (Westfall et al., 2001); however, convincing images of a surrounding membrane are not provided in Westfall's paper (2001) and similar "zymogen granules" identified by Haynes and Davis (1969) in *Hydra viridis* are said to lack a surrounding membrane. In order to test the identity of these characteristic cnidarian 'zymogen-like' granules, a recent ultrastructural investigation tested their contents in a symbiotic coral using DMAB-nitrite and Bromophenol blue (Goldberg, 2002). They concluded that the primary composition of the inclusions was similar to that of vertebrate zymogen precursors (Goldberg, 2002).

Although no surrounding membrane could be distinguished in association with the large dense granules observed in this study, their morphology and organization appeared strikingly similar to previous descriptions in *A. pallida* (Westfall et al., 1997; 2001). The combined results of the current ultrastructural study with recent ultrastructural-biochemical investigations (Goldberg, 2002) suggest that these large electron-dense inclusions in the gastrodermis of *A. pallida* are zymogenic granules. However, histochemical testing is necessary to determine the true identity of the contents of these granules in *A. pallida*.

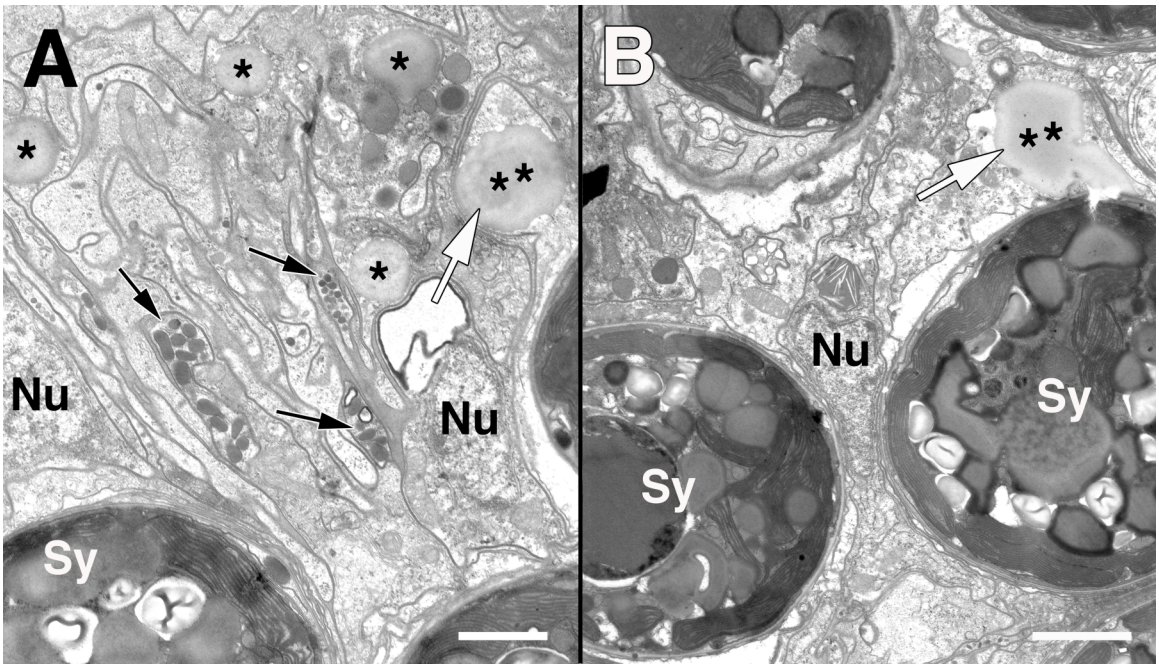

Figure 4. TEM: Transverse sections of symbiotic gastrodermal *Aiptasia pallida* tentacle tissues with gland cells containing various types of vesicular inclusions. A. Numerous putative gland cells containing small electron-dense (arrows) or large pale inclusions (indicated by asterisks) that are commonly present throughout the gastrodermis. B. A symbiont cell appears to be exuding a pale substance (indicated by white arrow and the double asterisks), which has the same appearance as the pale inclusions located in other cells throughout the gastrodermis in 4A (indicated by asterisks).This suggests that the pale inclusions (double asterisks) may be a translocation product released to the host. Nu, nucleus; Sy, symbiont cell. Scale bar A=1μm, B=2μm.

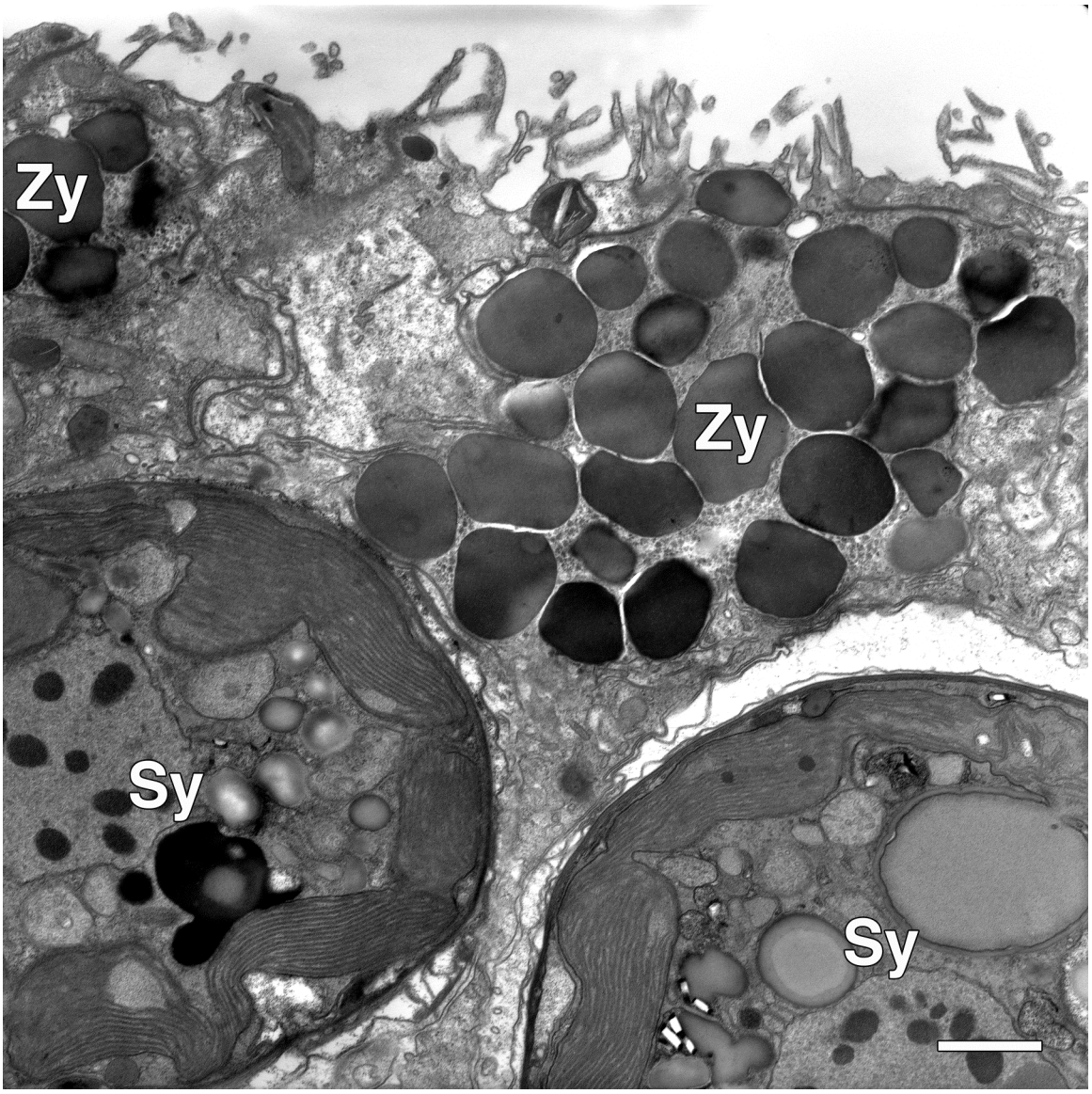

Figure 5. TEM: Transverse sections of symbiotic gastrodermal *Aiptasia pallida* tentacle tissues with gland cells containing putative zymogenic granules. Gland cells containing putative zymogenic granules (Zy) were commonly observed in the gastrodermis. Sy, symbiont cell. Scale bar =1μm.

Nerve plexus

Structures associated with the nerve net of *A. pallida* were generally observed as putative neurites (Fig. 6A-C) that at times clumped together as a bundle of nerve fibers (Fig. 6A,B). Interestingly, the most commonly observed structures that were presumably associated with the nervous system appeared as densely packed concentric circles within a cell or cell process

located near or adjacent to the mesoglea (Fig. 6D). Due to their abundance within a cell or cell process, it is not likely that they are axons surrounded by an associated cell; however, evidence for small and densely packed neurites has been documented in *A. pallida* (Westfall, 2002). Alternatively, it is possible that they are dense-core vesicles that have undergone some extraction as a result of processing for TEM.

Cnidarians are the simplest multicellular organisms to possess a nervous system, which is a diffuse nerve plexus called a "nerve net" (Schick, 1991; Grimmelikhuijzen and Westfall, 1995). In most cnidarians the gastrodermal nerve plexus consists of numerous neurites located near the bases of digestive cells (Westfall and Elliot, 2002) that appear similar to those observed in this study (Fig. 6A, B and 9B). The nerve plexus is found just beyond the musculature and transmits signals to various regions throughout the anemone where it contacts other nerve or muscular cells (Schick, 1991; Westfall et al., 2002). In order to carry out this cascade of cellular events, several types of cells are necessary, including specialized neurons and ganglion cells (Westfall, 1970; 1973; Anderson and Schwab, 1982). Ganglion cells have been shown interconnect to other ganglion cells through synaptic connections, which suggests that these cells facilitate "through-conduction of impulses in the nerve net" (Westfall and Elliot, 2002). These cells receive stimuli from sensory cells then process and transmit the signal to smooth muscle for contraction to occur (Parker, 1919). (See Epidermis Nerve plexus for more information)

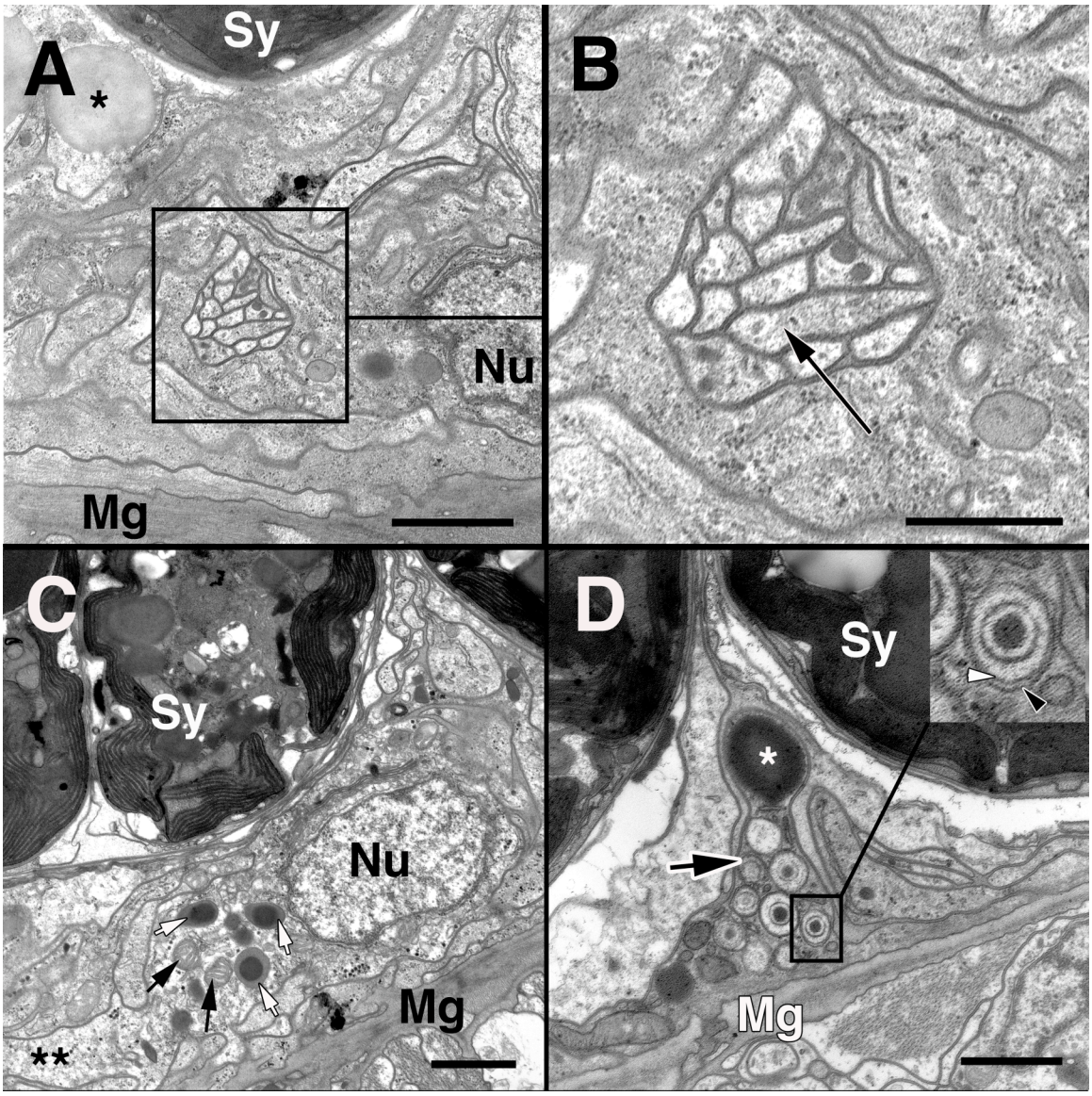

Figure 6. TEM: Transverse sections of symbiotic gastrodermal *Aiptasia pallida* tentacle tissues containing putative structures associated with the gastrodermal nerve plexus. A. A region of putative neurites passing amongst other cellular processes. B. Higher magnification of putative neurites (black arrow) showing detail. C. A large cell body containing dense core vesicles (white arrows) and mitochondria (small black arrows) is present at the basal region of the gastrodermis adjacent to the mesoglea (Mg). This cell appeared to narrow at one end (indicated by the double asterisks) in a manner suggestive of a neural projection. D. Putative dense core vesicles were commonly observed in cross-section and appeared to aggregate within a cell or cell process (black arrow) that contains a large lipid droplet (indicated by asterisk) and attaches directly along the mesogleal surface. The inset provides higher magnification of the boxed region showing what appears to be three concentric membranes, the first that of the dense core vesicle and then two additional membranes (white arrowhead and black arrowhead). The presence of these two additional membranes suggests the possibility that this is a process from a neuron that penetrates through an associated cell. Nu, nucleus; Sy, symbiont cell. Scale bars=1μm.

Nutritive-muscular cells

Host cells that harbored one or more symbionts were the most conspicuous type in the gastrodermis (Fig. 2 and 3). These abundant gastrodermal cells have historically been referred to as 'nutritive-muscular' (Hyman, 1940; Brusca and Brusca, 2002) and more commonly, 'epitheliomuscular' (= myoepithelial; Doumenc and Van-Praet, 1987; Schick, 1991; Fautin and Mariscal, 1991; Westfall et al., 2001; Brusca and Brusca, 2002) cells. However, we will refer to them exclusively as nutritive-muscular cells throughout the remainder of the text 1) in order to differentiate them from similar but distinct non-symbiont containing cells in the epidermis and 2) to recognize the digestive role of these cells.

Nutritive-muscular cells are exclusively found in the gastrodermis and exhibit basal projections that extend circumferentially adjacent to the mesoglea (Fig. 7). Sparse muscular threads were observed within the basal projections that contribute to the circular smooth muscle of the tentacles (Fig. 7). These structures were further identified as putative myosin (thick) and actin (thin) filaments (Fig. 7) based on their measurements of ~17.5nm and ~7 nm in diameter, respectively, which are both within the expected size ranges of smooth muscle myofilaments in *Aiptasia* (Amerongen and Peteya, 1976; 1980) (Fig. 7). A similar description of nutritive-muscular cells was made by Hyman (1940) in *Hydra* as having bases that are "drawn out into extensions containing a [contractile] myoneme". "Myoneme" is a term originally used to describe contractile fibers in the cytoplasm of protists (Butschli, 1887). Alternatively, Hyman described the muscular component of gastrodermal cells in Anthozoa as cells "whose bases are drawn out into circular muscle fibers" and fails to describe any basal processes or myoneme within them; rather describing the base of the cell itself as the muscle fiber.

Our observations of the muscular components of nutritive-muscular cells in *A. pallida* differed from previous descriptions of 'myoneme'-bearing gastrodermals cells in *Hydra* (Hyman, 1940; Slautterback, 1967; Haynes et al., 1968; Haynes, 1973; Davis, 1973) and those described in other anthozoans (Doumenc and Van-Praet, 1987; Fautin and Mariscal, 1991; Schick, 1991; Westfall et al., 1997; Brusca and Brusca, 2002; Westfall and Elliot, 2002; Tucker et al., 2011). In many of these studies, the organization of the muscular filaments exhibited a rod-like appearance (=myoneme) that has been suggested to result from numerous individual myofilaments stacked together as one contractile unit (Haynes, 1973). In contrast, only sparse single myofilaments were observed as short segments in this study, which may suggest that the filaments are convoluted within the basal processes in *Aiptasia pallida.*

A previous study suggested that symbiotic anemones contain two distinct types of nutritive-muscular cells in the gastrodermis (Doumenc and Van-Praet, 1987). The first type fits the 'classical' definition of an'epitheliomuscular' cell by exhibiting highly elongated contractile basal projections and associated myofilaments (i.e., myoneme) that extend circumferentially along the mesoglea (Doumenc and Van-Praet, 1987). But the projections and myofilaments of the second type are not as elongated as the previously mentioned cell and these cells often harbor symbiont cells (Doumenc and Van-Praet, 1987).

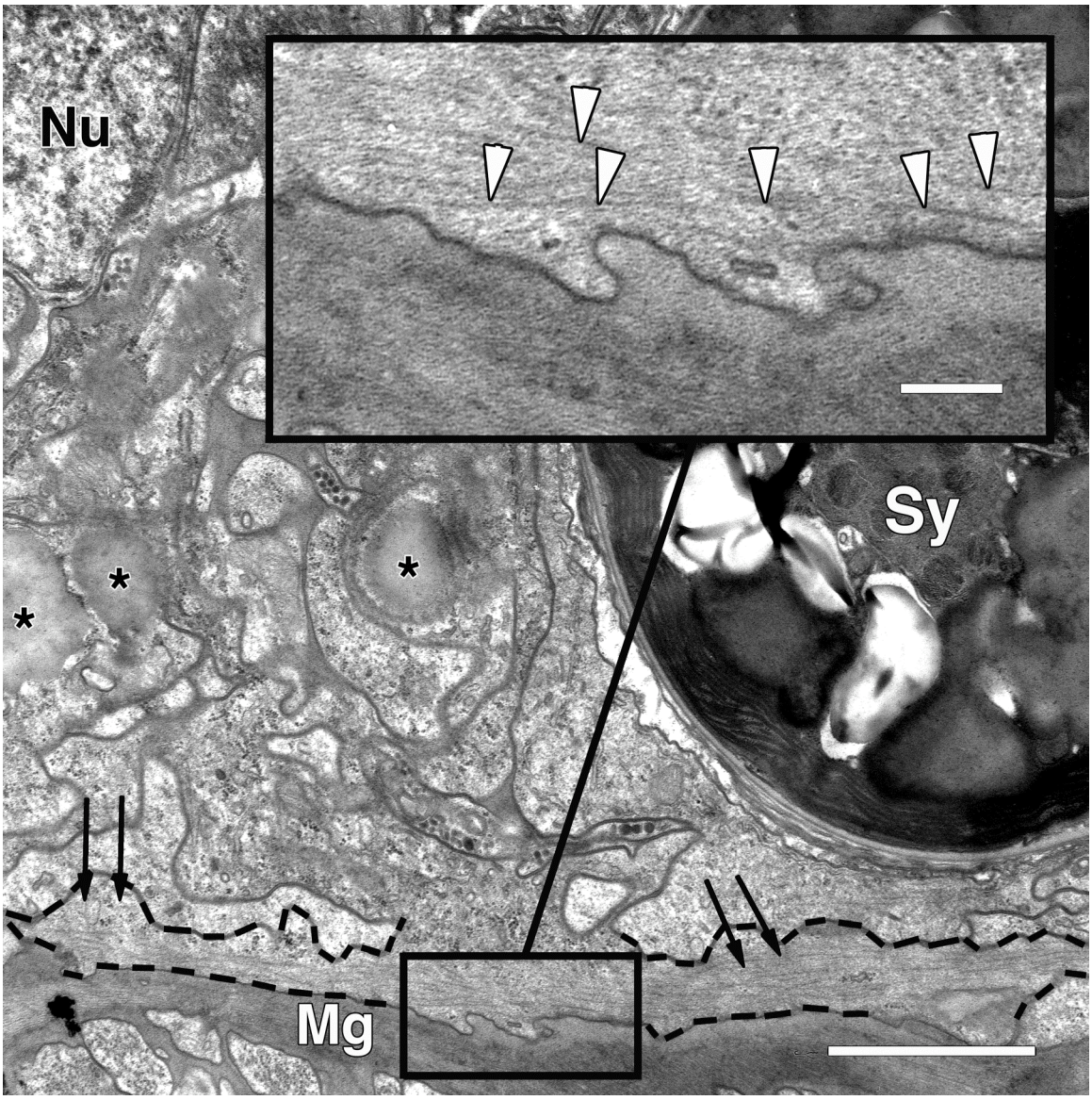

Figure 7. TEM: Transverse sections of symbiotic gastrodermal *Aiptasia pallida* tentacle tissues displaying a nutritive-muscular cell. Numerous nutritive-muscular cells were observed throughout the basal region of the gastrodermis. The processes of nutritive-muscular cell (visible portion outlined by the dashed lines) extend circumferentially (double arrows) and attach directly adjacent to the mesoglea (Mg). The inset provides higher magnification of the boxed region allowing visualization of the myofilaments (white arrowheads) that are present in the cytoplasm. Note: Asterisks indicate putative mucous-containing inclusions. Nu, nucleus; Sy, symbiont cell. Scale bar=2μm; inset:= 1μm.

A basal process clearly associated with a nutritive-muscular cell-containing symbionts was only observed in one instance (Fig. 8A,B). In this longitudinal section of tentacle, the base of the symbiont containing nutritive-muscular cell could be seen in direct contact with the mesoglea and no micro- or intermediate filaments were evident; unfortunately, the extent of

projection of the basal processes cannot be determined from this single section. Two different scenarios are possible. 1) The projections of symbiotic nutritive-muscular cells in *A. pallida* are reduced in length and musculature compared to the processes of non-symbiotic nutritive-muscular cells. 2) Gastrodermal cells that are capable of harboring symbionts may lack myofilaments or basal processes entirely. Without further ultrastructural analysis, the true morphology of these symbiont-containing cells remains uncertain.

Mesoglea

In anemones, and other cnidarians the mesoglea exists as an extracellular matrix that exhibits ultrastructural and molecular features similar to the extracellular matrix of vertebrates (Tucker et al., 2011). Previous studies revealed that the mesoglea of *Hydra* contains both striated (Davis and Haynes, 1968) and beaded (Weber and Schmid, 1985) fibrils, which are likely collagen (Zhang et al., 2007) and fibrillin (Megill et al., 2005). The mesogleal layer serves several purposes, including overall structural support and epithelial attachment (Wood, 1961) while facilitating movement of the body wall (Chapman, 1953). Basal processes of presumably non-symbiotic nutritive-muscular cells were commonly located adjacent to the mesoglea (Fig. 7). Immediate contact between nutritive-muscular cells and mesoglea has been reported in other cnidarians (Wood, 1961; Fautin and Mariscal, 1991) and was observed in *A. pallida* (Fig 8A, B).

Longitudinal sectioning of *A. pallida* tentacles revealed that numerous narrow projections of mesoglea also extend deeply between adjacent cells and cell processes in the gastrodermis (Fig. 8C, D). As such, the bases of gastrodermal cells and their processes appear to be embedded within a web-like system of mesogleal extensions, rather than simply attached to the mesoglea along their basal surface (Fig. 8C, D).

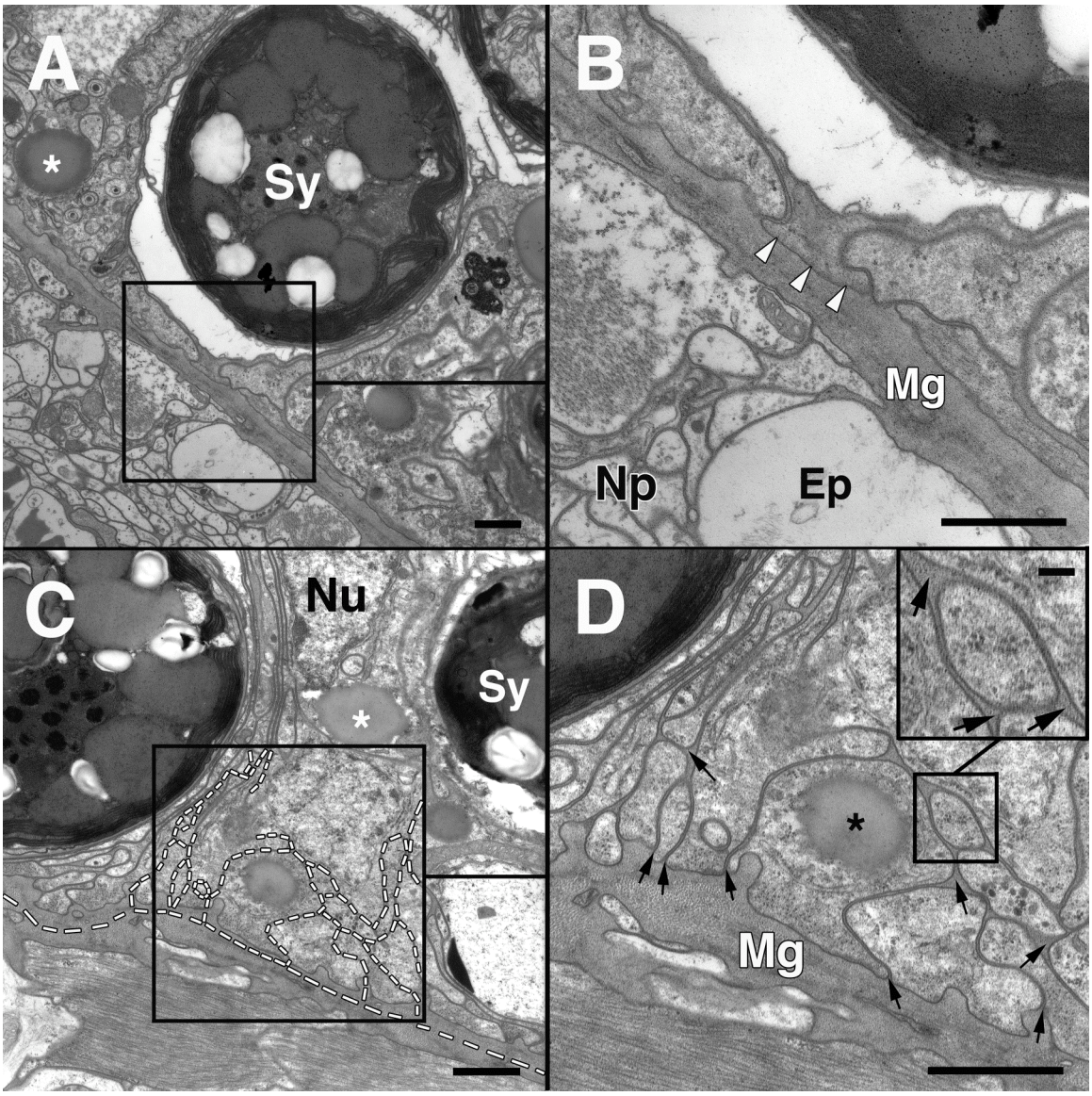

Figure 8. TEM: Transverse and longitudinal sections of symbiotic gastrodermal *Aiptasia pallida* tentacle tissues at the region of attachment to the mesoglea. A. Transverse section. Occasionally the attachment of a symbiotic nutritive-muscular cell to the mesoglea (Mg) could be observed. B. Higher magnification of the region where the symbiotic nutritive-muscular cell is directly adjacent to the mesoglea (arrowheads). The lateral processes of this cell appear to be possibly reduced in length compared to the processes of non-symbiont containing nutritive-muscular cells. C. Longitudinal section. Numerous projections of mesoglea extended between and around cells or cell processes as indicated by the white dashed lines. D. At higher magnification substantial portions of mesoglea could be seen surrounding each visible cell process (arrows). One large process containing a large granule (asterisk) was completely surrounded by a prominent layer of mesoglea. The inset shows a higher magnification view of another process surrounded by mesoglea (black arrows). Ep, epidermis; Np, nerve plexus; Nu, nucleus; Sy, symbiont cell. Scale bars=1μm; inset=0.25μm.

The mesoglea of *A. pallida* appeared almost exclusively as an acellular fibrous matrix throughout various regions of the tentacle (Fig. 3-7). However, the mesoglea appeared to be penetrated by adjacent cells on occasion (Fig. 9). Past studies have reported regions of mesoglea traversed by narrow cytoplamic processes (Wood, 1961). In this study, large portions of processes from adjacent cells protruded into the mesoglea (Fig. 9A,B). Such cellular processes occasionally appeared to cross the mesoglea and extend between cells of the opposite tissue layer (Fig. 9C, D). These extensions represent regions of contact between gastrodermis and epidermis.

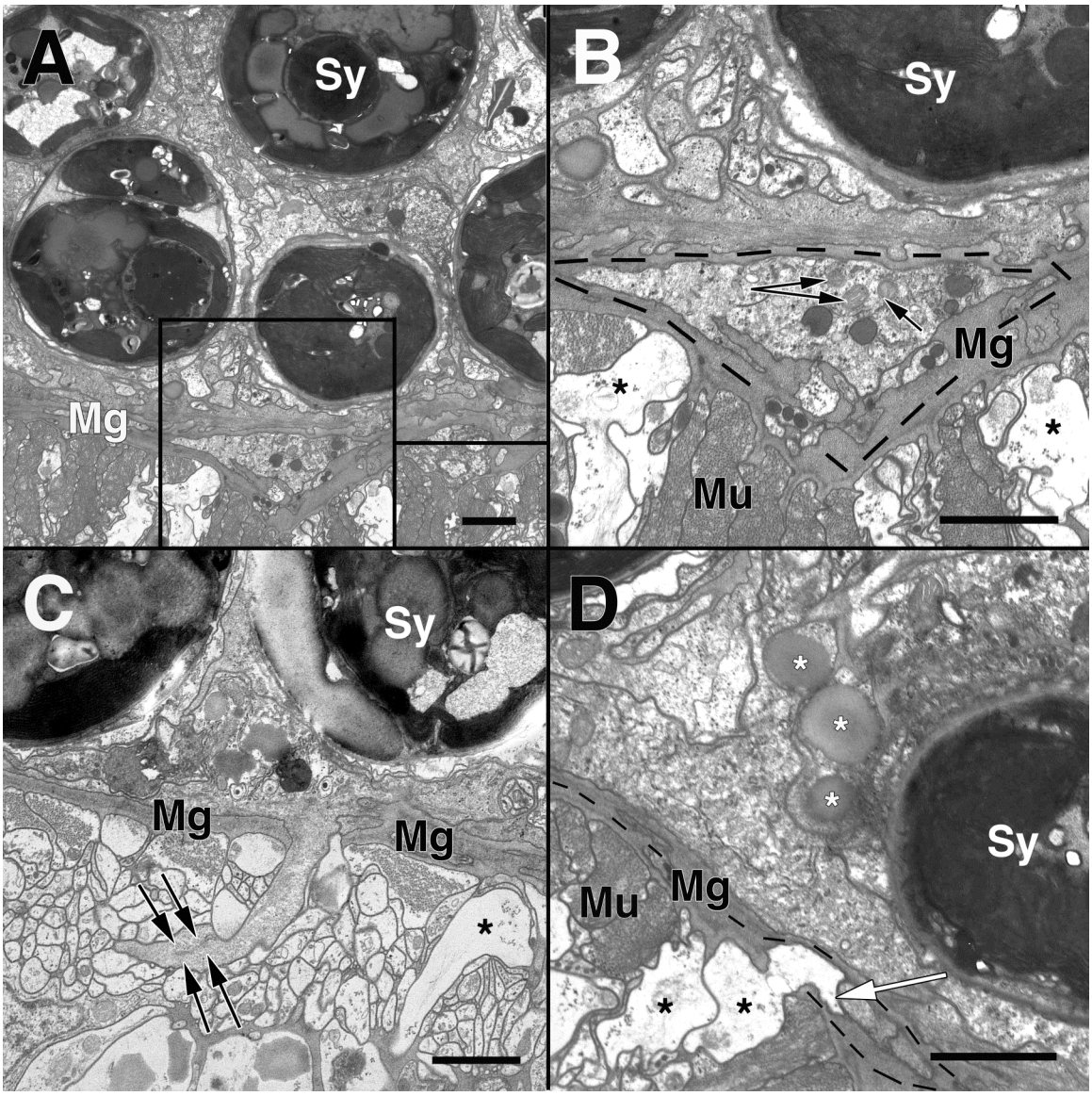

Figure 9. TEM: Transverse sections of symbiotic gastrodermal *Aiptasia pallida* tentacle tissues at the region of attachment to the mesoglea. A. Situations where the mesoglea (Mg) appeared to be interrupted by an adjacent cell were occasionally observed. B. At higher magnification, a cell process penetrates the mesoglea (indicated by the dashed line). The cellular process protruding into the mesoglea, appeared to be a portion of an adjacent gastrodermal cell based on its lack of myofilaments that would be characteristic of epithelia-muscular cells in the epidermis. The penetrating process contains various organelles, including vesicles and mitochondria (black arrows). C. Occasionally, an adjacent gastrodermal cell was observed crossing the mesoglea and extending deeply into the epidermis (double arrows). D. Less commonly, adjacent processes of epithliomuscular cells (indicated by black asterisks) appeared to extend across and into the mesoglea (indicated by dashed line) and directly contacting the gastrodermis (white arrow). Note: occasionally basal processes exhibited a vacuous appearance, which is likely due to the section cutting through a distal region of the process where the myofilaments no longer extend through the cytoplasm. Putative mucus-inclusions are indicated by white asterisks. Ep, epidermis; Mu, longitudinal smooth muscle; Nu nucleus; Sy, symbiont cell. Scale bars A-C=2 μm, D=1μm.

Epidermis

The epidermis is the most complex tissue layer in cnidarians and serves multiple functions for the organism, including defense and prey capture (Fautin and Mariscal, 1991). Several cell types can be found in the epidermis of *A. pallida*, and the cellular organization can be divided into specific regions according to cell type (Fig. 10).

Epitheliomuscular cells

The cells located in the closest proximity to the mesoglea (Zone I in Fig. 10) are columnar epitheliomuscular cells (Hyman, 1940; Chapman, 1974, Fautin and Mariscal, 1991). Epitheliomuscular cells are columnar cells that, like the presumptive non-symbiotic nutritive-muscular cells of the gastrodermis, exhibit muscular filaments that appear to be located within prominent longitudinal basal processes (Fig. 7). However, unlike nutritive-muscular cells, epitheliomuscular cells of the epidermis exhibit numerous myofilaments that are organized into 'bundles' (Fig. 11). These myofilaments make up longitudinal smooth muscle of the epidermis in the tentacles of *Aiptasia* spp. (Amerongen and Peteya, 1980) that works antagonistically against the circular muscle of the gastrodermis (Fautin and Mariscal, 1991). Longitudinal muscle appears stippled in cross section (Fig. 11A) and striated in longitudinal section (Fig. 11B). This appearance results from the presence of thick and thin myofilaments, which likely correspond to the presence of myosin and actin filaments, respectively, both of which have been previously documented in cnidarian muscle (Keough and Summers, 1976). In the epithelium, the myofilaments of epitheliomuscular cells are more far more dense and abundant than those found in the gastrodermis (Fig. 7), which likely form from numerous myofilaments stacking together as one contractile unit (Haynes, 1973).

Densely packed myofilaments concentrated in processes at the base of the cnidarian epidermis have been generally described as 'myonemes' in numerous studies (Hyman, 1940; Slautterback, 1967; Davis, 1973; Doumenc and Van-Praet, 1987; Fautin and Mariscal, 1991; Schick, 1991; Westfall et al., 1997; Brusca and Brusca, 2002; Westfall and Elliot, 2002; Tucker et al., 2011). It has also been suggested that the myofilament bundles (=myonemes) may function as independent muscle cells that are separated from adjacent epitheliomuscular cells (Hyman, 1940). In this study, myofilaments were arranged into well-structured bundles that extended through the longitudinally oriented processes located at the bases of epitheliomuscular cells (Fig. 10). Occasionally basal processes of epitheliomuscular cells exhibited a vacuous or 'empty' appearance, which is likely due to the section cutting through a distal region of the cell where the myofilaments no longer extend through the cytoplasm Fig 9A-D).

Nerve plexus/ Sensory structures

Cellular structures associated with the nerve plexus are typically observed directly adjacent and exterior to the bundles of epitheliomuscular cell processes and their contained myofilaments (Zone II in Fig 10). The nerve plexus of the epidermis is more extensive than the gastrodermis (Westfall and Elliot, 2002; Fig. 6) and appears as a complex network of neurites (Fig. 10 and 11). These neurites can be ganglionic or sensory in origin but cannot be distinguished (Westfall and Elliot, 2002).

Clear evidence has been provided in previous investigations of chemical synapses in the epidermal nerve plexus of several anthozoans (Westfall, 1970; Westfall and Elliot, 2002), including *A. pallida* (Westfall et al., 1998, 1999, 2001; Westfall and Elliot, 2002).

However, the overall organization of the nerve net and how muscle contraction is modulated in sea anemone tentacles remains misunderstood (Westfall and Elliot, 2002) and needs further investigation.

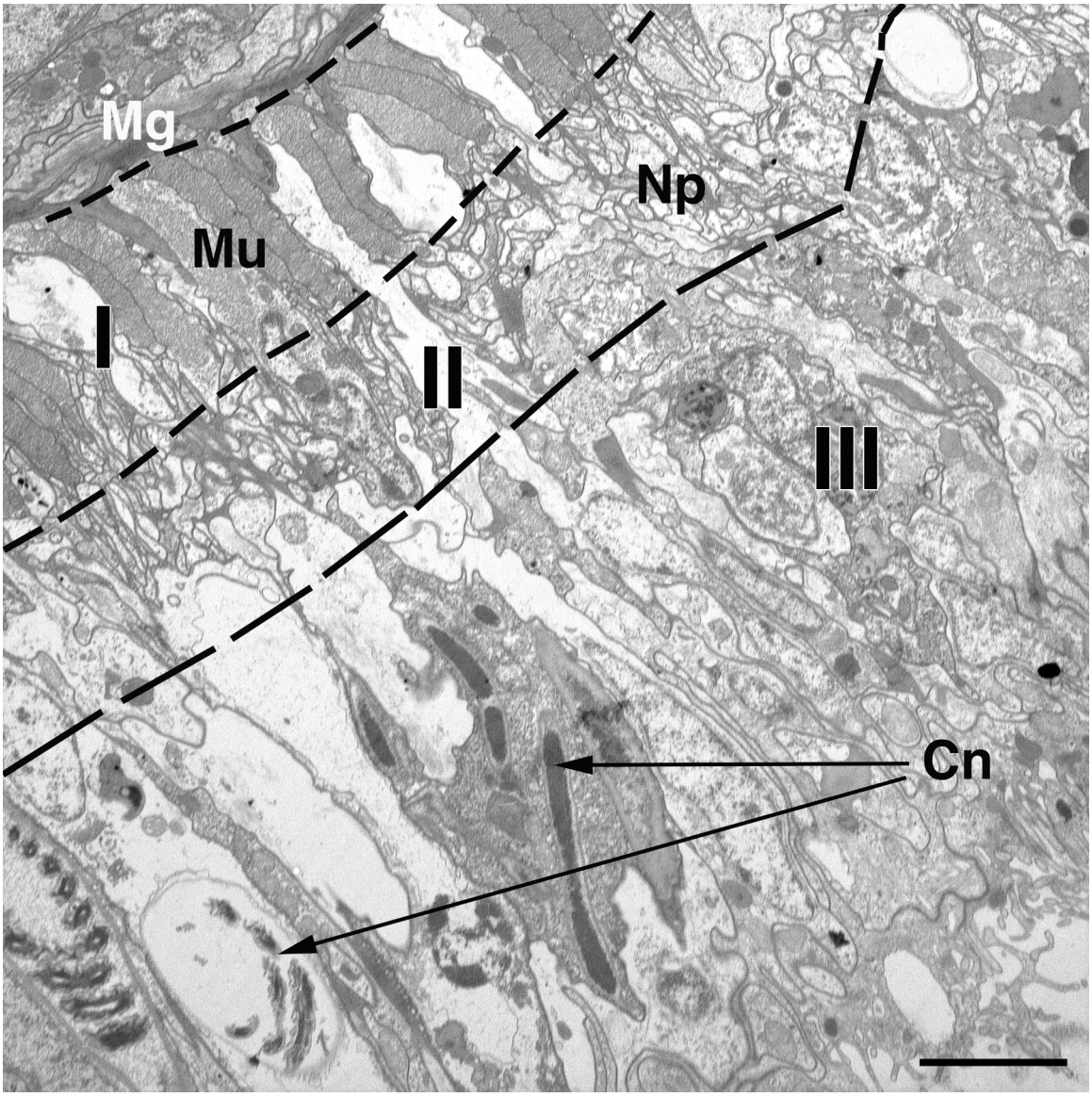

Figure 10. TEM: Transverse sections of symbiotic epidermal *Aiptasia pallida* tentacle tissues. Several cellular structures were observed throughout the epidermis that can be organized within specific zones based on their general location. In Zone 1, longitudinal smooth muscle (Mu) projects from epitheliomuscular cells directly adjacent to the mesoglea. In Zone 2, the nerve plexus (Np) is located directly adjacent to the muscle cells. Zone 3 consitutes the remaining breadth of the epithelium, where various cnidae (Cn) and other specialized cells are located. Scale bar=3μm.

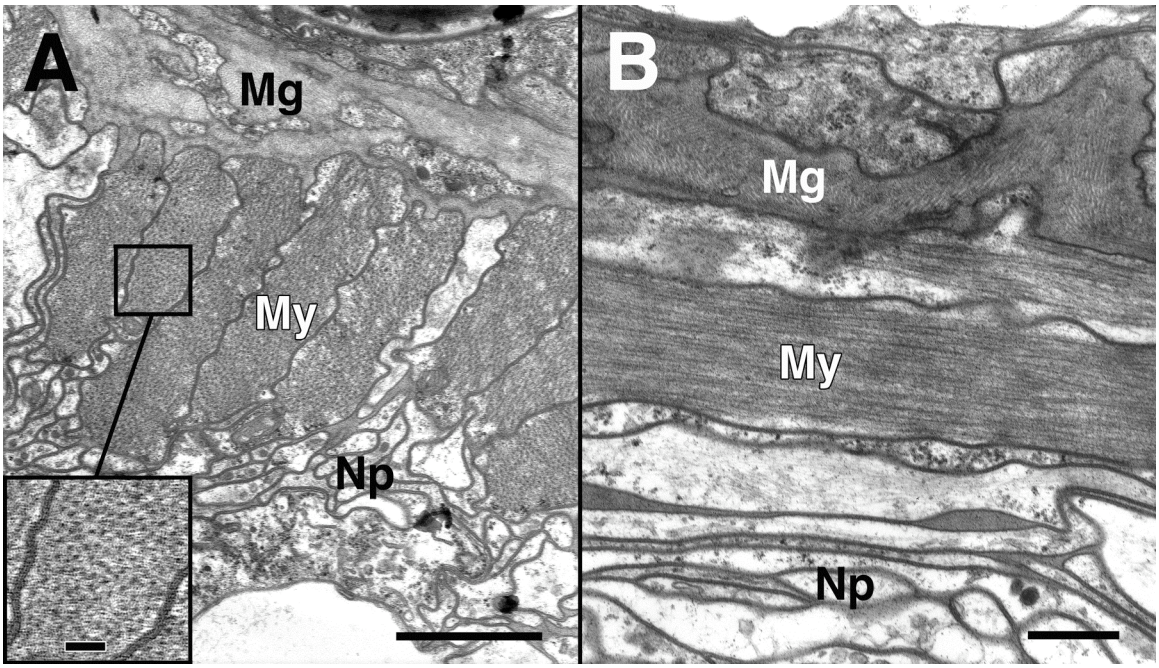

Figure 11. TEM: Transverse and longitudinal sections of symbiotic epidermal *Aiptasia pallida* tentacle tissues displaying longitudinal muscle cells. A. Transverse section showing densely packed myofilaments (My) longitudinally oriented within basal processes of numerous epitheliomuscular cells adjacent to the mesoglea (Mg). High magnifacation of a process allows visualization of individual densely packed thick and thin filaments (inset) The nerve plexus (Np) often appeared as small clear cell processes located immediately adjacent to the muscular processes. B. Longitudinal section showing the orientation of My running parallel to the neurites of the Np. Scale bars A=1μm; inset=0.25μm, B=1μm.

Cnidae

Additional cell types were distributed throughout the remaining breadth of the epithelium (Zone III in Fig. 10) where various cnidae and other specialized cells are located (Fig. 10). Cnidae serve as the diagnostic characteristic for the phylum and come in several forms based on function and morphology. All cnidae are encapsulated in a sheath or tube that is everted upon physical or chemical stimulation (Fautin and Mariscal, 1991). Depending on the type of cnida, the tubule may deliver a toxin, entangle an object, or stick to a prey item (Fautin and Romano, 1997). There are three major types of cnidae: spirocysts, nematocysts, and ptychocysts, but only the former two have been described in *A. pallida* (Westfall et al., 1998). Both spirocysts and

nematocysts were identified in this study (Fig. 12A,B), but the most prominent type observed in tentacle sections was the spirocyst (Fig. 12A,B). When discharged, these adhere to prey or adjacent substratum and are only known to occur in Anthozoa (Fautin and Mariscal, 1991). Spirocysts appeared as a spiral tubule within an elongated capsule that was housed within a hollow spirocyte (Fig. 12A,B), similar to those described by Westfall (1998). Alternatively, the epidermis of *A. pallida* also contains nematocysts (Fig. 12A,B), which are the "stinging" cnidae and typically display spines that latch onto prey or predator when everted and inject toxic venom (Fautin and Mariscal, 1991). Nematocysts are easily identified by their thick-walled capsules (Fig. 12B,C), which are basophilic (Kass and Scappaticci, 2002) and often impermeable to fixatives and thus, often obstruct the view of the internal spine (Westfall et al., 1998) (Fig. 12B). Cnidae are actually secreted by the golgi apparatus of specialized cells called 'cnidoblasts' (Watson, 1988), which were commonly observed in *A.pallida* epithelia (Fig. 12C). Thus, cnidae are not actually organelles, but, rather, the most complex secretory product known (Fautin and Romano, 1997). Typically, a cnidoblast cannot be identified as a nematocyst or spirocyst until a thick capsule becomes visible (Fig. 12C), which is suggestive of further differentiation into a nematocyst (Westfall et al., 1998).

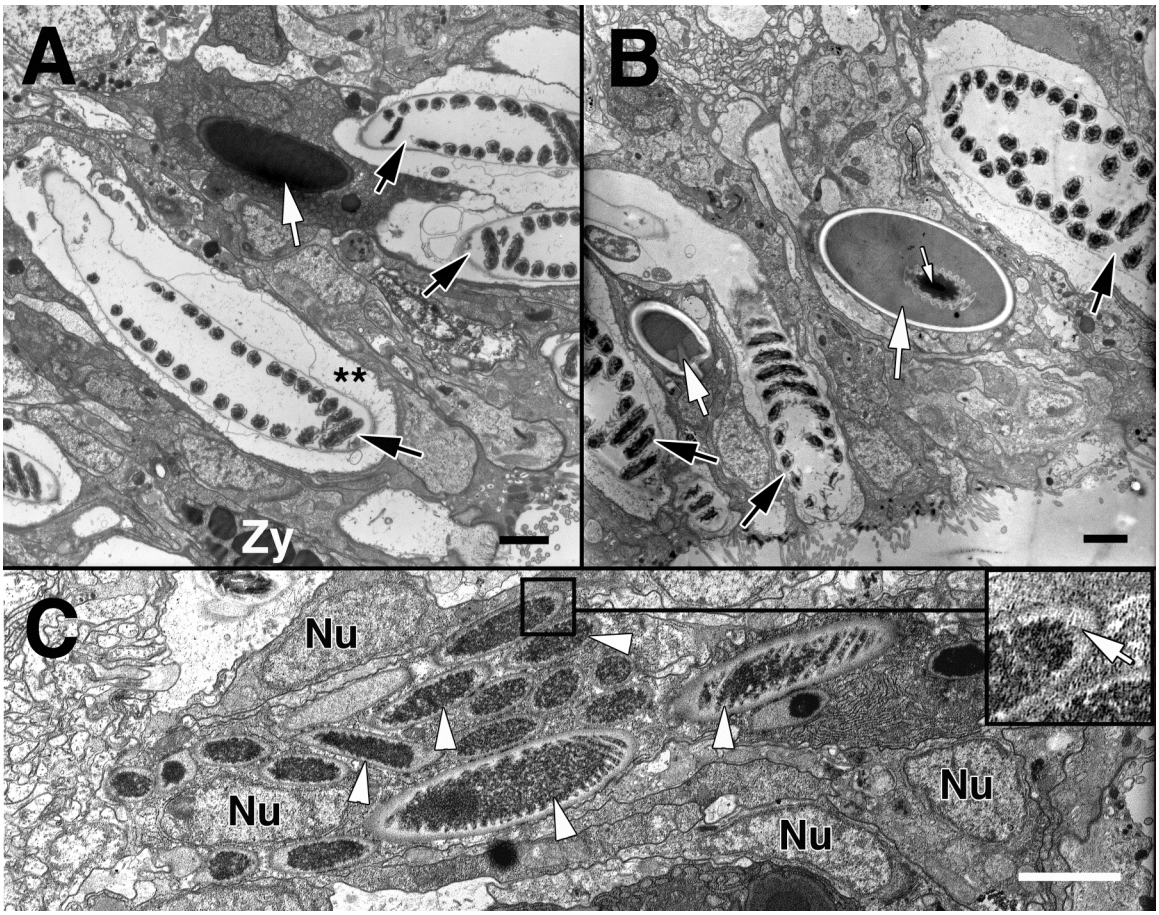

Figure 12. TEM: Transverse sections of symbiotic epidermal *Aiptasia pallida* tentacle tissues displaying various cnidae. A. Numerous nematocysts (white arrows) and spirocysts (black arrows) were observed throughout the epidermis, the latter being the most common. Spirocysts appeared as a spiral tubule within an elongated tube, which was housed within a hollow spirocyte (indicated by the double asterisks). B. The thick walled capsules of nematocysts were commonly observed, and occasionally the internal spined tube could also be visualized (small white arrow). C. Cnidoblasts (white arrowheads) were also commonly observed in epidermal tissues. Those developing into nematocysts were often identified based on the presence of the forming thick capsule (inset, white arrow). Numerous cnidoblast nuclei (Nu) were often observed in the region where developing cnidoblasts were present. Zy, zymogen granules. Scale bars =2μm.

Sensory structures in the epidermis and gastrodermis

Sensory cells and their associated structures were also occasionally observed (Zone III in Fig. 10) in both the gastrodermis and epidermis of *A. pallida* (Fig. 13). Sensory cells were most commonly identified based on the presence of an apical cone of stereovilli that surrounded a central cilium that extended beyond the microvilli of adjacent cells (Fig. 13A). In this study, stereovillar cones and their associated sensory cilium were most often observed in regions

nearby an epidermal nematocyte. This would suggest that they may function in nematocyst discharge in *A. pallida* as has been shown in other anthozoans (Mariscal and Bigger, 1976; Mariscal, et al. 1978). Apical ciliary cone is the term used to refer to this ciliary-nematocyte receptor complex that is unique to anthozoans and that are conspicuous in their lack of a cnidocil, or hair-like trigger on the nematocyte (Kass and Scappaticci, 2002); however, this term is also used to reference non-nematocyte associated sensory cells (Fautin and Mariscal, 1991). It should be noted that the stereovilli of the sensory and sometimes adjacent cells actually form the cone-like structure that surrounds the central cilium originating from the sensory cell.

Within the epidermal nerve plexus of *A. pallida*, various types of neural synapses have been documented, including neuron-spirocyte (Westfall et al., 1999), neuron-nematocyte (Westfall et al., 1998) and neuron-muscular synapses (Westfall and Elliot, 2002). Previous studies have shown that ciliary-nematocyte receptor complexes may be formed entirely by the cilia and microvilli of the nematocyte itself or may include projections of supporting cells that surround the nematocyte (Kass and Scappaticci, 2002). The latter scenario is similar to the sensory cell observed in the epidermis in this study (Fig. 13A), since it appears that at least some of the stereovilli that are contributing to the cone-like structure belong to adjacent supporting cells.

The cross-sectioned stereovilli and central cilium in Fig. 13B displays a similar appearance, where it there is a central large cilium surrounded by several stereovilli. These stereovilli were unique in their appearance in that they appeared to have remained directly apposed to the central cilium and partially connected to the adjacent tissue. Similar structures have been previously reported in anthozoans in both sensory cells and phagocytic cells of the gastrodermis (Fautin and Mariscal, 1991). Further sectioning is necessary to determine whether

the morphology of the putative ciliary cone in 13B from the gastrodermis is similar to that which we observed in the epidermis. Additionally, with semi serial sectioning of a complete sensory cell receptor complex it would be possible to determine a significant amount of information about signal transduction in anthozoan sensory cells.

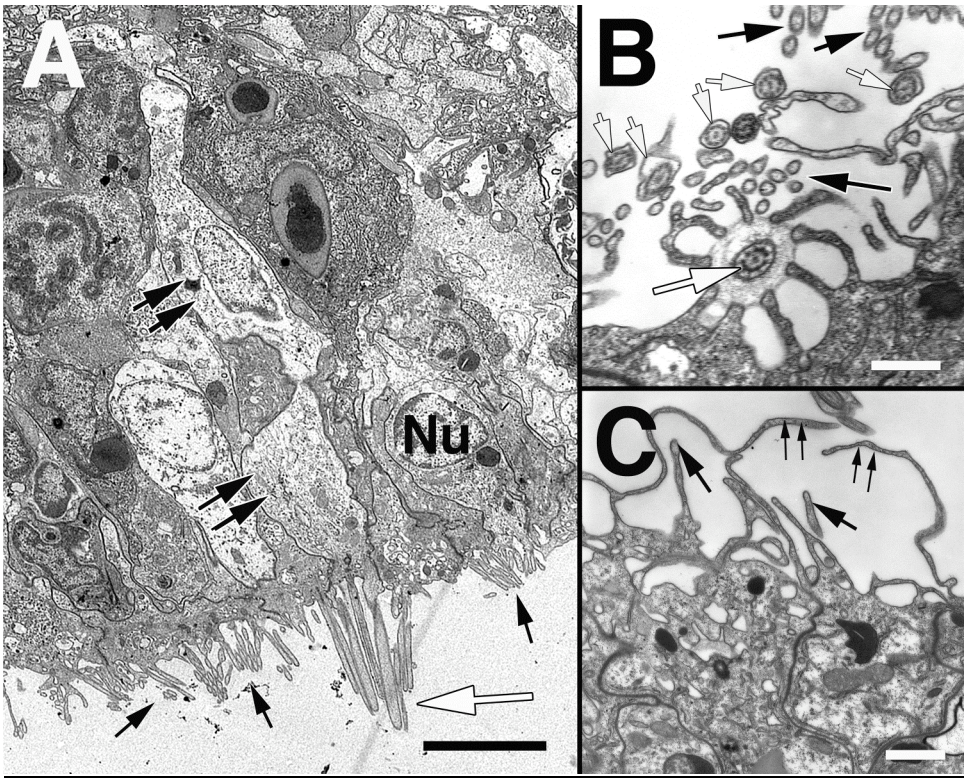

Figure 13. TEM: Transverse sections of symbiotic epidermal (A) *Aiptasia pallida* tentacle tissues displaying a sensory cell and associated structures. A. A putative sensory cell (double black arrows) was observed in the epidermis that displayed an apical ciliary cone (large white arrow) that protruded out past the microvilli (black arrows) of adjacent cells. This cell extended through the length of the epidermis (double arrows). The apical ends of most epidermal cells displayed numerous microvilli (black arrows). B. Several cilia (small white arrows) were also commonly observed at the apical end of many gastrodermal cells along with numerous smaller microvilli (black arrows heads). Occasionally, a cross-sectioned modified cilum would be seen surrounded by several directly adjacent stereovilli. This appears to be a cross-section of an apical ciliary cone in the gastrodermis. C. In the gastrodermis, many cells displayed numerous microvilli (black arrows) as well as what appear to be long thin stereovilli (double arrows) that projected into the gastrovascular cavity. Nu, nucleus. Scale bars A=1μm, B=0.5μm

Bacterial aggregates

Cyst-like aggregations of bacteria were observed in the epidermis of healthy symbiotic *A. pallida* (Fig. 14) similar to what has previously been described in this species by Palinscar (1989). In both the previous study as well as the current investigation, the bacteria appeared packed closely together within a large single vacuole (Fig. 14A). Higher magnification of the bacteria within the cyst revealed that they contained numerous vacuoles and central nucleoids (Fig. 14B). Palinscar and colleagues (1989) determined the identity of identical-looking bacteria to be *Vibrio,* which have been reported to cause disease outbreaks in sclearactinian anthozoans. Endosymbiotic bacteria have often been documented in cells of a variety of organisms, including cnidarians (Margulis et al., 1978; Thorington et al., 1979). Our observation of bacterial cysts provides further evidence that *A. pallida* can be 'infected' by bacterial communities; however, whether this association is parasitic or mutualistic remains to be determined. Future investigations would benefit by considering the role of bacterial symbioses when measuring the cellular or molecular responses of any metazoan.

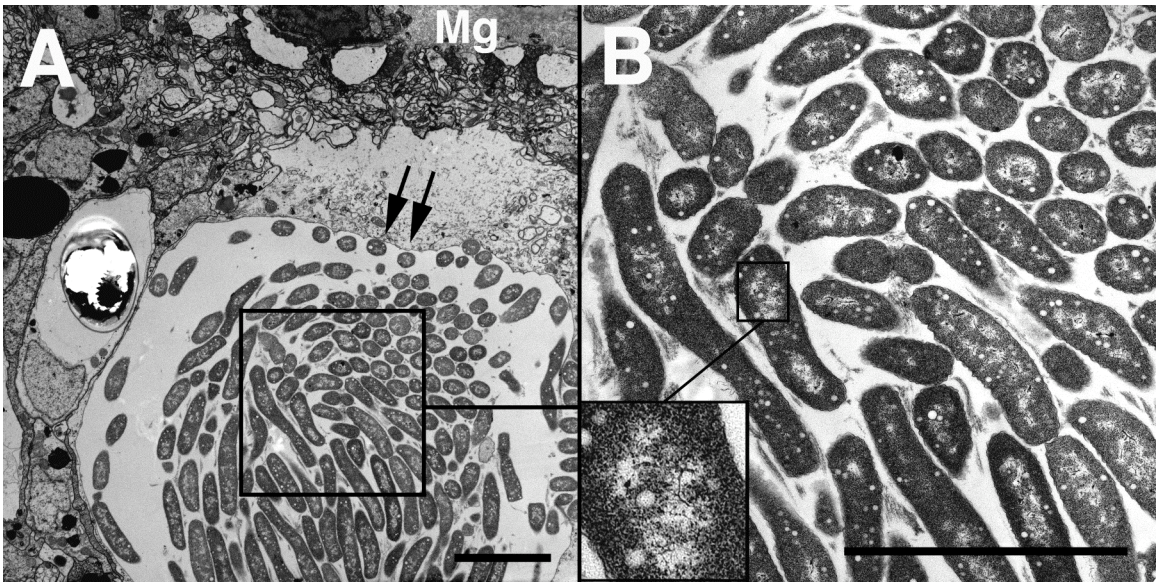

Figure 14. TEM: Transverse sections of symbiotic epidermal *Aiptasia pallida* tentacle tissues displaying a bacterial cyst. A. A bacterial cyst-like aggregate (double arrows) was observed in the epidermis of an otherwise healthy symbiotic anemone. B. Higher magnification of the bacteria within the cyst revealed that they contained numerous vacuoles and central nucleoids (inset). Mg, mesoglea. A. Scale bars A=5μm, B=0.5μm.

Conclusions

A thorough examination of host symbiotic *A. pallida* tentacle tissues revealed several interesting results that contradict previous ultrastructural studies. For example, in contrast to earlier descriptions of the mesoglea as an acellular layer to which epithelial cells exhibit simple basal attachment (Gates et al., 1992), our results suggest that the mesoglea functions as a complex network of collagenous substrate that is basally entangled with the cells and cell processes of the gastrodermis.

The gastrodermal-mesogleal interface has been an important area of interest since Gates *et al.* (1992) proposed "host cell detachment" as a potential cellular bleaching mechanism. Evidence of host cell detachment was originally documented in cold-shocked (12^{o}C) and thermally stressed (32 ^{o}C) *Aiptasia pulchella* and *Pocillopora damnicornis*, where it appeared that entire host cells containing intracellular symbionts detached from the mesoglea and were

expelled as a result of stress induced-cell adhesion dysfunction. Our observations, suggest that the complex entanglement of gastrodermal cells, cell processes and the mesoglea observed in symbiotic *A. pallida* make simple basal separation of symbiont containing cells from the mesoglea an unlikely mechanism for bleaching in this species. The entanglement would make the simple release of cells from the mesoglea very difficult. Alternatively, it is possible that during severe cellular stress, symbiotic host cells remain basally anchored to the mesogleal network, but undergo extensive cellular degradation. When structural integrity significantly declines, a portion of the deteriorated host cell may become detached apically along with the intracellular symbiont and symbiosome in an apocrine-like apical detachment mechanism and be expelled into the gastrovascular cavity (Chapter 3). During this process, the remaining host gastrodermal cell maintains its entangled connection to the mesoglea that prevents it from detaching along with the apical portion. The work of Gates *et al.* (1992) consisted of a few ultrastructural snapshots of degrading tissues of *A.pallida* and *P. damicornis*, whereas a subsequent study by Brown *et al*. (1995) used the light microscope and histological techniques in determining that whole cell detachment occurred. Our results suggest that previous descriptions of host cell detachment (Gates et al., 1992; Brown et al., 1995) may be in need of revision and would benefit from a more in depth ultrastructural re-examination of bleaching in the species and conditions used in those earlier studies.

Increased mass mortality bleaching events are predicted to occur in the future (Hoegh-Guldberg, 1999; Donner et al., 2007). Thus, having detailed ultrastructural information of a tractable symbiosis model is critical if we wish to understand the cellular mechanisms that underlie the bleaching response. This investigation provides an ultrastructural analysis of tentacle tissues in healthy, unstressed examples of the model symbiotic anemone, *A. pallida.* The cellular

information provided here can be used as a baseline against which the health of the *Aiptasia* model system can be assessed as it is manipulated in the lab or in the field.

III. Host autophagic degradation and associated symbiont loss occur in response to heat stress in the symbiotic anemone, *Aiptasia pallida*.

Abstract

Coral bleaching involves the loss of essential, photosynthetic dinoflagellates (*Symbiodinium* sp.) from host gastrodermal cells in response to temperature and/or light stress conditions. Although numerous potential cellular bleaching mechanisms have been proposed, there remains much uncertainty regarding which of them occur during early breakdown of the host-dinoflagellate symbiosis. In this study, transmission electron microscopy was utilized to conduct a detailed examination of symbiotic tissues of the tropical anemone *Aiptasia pallida* during early stages of host stress. Bleaching was induced by exposing specimens to a stress treatment of 32.5±0.5^{o}C at 140 ± 5 μmol photons $m^{-2}s^{-1}$ light intensity for 12 h followed by 12 h at 24±0.5^{o}C in darkness repeated over a 48 h period. Ultrastructural examinations revealed numerous dense, autophagic structures and associated cellular degradation in tentacle tissues after ~12 h of stress treatment. Anemones treated with rapamycin, a known autophagy inducer, exhibited the same ultrastructural characteristics as heat stressed tissues, confirming that the structures observed during heat stress treatment were autophagic. Additionally, symbionts appeared to be expelled from host cells via an apocrine-like detachment mechanism from the apical ends of autophagic gastrodermal cells. This study provides the first ultrastructural evidence of host autophagic degradation during thermal stress in a cnidarian system and also supports earlier suggestions that autophagy is an active cellular mechanism during

early stages of bleaching.

Introduction

Coral reefs are one of the most productive and economically valuable ecosystems on Earth, providing numerous services to people worldwide (N.O.A.A., 2011). However, coral abundance and diversity have dramatically declined over the past few decades as a result of growing anthropogenic pressures (Donner et al., 2007). Although a wide variety of environmental stressors currently threaten corals, one of the primary causes of large-scale reef degradation is mass mortality bleaching events that have been linked to global climate change and associated elevated sea surface temperatures (Hughes, 2003; Hoegh-Guldberg et al., 2007). Coral bleaching occurs as a stress response during periods of elevated temperature and irradiation. This results in loss of intracellular dinoflagellates from the genus *Symbiodinium* (Freudenthal, 1962) from host tissues and/or degradation of symbiont photosynthetic pigments (Hoegh-Guldberg, 1999; Fitt et al., 2001), producing a whitened appearance to the host as the underlying calcareous skeleton is exposed through translucent coral tissue. Significant reductions in symbiont densities often lead to reduced growth and fitness of the host as well as increased disease susceptibility (Kushmaro et al., 1997; Harvell et al., 1999; Hoegh-Guldberg, 1999). Ultimately, if new symbionts are not re-established within a small window of time, death of the coral host will occur (Brown, 1997; Hoegh-Guldberg, 1999).

Collapse of the coral-dinoflagellate symbiosis is initiated with increased production of damaging reactive oxygen species (ROS) that occurs during temperature and light stress (Lesser, 1996; Franklin et al., 2004). Elevated ROS concentrations have been shown to decrease photosynthetic capability of symbionts through photoinhibition and damage to photosystem II

(PSII) (Warner et al., 1999; Lesser, 2006). Also, as a result of host mitochondrial membrane damage, high levels of ROS have been shown to diffuse into host cell cytoplasm (Nii and Muscatine, 1997; Dunn et al., 2012), where they can directly damage host membranes, proteins (Richier et al., 2005), and DNA (Lesser and Farrell, 2004).

Although coral bleaching has been extensively studied for the past few decades, there remains a great deal of uncertainty regarding which cellular events occur during a natural bleaching episode (Weis, 2008). Microscopic examinations of both natural and experimentally manipulated bleaching tissue have yielded a wide variety of descriptions of potential cellular bleaching mechanisms that have been covered in several reviews (Gates et al., 1992; Douglas, 2003; Lesser, 2004; Weis, 2008). These include exocytosis (Steen and Muscatine, 1987), host cell detachment (Gates et al., 1992; Sawyer and Muscatine, 2001), and *in situ* degradation (Taylor, 1973; Brown et al., 1995; Ainsworth and Hoegh-Guldberg, 2008), as well as multiple forms of ROS-mediated cell death in the form of apoptosis (Dunn et al., 2002; 2004; 2007; Franklin et al., 2004; Strychar et al., 2004; Richier et al., 2006; Ainsworth et al., 2008; Strychar and Sammarco, 2009; and Tchernov et al., 2011) and necrosis (Glynn et al., 1985; Dunn et al., 2002; 2004; Strychar et al., 2004; Ainsworth et al., 2008; Strychar and Sammarco, 2009). Most recently, an additional form of cell death, resulting from autophagy, has been implicated as an active mechanism of symbiont loss (Dunn et al., 2007; Downs et al., 2009). The autophagic process functions to isolate old or damaged proteins and/or organelles by isolating them within membrane-bound autophagosomes and degrading the contents for recycling. An alternative form of autophagy, called 'symbiophagy', has been reported in a thermally-stressed coral, *Pocillopora damicornis*, whereby the symbionts themselves were digested within their host-derived symbiosomes (Downs et al., 2009).

The variation among previously described cellular bleaching investigations likely results from several factors. First, microscopical observations have been made in numerous different anthozoan host-symbiont complements under a wide range of environmental bleaching conditions, including methods such as cold shock (e.g., Gates et al., 1992), which is less commonly observed in the natural environment. Second, much emphasis has been placed on the stress response of the symbiont during bleaching rather than that of the host (Baird et al., 2008; Weis, 2008). However, increasing evidence suggests that the host cellular response plays an important role in the bleaching process (Baird et al., 2008) and may precede that of the symbiont (Ainsworth et al., 2008; Dunn et al., 2012). Third, a majority of previous investigations have relied on 'snapshots' in time of stressed tissues (often without comparison to controls) as a basis for their histological interpretations, rather than a sequential examination of bleaching tissues throughout the process. Thus, much of our current information has been gained from brief glimpses of the bleaching response, particularly focusing on late stages in the process. As a result of these limitations, our current understanding of the cellular mechanisms of bleaching is far from complete (Weis, 2008). It has been suggested that in order to accelerate our understanding of cellular bleaching, a tractable model species, such as the symbiotic anemone, *Aiptasia pallida (*Agassiz in Verrill, 1864), should be utilized in experimental studies under naturally relevant environmental conditions (Weis et al., 2008).

In this study, we aim to elucidate some of the missing pieces of information surrounding the cellular bleaching process by conducting a thorough ultrastructural examination of host anthozoan tissues at multiple stages of the early stress response using the symbiotic anemone, *Aiptasia pallida*. Heat stress conditions were used to induce gradual bleaching, and ultrastructural changes were systematically analyzed and compared to unstressed, healthy control

animals. Results from this study provide a better understanding of how the anthozoan host responds during the early stages of a bleaching event and examines the role of autophagy in the host stress response during symbiont loss.

Materials and Methods

Culture conditions

Aiptasia pallida harboring symbionts typed as Clade A4 *Symbiodinium* (Santos et al., 2002; Scott Santos, pers. comm.) were collected in the Florida Keys and maintained in artificial seawater (Reef Crystals) at 28-30 ppt salinity. Anemones were kept in two 150 gal tanks at 24±1°C. The bottom of each tank, where most anemones were located, was ~ 1 m below a light source that covered the length of each tank. The light source consisted of two fluorescent light fixtures per tank that were each equipped with two 32W bulbs (Phillips F32T8/TL841) producing a 50±5 μmol photons $m^{-2}s^{-1}$ irradiance at the bottoms of the tanks. Lights were set on a 12:12 h light/dark regime. The anemones were fed freshly hatched *Artemia* nauplii three times per week.

Field seawater temperature determination

In order to approximate ecologically relevant bleaching conditions in this study, diurnal changes in surface water temperature were measured at the collection site in Key Largo, Florida using a standard ethanol thermometer at six regular daily intervals for 5 days. Average temperature values were calculated at 30±1°C during the day and 24±1°C at night. Stressed *A. pallida* were subjected to similar daily temperature changes with the daytime temperature adjusted to a value that would cause bleaching (as described below).

Bleaching conditions

Twelve medium sized anemones were placed in identical, individual dishes that contained ~200 ml 0.45 μm Millipore-filtered artificial aquarium sea water (MFAW) and allowed to acclimate for ~5 days at the ambient room temperature of 24±1° C with 50±5 μmol photons $m^{-2}s^{-1}$ ambient light intensity. Water in these dishes was changed daily and the anemones were fed once during the first 3 days. They were then held unfed for 48 h prior to the beginning of the experiments. Six anemones were then randomly selected and transferred in their containers to an incubator at 32.5±0.5° C and placed ~14 cm beneath two light fixtures each equipped with two 20W fluorescent bulbs (GE Ecolux F20T12/G50-ECO) that emitted 140±5 μmol photons $m^{-2}s^{-1}$ light intensity at the level of the anemones. The anemones were held in the incubator for 12 h and then removed to a dark, well-ventilated box on the lab bench for 12 h in darkness at 24±1° C. The incubator and dark box treatments were then repeated over the following 24 h for a total treatment time of 48 h. It took approximately 2.5 h for the 24±1° C dishes to warm to 32.5±0.5° C in the incubator under these conditions. This study primarily focuses on the effects of heat stress. There was a small difference in light intensity between the anemone culture tanks (50±5 μmol photons $m^{-2}s^{-1)}$ and the incubator (140±5 μmol photons $m^{-2}s^{-1}$); however, this is well within the field light intensities (0 to > 1000 μmol photons $m^{-2}s^{-1}$) that these symbiotic anemones experience and was not considered to be a stressor in our experiments. In order to test for effects of any ambient environmental factors, six additional anemones acclimated as described above were randomly selected as controls (no stress treatment) and were placed in the same type of dishes used for stressed anemones at 24±1°C with 50±5 μmol photons $m^{-2}s^{-1}$ irradiance for 12 h daily followed by 12 h in darkness over a 48 h period in a subsequent

experiment. In all cases water was changed daily and anemones were not fed during the 48 h treatment period.

Biochemical induction of autophagy

Anemones were maintained in their standard culture conditions at 24±1^{o}C and 50±5 μmol photons $m^{-2}s^{-1}$ irradiance with a 12:12 h light/dark regime. Several symbiotic anemones (n=6) were exposed to one treatment of 25 μM rapamycin (Sigma-Aldrich) in a solution of 1% DMSO in MFAW for 12 h (Dunn et al. 2007). Control anemones (n=6) were exposed to 1% DMSO in MFAW for 12 h under identical conditions.

Fixation, embedment and sectioning for TEM

Treatment anemones exposed to heat stress (0, 12, 24, or 48 h) or to 24 μM rapamycin (12 h) and control anemones exposed to no stress (0 and 48 h) and to 12 h of 1% DMSO were all prepared for TEM following the same protocol. First they were relaxed by removing the seawater from each anemone container and replacing it with ~300 mL high Mg/low Ca seawater (Audesirk and Audesirk 1980) for 30 mins, followed by the addition of ~ 2 mL chlorotone saturated seawater for 30 mins. Then a subset of tentacles (n=6) was clipped from each of 3 randomly selected anemones at each time point (stress treatments and controls). Tissues were fixed using methods similar to the protocol of Carroll and Kempf (1994) in Millonig's phosphate buffered, 2.5% gluteraldehyde fixative solution for 1 h followed by rinses with a 1:1 0.34M NaCl/Millonig's phosphate buffer solution. The tentacles were secondarily fixed in a 1.25% $NaHCO_3$ buffered, 2% OsO_4 solution for 1 h. Following secondary fixation, tentacles were rinsed three times in 1.25% $NaHCO_3$ buffer, dehydrated through an ethanol series to 100%

ethanol, transferred through 3 changes of propylene oxide, and infiltrated and embedded using EMbed 812 resin (Electron Microscopy Sciences). All treatments were carried out at room temperature (24±1°C). Embedded tentacles were sectioned (~60nm) using a diamond knife (Diatome) on a Reichert-Jung Ultracut E microtome. All sections were stained with uranyl acetate and lead citrate for transmission electron microscopy (TEM). Tissues were visualized and photographed in sections from mid-tentacle length and around the circumference of each tentacle using a Zeiss EM 10C 10CR transmission electron microscope. Negatives from TEM were scanned as positives on an Epson Perfection 3200 Photo flatbed scanner at 1200 dpi and contrast and levels were adjusted using Adobe Photoshop 8.0 (n=142).

A detailed ultrastructural examination of healthy, symbiotic, control *A. pallida* tentacle tissues from 0 and 48 h provided baseline data that were used for comparison to tissues exposed to various time periods of heat stress or to rapamycin treatment. Such comparisons allowed ultrastructural variations in stress and rapamycin treated tissues to be identified. The possible occurrence of cell death mechanisms, such as apoptosis and necrosis, was determined based on cellular ultrastructural characteristics specific for these mechanisms as reported for *A. pallida* and its intracellular symbionts (Dunn et al., 2002; 2004). Cells were considered apoptotic when they exhibited condensed chromatin with cell shrinkage and/or membrane blebbing, and in contrast, necrotic when the presence of lysed cellular material and/or cell swelling was observed (Dunn et al., 2002; 2004). Additionally, cells were determined to be autophagic if autophagy-derived structures (i.e. autophagosomes, autophagolysosomes, tertiary lysosomes, residual bodies) similar to those previously described in vertebrate (Hand, 1970; Fawcett, 1981; Holtzman, 1989; Jing and Tang, 1999; Nixon, 2007) and invertebrate (Kov et al., 2000; Rost-Roszkowska et al., 2008) tissues were observed in either host or symbiont cells. These structures

are commonly identified by the presence of cellular material at various stages of degradation within their membranes (Holtzman, 1989; Jing and Tang, 1999; Levine and Yuan, 2005; Nixon, 2007; Rost-Roszkowska et al., 2008).

Algal cell counts

In order to quantify symbiont loss resulting from stress-induced bleaching, expelled *Symbiodinium* cells were collected from both control and stressed anemone containers (n=3) after 48 h of treatment. For each anemone the collected algae were centrifuged, and then re-suspended in 250 ml of 0.45 μm MFAW. Cells were then counted with a Neubauer hemacytometer (according to Perez and Weis, 2006) and the average number of algal cells that were expelled per anemone after 48 h was calculated for controls and heat stress treatment anemones.

Statistical analysis

Significance of the difference in average number of expelled *Symbiodinium* cells/anemone after 48 h for both control and heat stress anemones was determined using a t-test at significance level of 5% (alpha=0.05) using SAS 9.2 software.

Results and Discussion

Examination of symbiotic anemone tentacle tissues prior to the heat stress treatment (at 0 h) revealed a healthy overall appearance (Fig. 15A-C) identical to that of control anemones at 0 and 48 h (Fig. 15D-E). In general, unstressed host tissues consisted of intact gastrodermal and epidermal cell layers separated by a thin layer of acellular mesoglea (Fig. 15A). The epithelial cells that make up each layer consistently exhibited a characteristically healthy cellular composition (Fautin and Mariscal, 1991; Shick, 1991) with a normal distribution of organelle types (e.g. nucleus, mitochondria, etc.) surrounded by abundant dense cytoplasm. In the cytoplasm of the epidermis, nematocyst capsules were often observed, appearing as capsule membrane surrounding dark, oval-shaped structures of varying size depending on the plane of section (Fig. 15B). In the gastrodermis, numerous epithelial cells harbored intact, healthy *Symbiodinium* cells within a host derived symbiosome membrane (Fig. 15A, C, E) (Wakefield and Kempf, 2001). In both tissue layers, electron dense lipid droplets were occasionally observed, which were easily recognized by their characteristic smooth and approximate circular or oval shape, homogeneous osmophilic appearance, and lack of a surrounding membrane (Fig. 15B). There was little or no evidence of apoptotic, necrotic or autophagic activity present in host or symbiont cells from control anemones or from treatment anemones prior to stress. However, *in situ* degradation of symbionts was occasionally observed in some sections.

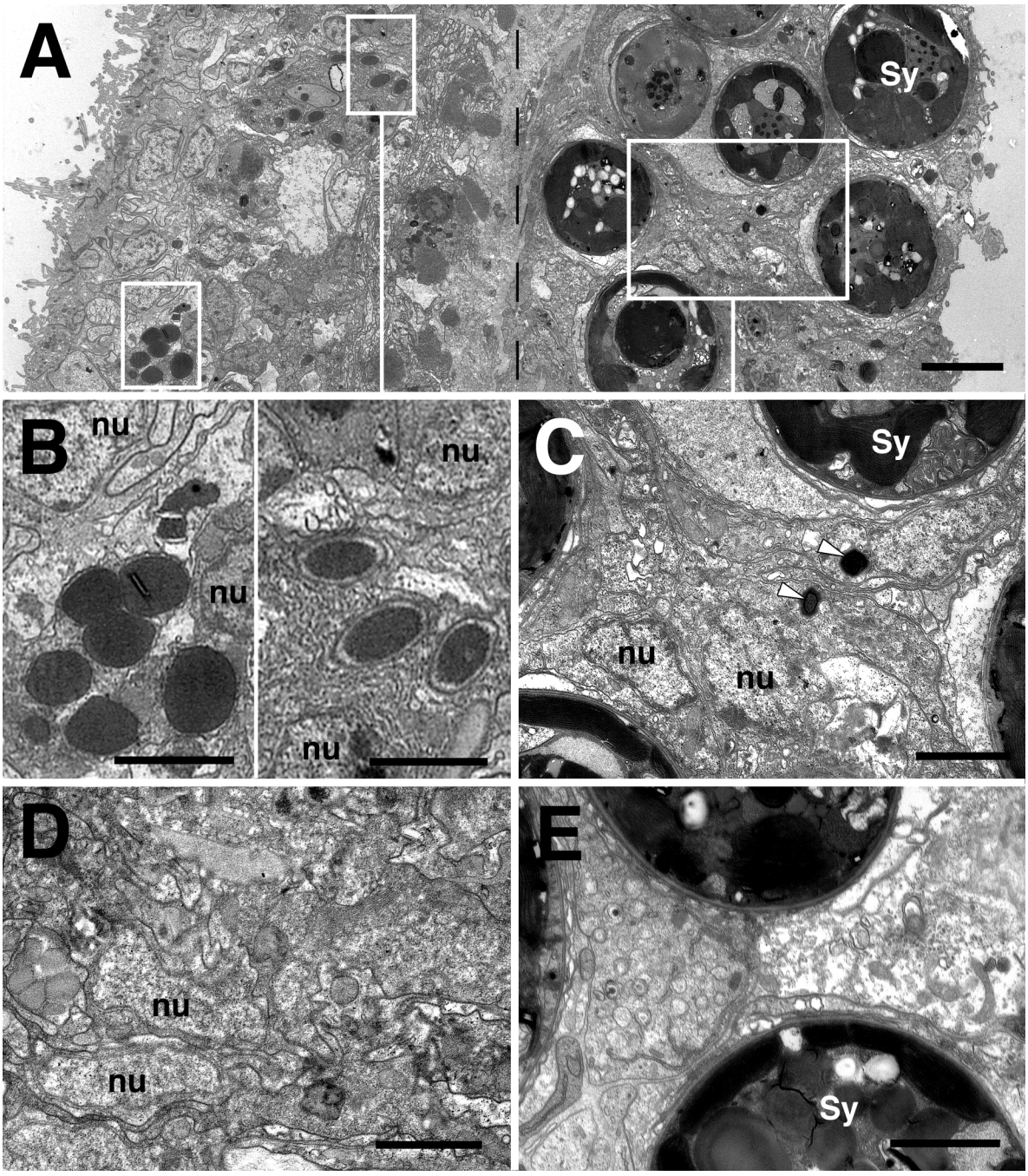

Figure 15: TEM: Transverse sections of control and unstressed treatment (t=0) symbiotic *Aiptasia pallida* tissues. A-C) Healthy unstressed tissues (0 h of heat treatment): A) Host cells exhibit a normal appearance with abundant dense cytoplasm in both gastrodermis and epidermis. In the cytoplasm, electron dense circular or oval structures were occasionally observed (boxed regions). Numerous intact *Symbiodinium* cells (Sy) were observed within host gastrodermal cells. B) Higher magnification of the epidermal tissue layer, showing homogeneous osmophilic appearance and regular shape of lipid droplets (left panel) and nematocyst capsules (right panel). C) Higher magnification of the gastrodermal tissue layer (large, right boxed region in A) showing the healthy condition of host cells. Two dark structures are indicated (white arrowheads with black border) that are likely small lipid droplets. D and E) Control (48 h at ambient temperature and irradiation) tissues for comparison: D - Epidermis and E - Gastrodermis. nu = host cell nucleus. Scale bars = 5 μm (A) and 2 μm (B-E).

The ultrastructure of anemone tissues changed dramatically after exposure to the heat stress treatment described above. Examination of stressed tissues starting at 12 h of treatment revealehd that both the gastrodermis and epidermis contained increasing numbers of electron dense, irregularly shaped cytoplasmic bodies that exhibited a heterogeneous appearance (Fig. 16) and were easily distinguishable from smooth, homogeneous lipid droplets. At higher magnification, it became apparent that these dense structures contained varying amounts of accumulated and/or partially digested cytoplasmic material (Fig. 16B-C), which is a characteristic of active autophagic structures (APSs). Other cell death activities, including apoptosis and necrosis (see methods) were infrequently observed in host and/or symbiont cells throughout the duration of heat stress. Additionally, no evidence of exocytosis of symbionts from host gastrodermal cells or of host cell detachment was observed; however, as in the controls (see above) *in situ* degradation of symbionts was occasionally observed in treatment tissues (see below).

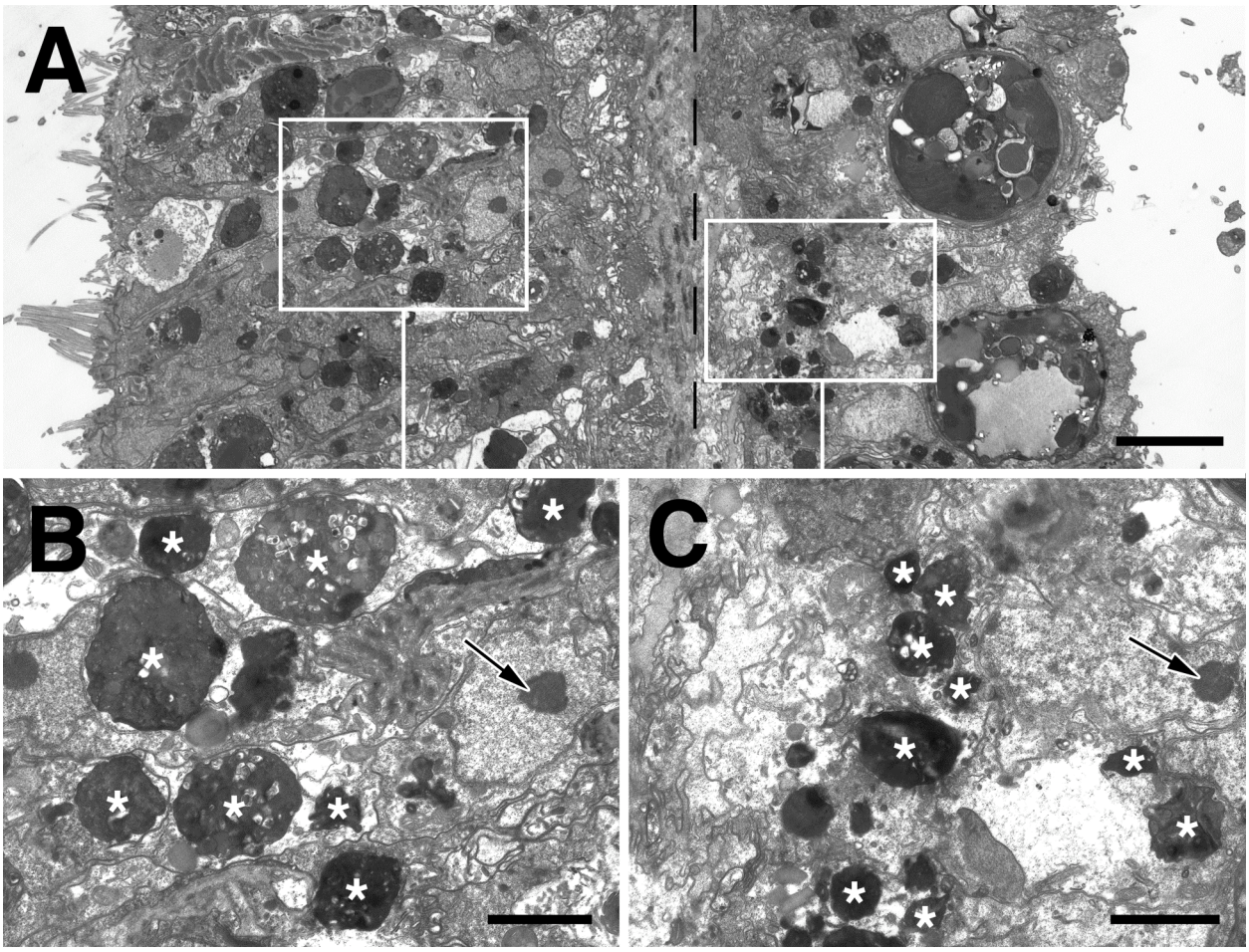

Figure 16: TEM: Transverse sections of symbiotic *Aiptasia pallida* tissues after 48 h of exposure to heat stress. A) Host tissues exhibit numerous dense APSs throughout both the gastrodermis and epidermis. B) Higher magnification of the epidermis where sequestered and partially digested cellular materials can be seen within large APSs (indicated with asterisks). C) Higher magnification of the gastrodermal tissue layer with smaller but similar APSs (indicated with asterisks) that also have a heterogeneous appearance. Nucleoli are indicated in B and C (black arrow with white outline) within host nuclei for comparison. Scale bars = 5 μm (A) and 2 μm (B, C).

The observed APSs varied in their appearance as they progressed through several stages of development, (Fig. 17). These include 1) initial formation of a characteristic 'cup-like' pre-autophagosome structure (Fig. 17A), 2) sealing of pre-autophagosomes and early sequestration of surrounding cytoplasmic and organellar materials for digestion (Fig. 17B), and 3) further sequestration/digestion of contents and retention of indigestible material forming electron dense APSs (Fig. 17B-D). Autophagic degradation within cells and their processes resulted in regions with sparse cytoplasm and numerous dense APSs (Fig. 17D). Both 'young' and 'mature'

(electron dense) APSs were often observed in what appeared to be the active sequestration of cellular materials (note invagination of several APSs - double asterisks, in Fig. 17B-D).

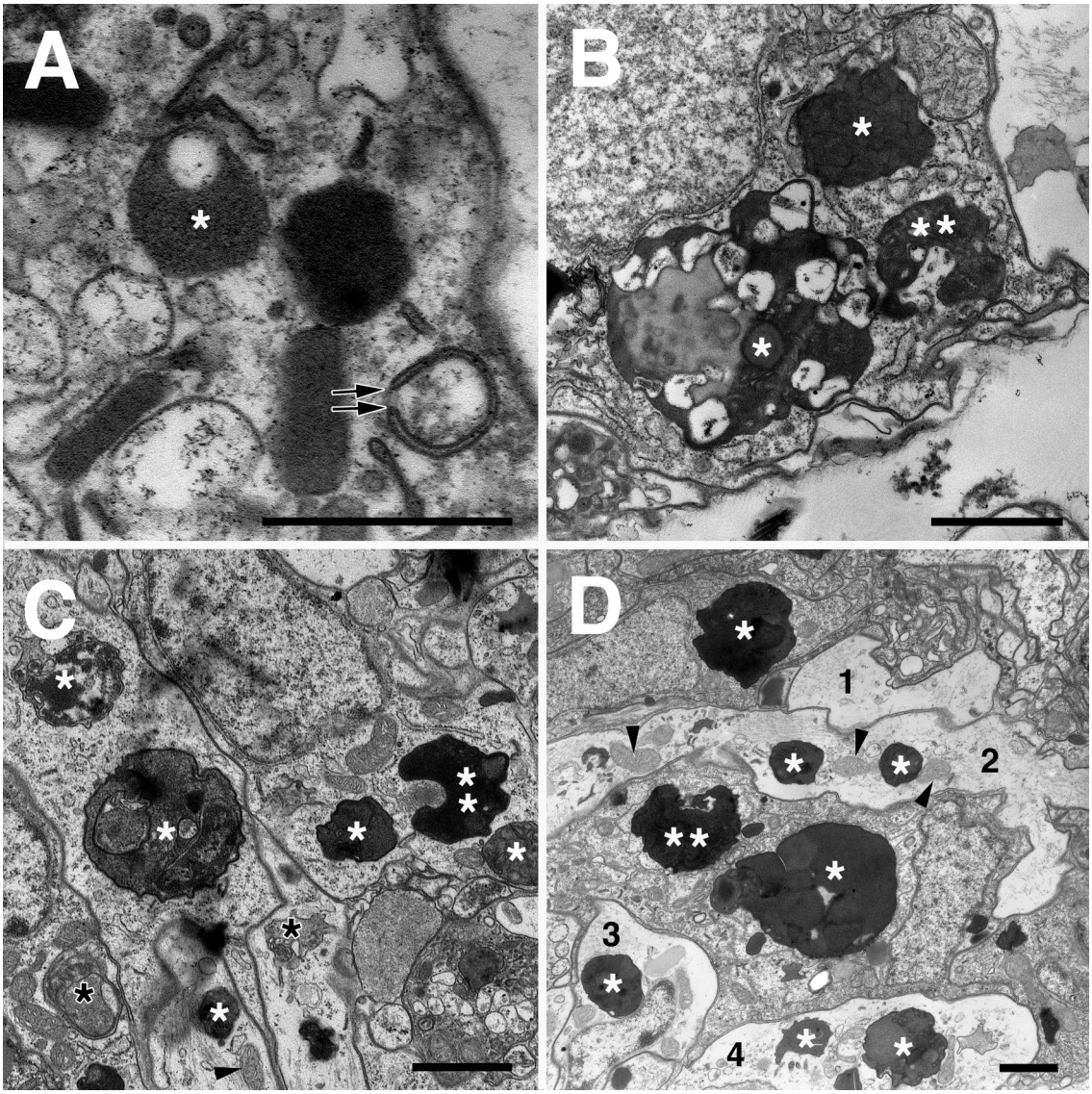

Figure 17: TEM: Transverse sections of symbiotic *Aiptasia pallida* tissues after 48 h heat stress showing various stages of APS formation (indicated with 1 or more white asterisks). A) Induction: Pre-autophagosome formation via 'cup-like' structure (double arrows point to lip of cup) located nearby a mature APS (asterisk). B) Sequestration: Surrounding cellular materials are sequestered into an autophagolysosome (double asterisks) where they are actively degraded. Other nearby autophagosomes (single asterisks) are also indicated. C) Retention and further sequestration: APSs can vary in size and density depending on the type and amount of materials that are retained and the extent of digestive breakdown of sequestered materials. Note: Early APSs often appear less dense (black asterisks with white outline) D) Formation of large, dense APSs that result from accumulation and digestion of cellular material. Cytoplasmic degradation is often observed as regions of 'cleared' cytoplasm where numerous APSs and suspended organelles (black arrowheads) are found (e.g., regions 1, 2, 3, 4). Double asterisks indicate APSs that appear to be actively sequestering cytoplasmic or organellar material. Scale bars = 0.5μm (A) and 1μm (B-C).

Biochemical induction of autophagy

In order to confirm the role of autophagy in APS formation and subsequent cellular degradation during heat stress, several symbiotic anemones were exposed to 25 μM rapamycin in seawater containing 1% DMSO for 12 h (Dunn et al. 2007) (Fig. 18) and the ultrastructural appearance of their tissues was compared to that of anemones experiencing heat stress (Fig 16). Ultrastructural examination of tentacle tissues from rapamycin treated anemones (Fig. 18E-F) revealed a strikingly similar cellular response to that seen in heat stress-induced anemones (Fig. 18B-C) with numerous APSs and highly degraded cellular regions present when compared to controls (Fig. 18A,D). As was the case with heat stressed anemones, a significant amount of expelled algae was observed at the bottom of each rapamycin treatment anemone container. All treatment anemones exhibited reduced brown coloration (presumably resulting from symbiont loss) after 12 h of rapamycin incubation when compared to controls.

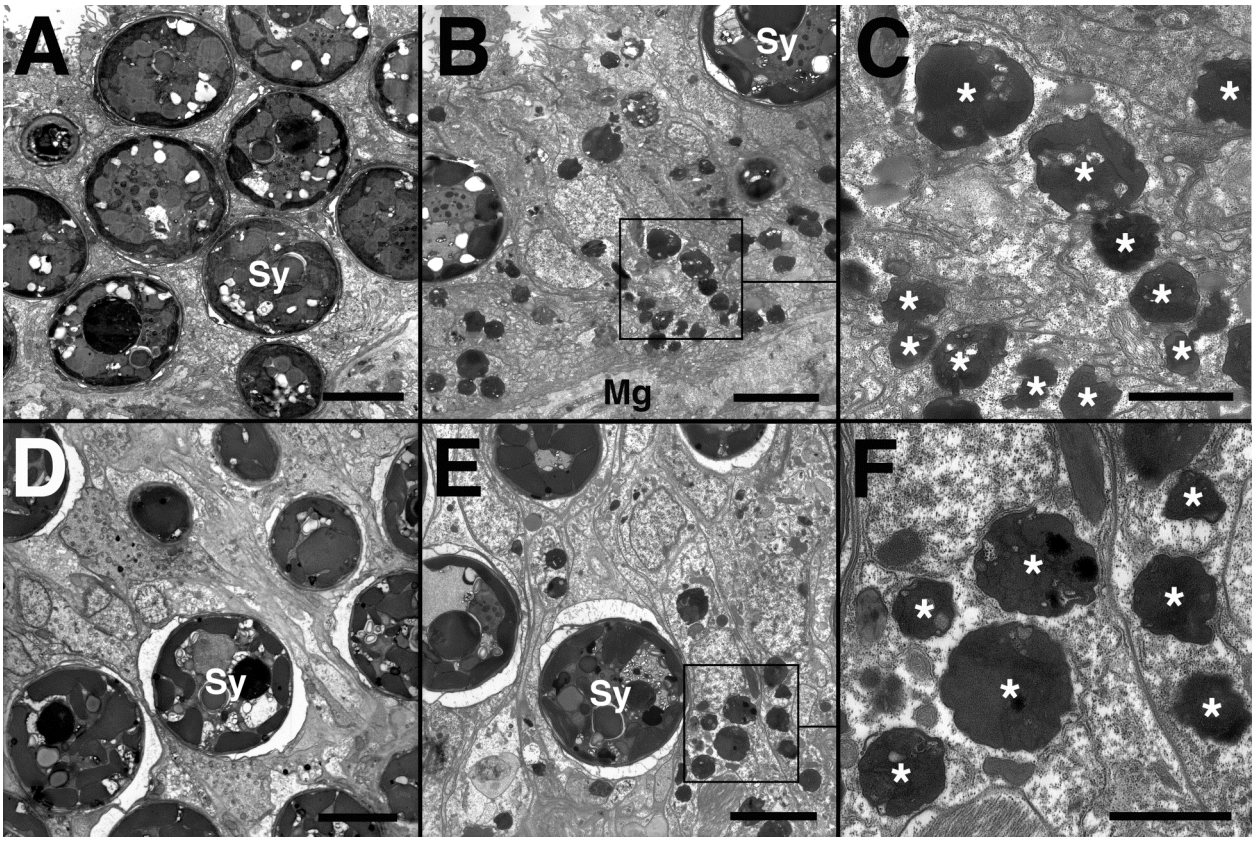

Figure 18: TEM: Transverse sections of tentacles at midlength showing autophagic structure formation in the gastrodermis of symbiotic anemones. A) Control tissues after 0 h of heat stress display healthy ultrastructural appearance with few to no visible autophagic structures, B) After 48 h of heat stress tissues reveal numerous dense autophagic structures, C) Higher magnification of the boxed region shows detail of the APSs (asterisks). D) Control tissues exposed to 1% DMSO for12 h (no rapamycin) exhibit few to no APSs with no degradation, E) Tissues exposed to 12 h of 25 μM rapamycin result in the presence of numerous dark APSs, F) Higher magnification of the boxed region shows detail of the APSs (asterisks). Sy = symbiont; Mg = mesoglea. Scale bars = 5μm (A, B, D, E) and 2μm (C, F).

Cellular bleaching mechanisms

After ≥ 12 h of heat stress, tissues often underwent excessive autophagic degradation resulting in loss of significant amounts of cytoplasmic material from either regions of cells and their processes or from entire cells (Fig. 18A-C). This degradation likely resulted from sequestration and subsequent digestion of cellular material by APSs, which were often observed within or near degraded cellular regions (Fig. 17D, 19A-D). Gastrodermal cells that harbored *Symbiodinium* cells frequently exhibited deterioration of their cytoplasm at the apical region of

the host cell between the symbiont and gastrovascular cavity (GVC) (Fig. 19A) and occasionally throughout the majority of the cell (Fig. 19B-C). Symbionts generally remained healthy in appearance (based on work of Taylor, 1968) with intact chloroplasts and other organelles throughout the duration of both the heat stress (Fig. 16A and 18B) and rapamycin (Fig. 18E) treatments. However, symbionts found within degraded host cells often appeared to have migrated or been moved toward the apical region of the host cell (Fig. 19A-B). Apically positioned symbionts were commonly observed bulging out into the GVC along with surrounding host cell cytoplasm and plasma membrane (Fig. 19B). These symbionts and surrounding host cell cytoplasm and plasma membrane appeared to be actively detaching from apical portions of host cells in what we describe as an apocrine-like manner, since both "secretion" (the symbiont) as well as a portion of the host cell are lost from the gastrodermal cell (Fig. 19D-F). During this detachment process (hereafter referred to as “apical detachment”), the separating, symbiont-containing bleb initially maintained a connection to th
e host cell via thin strands of host cytoplasm and plasma membrane (Fig. 19D) before apparent release into the GVC (Fig. 19E). Although fully detached symbionts remained surrounded by a thin layer of host cytoplasmic and membranous material (Fig. 19E), this host material appeared to be shed from symbionts as they moved further into the GVC (Fig. 19F). Additionally, degraded symbionts were occasionally observed in heat stressed tissues (Fig. 19E).

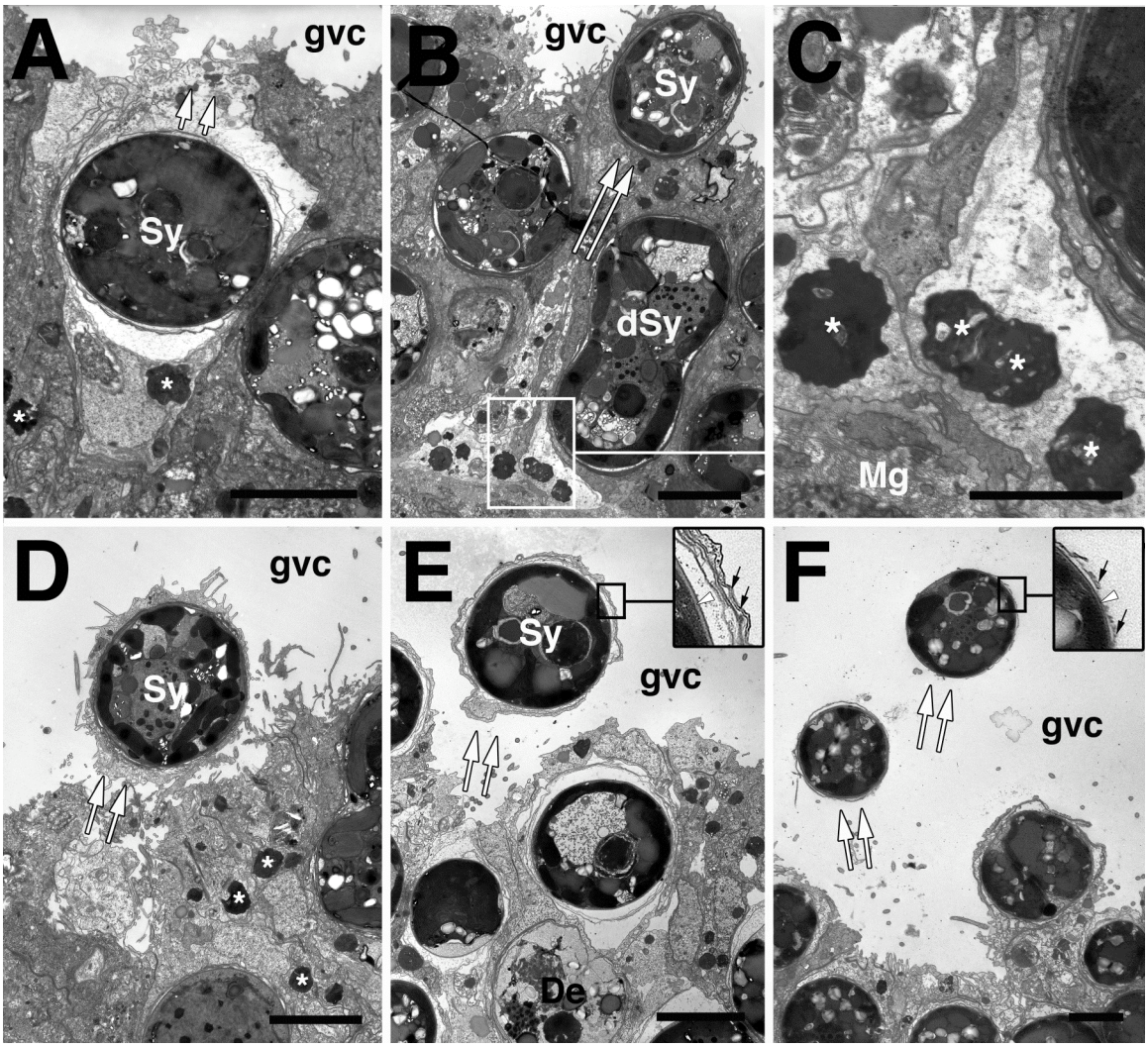

Figure 19: TEM: Transverse sections of symbiotic *Aiptasia pallida* after ≥ 12 h heat stress showing apparent apical detachment of symbiont containing blebs from autophagically degraded host gastrodermal cells (double white arrows with black border). Several large APSs are indicated with asterisks. A) After 48 h of treatment autophagic degradation results in sparse cytoplasm between symbiont and apical edge of host cell (double white arrows). B) After 12 h of treatment an apparently healthy symbiont has relocated toward the apical end of an extensively degraded host cell, where it bulges out into the gastrovascular cavity within the host plasma membrane. C) Higher magnification of boxed area in B, where autophagically degraded cytoplasm is apparent in basal region of a host cell. Note numerous large APSs are located within the heavily deteriorated region where only very sparse cytoplasm remains. D) After 24 h of heat stress treatment a symbiont and surrounding host cytoplasm and plasma membrane with microvilli is seen bulging into the GVC, as it appears to be completing its separation from the apical end of an autophagically degraded host cell in an apocrine-like manner. E) After 48 h of treatment an apparent fully detached bleb of symbiont containing host cell cytoplasm and associated plasma membrane floats free within the gastrovascular cavity. Inset shows higher magnification of host membrane (black arrows), underlying symbiosome structures, and symbiont cell wall (black arrowhead). F) After 48 h of treatment several symbionts are seen at various stages of apical detachment. The furthest symbiont from its detachment site has only small remnants of surrounding host cytoplasm and membranous components. Inset shows higher magnification of remaining host material (black arrows) and symbiont cell wall (black arrowhead). Scale bars = 5 μm (A, B, D-F) and 2μm (C). De = degrading symbiont; dSy = dividing symbiont; Mg = mesoglea ; Sy = symbiont.

After ~12 h of heat stress, anemones exhibited a noticeable loss of brown coloration, indicating that bleaching was actively occurring. Average symbiont loss was quantified in both control and heat-treated anemones after 48 h, the latter of which exhibited a significant 10-fold increase in the number of expelled cells per anemone (Fig. 20).

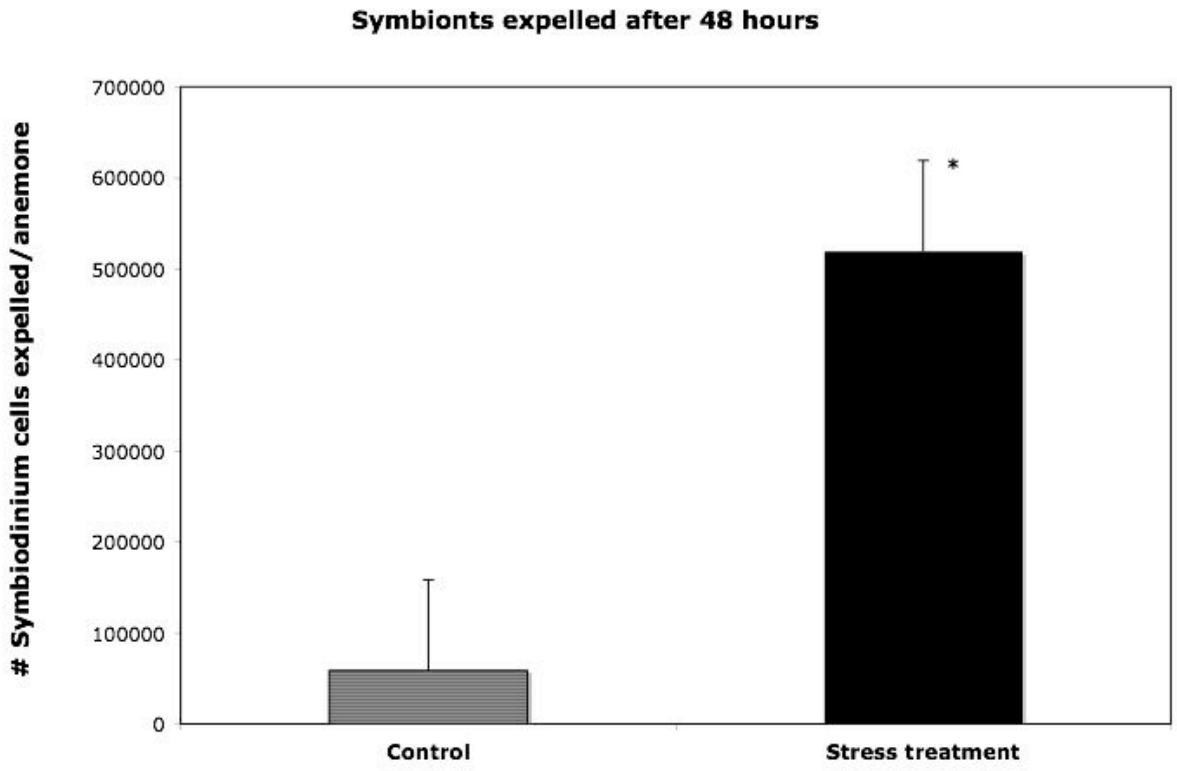

Figure 20: Average number of expelled *Symbiodinium* cells per anemone after 48 h of either heat stress or control treatment. (t-test, $p < 0.05$, n=3).

Conclusions

In this study, an abundance of autophagic structures (APSs) was observed within *A. pallida* tentacle tissues after exposure to heat stress. These were similar in structural appearance to those observed after 12 h of exposure to the autophagy inducer, rapamycin. Since rapamycin has previously been employed to biochemically induce autophagy in a variety of taxa, including *Hydra* (Chera et al., 2009) and *A. pallida* (Dunn et al., 2007), this provides ultrastructural evidence that elevated autophagic activity occurs as a cellular stress response in *A. pallida* during early stages of bleaching.

The autophagic process involves sequestration and intracellular breakdown of long-lived proteins and damaged organelles for recycling (Levine and Yuan, 2005; Mizushima and Klionsky, 2007). This occurs through a series of developmental stages, which were observed in heat stressed anemone tissues (Fig. 21). These begin with construction of a membranous pre-autophagosomal structure that seals around cytoplasmic material to form a complete "autophagosome" (Holtzman, 1989; Jing and Tang, 1999). At some point, autophagosomes must fuse with a primary lysosome in order to gain the necessary enzymes to degrade the sequestered contents (Fawcett, 1981; Jing and Tang, 1999) and are then generally termed "autophagolysosomes" (Holtzman, 1989). The APSs continue to sequester cytoplasmic materials as enzymes begin to degrade the contents, eventually leaving only electron dense, heterogeneous, indigestible materials within the autophagosome membrane (Fawcett, 1981; Holtzman, 1989). Interestingly, in tissues of *A. pallida,* even exceedingly electron dense APSs appeared to continue to sequester additional cellular material (Fig. 21). Variation in the density of APSs was observed, which likely correlated with the level of maturation (i.e. material degradation and retention) that each structure was experiencing at the time of fixation.

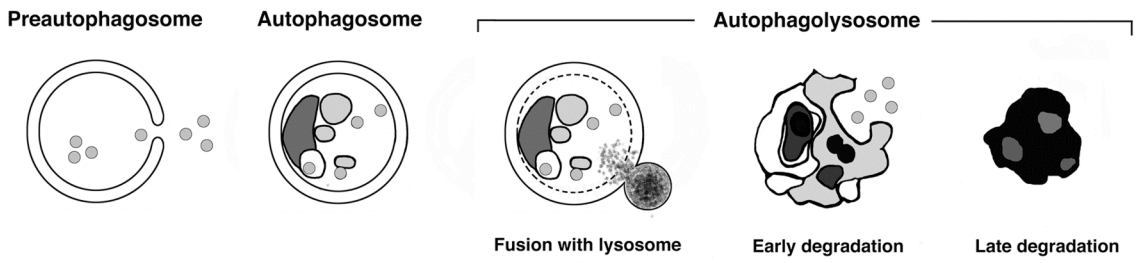

Figure 21: Stages of autophagy beginning with formation of the cup-like pre-autophagosome that extends around portions of cellular material (designated as gray circles) and eventually seals forming a double membrane bound autophagosome. Upon fusion with a lysosome the structures are often referred to as an autophagolysosome. Here, the inner membrane is quickly dissolved as lysosomal enzymes begin to degrade the sequestered cellular contents. Autophagolysosomes continue to sequester and degrade surrounding cellular material (early degradation stage) until only dense indigestible materials remain (late degradation stage- often referred to as a residual body). Autophagosomes and autophagolysosomes are collectively referred to as autophagic structures (APSs).

Since significant numbers of APSs were found in both symbiotic gastrodermal and non-symbiotic epidermal tissues, it would appear that stress induced-autophagy is primarily a host-mediated cellular activity. However, further investigation is necessary to determine any contributive role that the symbiont might have during this autophagic stress response (see comments on ROS below).

Autophagy-like cellular activities have been previously implicated in the bleaching process. One study conducted by Dunn et al. (2007) provided biochemical evidence of both autophagic and apoptotic activity during heat stress-induced bleaching in *A. pallida.* The authors suggested that no single cell death pathway could be implicated during the bleaching process and that both mechanisms contributed to the loss of symbionts. Their results suggested that apoptosis and autophagy were interconnected, such that when one is inhibited, the other is induced. However, the manner in which these two cellular processes progressed temporally throughout the bleaching episode was not described, and no ultrastructural evidence of the occurrence of

autophagy was provided. Additionally, no evidence of symbiont digestion or 'symbiophagy' (per Downs et al., 2009) was observed in our study. In this investigation, nearly all symbionts displayed a healthy appearance throughout the heat stress treatment, as evidenced by intact thylakoids in the chloroplasts as well as overall 'normal' ultrastructure (per Taylor, 1968). This may be due to the fact that the type A4 *Symbiodinium* strains present in *Aiptasia* from the Florida Keys have been previously shown to exhibit higher tolerance to temperature stress (Goulet et al., 2005) and thus, may better maintain its cellular structure under heat stress conditions. Additionally, *in situ* degradation of symbionts was occasionally observed in both heat stressed and control tissues in this study, suggesting that symbiont degradation may function as a naturally occurring means of population control rather than as a stress response.

Autophagic activity is an essential mechanism for cell survival and homeostasis (Ohsumi and Mizushima, 2003), but typically remains suppressed to low levels in most cells (Levine and Yuan, 2005). However, under various stress conditions, such as starvation (Scott et al., 2004) or heat stress (Prasad et al., 2007; Oberley et al., 2008; Swanlund et al., 2008), autophagy is often upregulated as a pro-survival response by maintaining mitochondrial ATP energy production through the recycling of nutrients (Levine and Yuan, 2005). Alternatively, autophagy has also been implicated as a cell death mechanism (Xue et al., 2001), whereby excessively damaged cells are removed from affected tissues (Kourtis and Tavernarakis, 2009).

Autophagy and other forms of cell death can be triggered by production of ROS (Scherz-Shouval et al., 2007; Chen and Gibson, 2008), which has been reported to induce cnidarian bleaching (Franklin et al., 2004; Perez and Weis, 2006). If the amount of cellular stress is minimal, then intracellular ROS levels remain low, and autophagy would be maintained at normal levels, thus, promoting survival. Alternatively, exposure to high temperature would

eventually result in excessive ROS levels in the host (Nii and Muscatine, 1997; Richier et al., 2006) that could result in damage to cytoplasmic organelles. The damaged intracellular debris would likely induce autophagic pathways and numerous APSs would be formed. These APSs would extensively digest surrounding cytoplasmic material and organelles, similar to the results we observed after 12 - 48 h of heat stress in *A. pallida*. Heavily stressed cells that become damaged beyond repair are likely to undergo autophagic cell death as they attempt to restore and maintain tissue homeostasis. This may facilitate bleaching during early stages of the stress response. Thus, ROS production by symbionts may act to facilitate host-mediated autophagy.

Expulsion of symbionts from gastrodermal cells via apical detachment appeared to be associated with autophagic degradation of cells. This may be a bleaching response that occurs when autophagy eliminates large amounts of cytoplasm and organelles from gastrodermal cells and both structural integrity and stability are systematically lost. As a result, intracellular symbionts may either migrate or be moved toward the apical end of the host cell, where they are eventually expelled along with surrounding host cellular material via an apocrine-like mechanism. A similar mechanism for symbiont loss, called “budding”, was suggested by Glider (1983) as a method of symbiont population control in non-stressed *A. pallida*. Similarly, Gates et al. (1992) suggested that "pinching off" might be a mechanism for symbiont release during bleaching, though they did not observe this process nor was it associated with autophagy or any similar cell death-related activity. Since symbionts exhibiting little or no associated host cytoplasm or plasma membrane were commonly observed in the GVC, but no evidence of exocytosis of symbionts was observed, it is possible that digestive enzymes or enzymes released from dying cells may quickly degrade the host-derived material that surrounds symbionts shed via apical detachment.

Although the majority of previous cellular bleaching studies have documented high levels of apoptotic or necrotic activity in both host and symbiont during heat stress (Dunn et al., 2002, 2004, 2007; Franklin et al., 2004; Strychar et al., 2004; Richier et al., 2006; Ainsworth et al., 2008; Strychar and Sammarco, 2009; Tchernov et al., 2011), the most prevalent cellular activity observed throughout the duration of the present study was host cell autophagy. These ultrastructural findings provide further evidence to support the suggestion of Dunn et al. (2007), that apoptosis is mostly suppressed while autophagic activity remains elevated during heat stress. Further investigation is necessary to determine whether autophagic cell death is replaced by apoptosis later in the stress response.

The results of this current investigation support the hypothesis that in *A. pallida* and perhaps other anthozoan species, elevated autophagic activity and autophagic cell death function as an early response to heat stress. Although these results suggest that autophagy may occur as the first cellular stress response during moderate to acute stress conditions (32.5^{o}C), it is possible that under more dramatic conditions, such as exposure to 1) exceedingly high temperatures or 2) longer periods of stress, that different cell death pathways may be initiated as has been previously suggested (Dunn et al. 2002, 2004).

Mass mortality bleaching events are predicted to increase in frequency and intensity over the next few decades (Hoegh-Guldberg, 1999; Donner et al., 2007). Therefore, it is critical to advance our current knowledge of the bleaching process by providing a complete analysis of how breakdown in the symbiotic association occurs. The results of this study provide a better understanding of the cellular stress responses in the common *Symbiodinium* symbiosis model, *A. pallida,* through a simulation of more natural bleaching conditions and a detailed examination of host tissues at multiple time points in heat stressed and control anemones. Results from this study

present the first ultrastructural evidence of autophagic digestion of host tissues during thermal stress in a cnidarian system. Additionally, we suggest that elevated autophagic activity may induce the loss of symbionts via apical detachment from degraded host cells. Further studies are needed both to verify this bleaching mechanism and to determine other cellular changes that may occur during later periods of heat stress-induced bleaching.

IV. Autophagic activity occurs as a host-derived mechanism in the symbiotic anemone, *Aiptasia pallida,* during heat stress-induced bleaching

Abstract

The process known as coral bleaching is characterized by the loss of essential, photosynthetic dinoflagellates, *Symbiodinium* spp., from host tissues in response to elevated temperature and/or light stress. Previous studies have implicated the involvement of several possible methods of cell death that underlie the cnidarian bleaching process, most recently highlighting the possible role of autophagic activity. In this study, transmission electron microscopy was utilized to conduct a detailed examination of symbiotic tissues of the anemone, *Aiptasia pallida,* during early stages of stress-induced bleaching. Both symbiotic and aposymbiotic anemones were exposed to a stress treatment of 32.5±0.5^{o}C at 140 ± 5 μmol photons $m^{-2}s^{-1}$ PAR light intensity for 12 h followed by 12 h at 24±0.5^{o}C in darkness during two consecutive 24 h cycles for a total of 48 h. In stressed symbiotic anemones, significantly higher numbers of autophagic structures (APSs) and associated cellular degradation were observed in both host gastrodermis and epidermis. Stressed aposymbiotic anemones exhibited significantly elevated autophagic activity in the gastrodermis, suggesting that autophagy occurs primarily as the result of a host-derived cellular pathway. Treatment of anemones with the known autophagy inducer, rapamycin, resulted in significant increases in APSs in both epidermis and gastrodermis with similar ultrastructural appearance to that of symbiotic heat stressed tissues. These results confirm previous suggestions that the structures observed during the heat stress treatment are autophagic. This study provides the first quantitative evidence in a symbiotic cnidarian that

autophagic activity is elevated during the initial 48 h of heat stress that results in bleaching.

Introduction

The coral bleaching process is characterized by the loss of essential, photosynthetic dinoflagellates of the genus *Symbiodinium* (Freudenthal, 1962) from gastrodermal tissues of corals or other symbiotic cnidarians. This phenomenon can occur in response to a variety of environmental stressors; however, elevated heat and/or light conditions are most commonly associated with episodes of mass mortality bleaching. During elevated temperature and light conditions, the cnidarian-dinoflagellate symbiosis breaks down through a complex series of cellular interactions which are initiated when the stress threshold of either or both member(s) is surpassed and excessive amounts of damaging reactive oxygen species (ROS) are produced by the symbiont (Franklin et al., 2004; Lesser, 1996) and/or host cells (Dunn et al., 2012; Dykens et al., 1992; Nii and Muscatine, 1997). If the rate of ROS generation exceeds the rate of detoxification, then accumulation of ROS may result in oxidative damage to cellular structure, loss of cell function, and ultimately death of the affected cell (Chen and Gibson, 2008; Lesser, 1997; Perez and Weis, 2006; Sherz-Shouval et al., 2007). Recent investigations suggest that such ROS-mediated stress is the underlying cause of symbiont loss during bleaching (Franklin et al., 2004; Lesser, 2007; Perez and Weis, 2006).

Several cellular bleaching mechanisms have been proposed that implicate the involvement of cell death-related activities in the host and/or symbiont. Such mechanisms include apoptosis (Ainsworth et al., 2008; Dunn et al., 2002; 2004; 2007; Franklin et al., 2004; Richier, et al., 2006; Strychar et al., 2004; Strychar and Sammarco, 2009; Tchernov, et al., 2011), necrosis (Ainsworth et al., 2008; Dunn et al., 2002; 2004; Glynn, 1985; Strychar et al.,

2004; Strychar and Sammarco, 2009), and autophagy or autophagy-like processes (Dunn et al., 2007; Downs, et al., 2009; Chapter 3). Although autophagic activity has been well documented in both vertebrate (Fawcett, 1981; Hand, 1970; Holtzman, 1989; Jing and Tang, 1999; Nixon, 2007) and invertebrate (Kov et al., 2000; Rost-Roszkowska et al., 2008) tissues, it has only recently been identified in stressed symbiotic cnidarians (Dunn et al., 2007; Chapter 3). This autophagic process is characterized as 'self-eating', whereby sequestration and intracellular breakdown of long-lived proteins and damaged organelles occurs during periods of cellular stress (Mizushima and Klionsky, 2007). In Chapter 3, numerous autophagic structures (APSs) were observed throughout both the gastrodermis and epidermis of the anemone, *Aiptasia pallida* (Agassiz in Verrill, 1864), after 12 h of heat stress treatment. These APSs contained sequestered host cellular material and were often found within highly degraded regions of the cell that often exhibited sparse cytoplasm. Gastrodermal treatment tissues that exhibited elevated autophagic activity also displayed significant levels of symbiont loss. Thus, the authors suggested that autophagic activity occurred as an early response to heat stress conditions, and resulted in bleaching.

Recent papers have highlighted the need for further investigations into the involvement of autophagy during breakdown of the cnidarian-dinoflagellate symbiosis (Davy et al., 2012; Weis, 2008). The aim of this study was to perform a quantitative examination of the abundance of APSs during heat stress in symbiotic and aposymbiotic, *A.pallida* tissues as well as in the tissues of anemones treated with the known autophagy inducer, rapamycin. We have employed previously established methods used to initiate the autophagic response in *Aiptasia pallida* (Chapter 3). Quantification of autophagic activity in both symbiotic and aposymbiotic anemones

allowed us to draw conclusions about the probable role of each symbiotic member in the autophagic response.

Materials and Methods

Culture conditions

Aiptasia pallida harboring symbionts typed as Clade A4 *Symbiodinium* (Santos et al. 2002; Scott Santos, 'personal communication') were collected in the Florida Keys and maintained in artificial seawater (Reef Crystals) at 28-30 ppt salinity. Symbiotic anemones were kept in two 150 gal tanks at 24±1°C (such notation indicates mean ± standard deviation) below fluorescent light fixtures, each equipped with two 32W bulbs (Phillips F32T8/TL841) producing 50±5 μmol photons $m^{-2}s^{-1}$ irradiance at the level of the anemones. Lights were set on a 12:12 h light/dark regime.

A separate group of anemones, also collected from the Florida Keys, were rendered aposymbiotic by long-term (years) maintenance in complete darkness (except during brief additions of food) in a 150 gal tank at 24±1°C. The absence of *Symbiodinium* was verified by using PCR nuclear 18S rDNA (Rowan and Powers, 1991) and chloroplast 23S rDNA (Santos et al, 2002). In both cases no PCR product was produced (Scott Santos, 'personal communication'). All anemones were fed freshly hatched *Artemia* larvae three times per week.

Temperature-light treatments for both symbiotic and aposymbiotic anemones

In order to assess whether or not elevated autophagy increases during heat stress-induced bleaching, two separate experiments were carried out. In a previously conducted experiment (Exp 1), symbiotic (n=3) anemones were exposed to heat stress conditions described in Chapter

3 known to cause non-lethal bleaching in *A. pallida*. In the second experiment (Exp 2), which is the present study and the focus of this investigation, both symbiotic (n=3) and aposymbiotic (n=3) anemones were exposed to the same heat-stress conditions as in Exp 1. In addition, controls were simultaneously run wherein symbiotic anemones were exposed to the same conditions as the stressed anemones but without the heat stress.

In preparation for Exp 2, six symbiotic and six aposymbiotic medium sized anemones were placed in identical, individual plexiglass dishes that each contained ~200 ml of 0.45 μm Millipore filtered artificial aquarium sea water (MFAW) and allowed to acclimate for ~5 days at the ambient lab temperature of 24±1° C with 50±5 μmol photons $m^{-2}s^{-1}$ ambient light intensity. Water in these dishes was changed daily. Anemones were fed once during the first 3 days and then held unfed for 48 h prior to the beginning of the experiments. Both symbiotic and aposymbiotic treatment anemones were then transferred in their containers to an incubator at 32.5±0.5° C and placed beneath two lamps each equipped with two 20W fluorescent bulbs (GE Ecolux F20T12/G50-ECO) that emitted ~140±5 μmol photons $m^{-2}s^{-1}$ light intensity at the level of the anemones. The anemones were held in the incubator for 12 h and then removed to a dark, well-ventilated box on the lab bench for 12 h in darkness at 24±1° C. The incubator and dark box treatments were then repeated over the following 24 h for a total treatment time of 48 h. It took approximately 2.5 h for the 24±1° C dishes to warm to 32.5±0.5° C in the incubator under these conditions. This study primarily focuses on the effects of heat stress. There was a small difference in light intensity between the anemone culture tanks (50±5 μmol photons $m^{-2}s^{-1}$) and the incubator (140±5 μmol photons $m^{-2}s^{-1}$); however, this is well within the field light intensities (0 to > 1000 μmol photons $m^{-2}s^{-1}$) that these symbiotic anemones experience and was not considered by itself to be a significant stressor in our experiments. Of the six symbiotic and six

aposymbiotic anemones exposed to heat stress, tentacles from three of each were sampled for fixation, embedding and examination with a transmission electron microscope (TEM) at t=0 h and t=48 h.

Six additional symbiotic anemones and six additional aposymbiotic anemomes were acclimated as described above, and used as controls (no stress treatment) in this experiment. These were placed in the same type of dishes used for stressed anemones at 24±1°C with 50±5 μmol photons $m^{-2}s^{-1}$ irradiance for 12 h daily followed by 12 h in darkness at 24±1°C over a 48 h period. In all cases water was changed daily and anemones were not fed during the 48 h treatment period. As was the case for the heat stressed anemones, tentacles from three symbiotic and three aposymbiotic anemones were sampled for fixation, embedding and TEM examination at t=0 h and t=48 h.

Biochemical induction of autophagy

Twelve symbiotic anemones were acclimated to lab conditions as described above. Six were then exposed to treatment conditions of 25 μM rapamycin (Sigma-Alrich) and 1% DMSO solution in MFAW for 12 h (Dunn et al., 2007), and the remaining six to control conditions of 1% DMSO in MFAW for 12 h. Both control and treatment anemones were maintained on a 12:12 h light:dark regime at 24±1°C as described above. Tentacles from three rapamycin treated anemones and three control anemones were sampled for fixation, embedding and TEM examination at t=12 h.

Fixation, embedment and sectioning for TEM

Anemones from heat stress treatments, rapamycin treatment, and control groups were prepared for TEM following the protocol outlined in Chapter 3. Heat treatment and control anemones (symbiotic and aposymbiotic) were sampled at 0 and 48 h and symbiotic rapamycin treatment and control anemones were sampled after 12 h. Anemones were relaxed in high Mg/low Ca seawater (Audesirk and Audesirk 1980) followed by the addition of chlorotone-saturated seawater. A subset of tentacles (n=6) was clipped from each of 3 randomly selected anemones at each time point (stress treatments and controls) (Fig. 22A). Tentacles were immediately fixed using methods similar to the protocol of Carroll and Kempf (1994) in Millonig's phosphate buffered, gluteraldehyde fixative solution followed by a secondary fixation in a $NaHCO_3$ buffered, OsO_4 solution. Tissues were dehydrated through an ethanol series, transferred through three changes of propylene oxide, and infiltrated and embedded using EMbed 812 resin (Electron Microscopy Sciences). Embedded tentacles were sectioned (~60nm) using a diamond knife (Diatome) on a Reichert-Jung Ultracut E microtome. All sections were stained with uranyl acetate and lead citrate and examined using a Zeiss EM 10C 10CR transmission electron microscope (TEM).

Quantification of autophagy

In order to quantify autophagic activity in *A. pallida,* tentacles were analyzed in each sampled anemone from each treatment [heat stress and controls (symbiotic and aposymbiotic) or rapamycin treated and controls] (Fig. 22) using a quantification method similar to that of Swanlund et al. (2010). First, one tentacle from each anemone was sectioned at mid-length in transverse orientation to generate one TEM section. Second, the transverse sections were viewed

in the TEM at low magnification and divided into four quadrants to ensure that regions representing the entire circumference of the tentacle could be analyzed. Third, both the gastrodermis and epidermis were photographed at the same magnification of 3,150X within the center of each quadrant (Fig. 22B). Negatives of the electron micrographs were scanned at 1200 dpi and converted to positive images. APSs were identified according to morphological characteristics previously used to assess autophagic response in symbiotic cnidarian tissues as described in Chapter 3. Of the various stages of autophagy that were observed in this study, only the denser, more easily identifiable stages (autophagolysosomes) were evaluated. In order to ensure consistency, each APS had to fulfill two main criteria: 1) must have overall irregular periphery (to help distinguish from primary lysosomes and lipid droplets), 2) must have heterogenous appearance and contain visible sequestered cytoplasmic material (to distinguish from lipid droplets). Fourth, each image was analyzed using ImagePro Plus 7.0 software and measurements were made for i) total cellular area outlined in the micrograph and ii) total area occupied by APSs (Fig. 22C) similar to Oberley et al. (2010). The area occupied by symbionts within their symbiosomes was also determined and subtracted from the total cytoplasmic area outlined giving the adjusted cytoplasmic area (= the total cytoplasmic area that could potentially contain gastrodermally derived APSs (Fig. 22C). The overall area-based abundance of APSs was calculated in stressed symbiotic and aposymbiotic anemones, controls and rapamycin-treated animals as a percentage of the adjusted cytoplasmic area in both gastrodermis and epidermis [% APSs = [(area occupied by APSs) / (adjusted cytoplasmic area)] X 100].

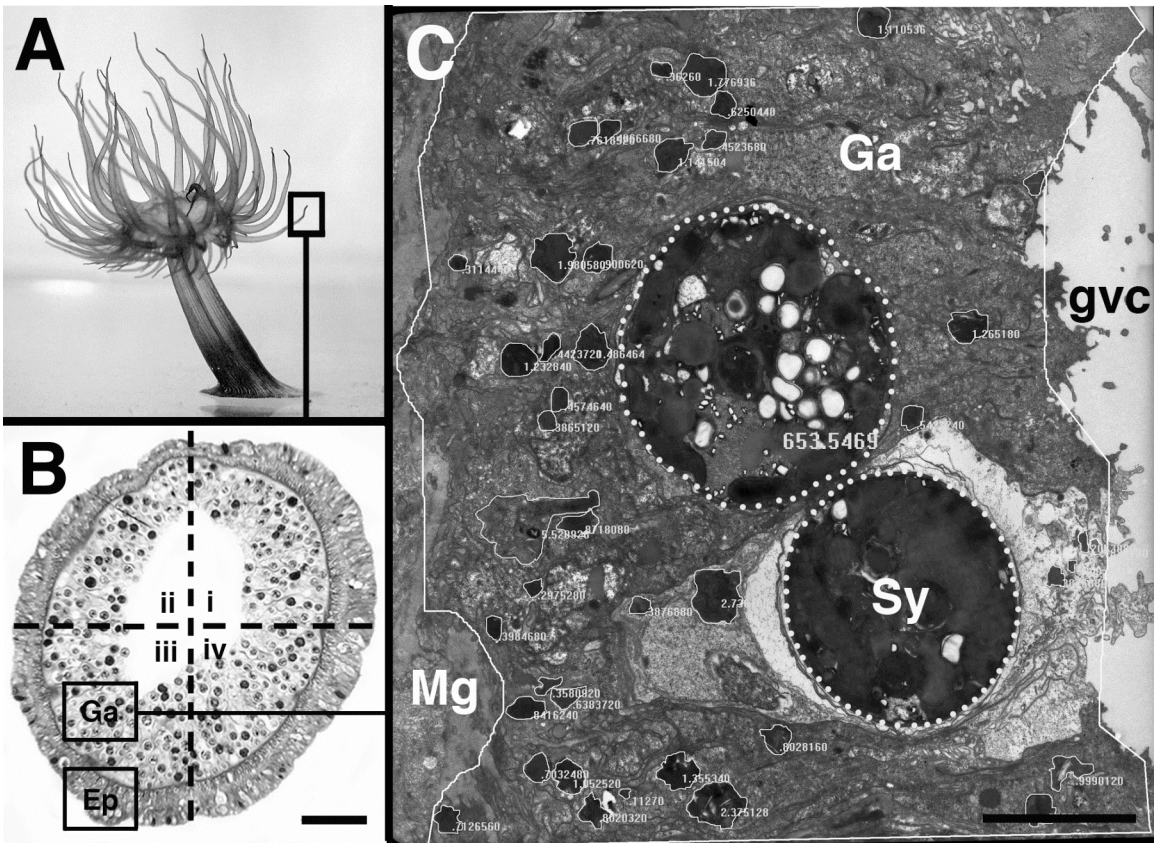

Figure 22: Quantification of autophagic structures within *A. pallida* tentacle tissues. A) Tentacles were excised from live anemones (treatment and controls) and prepared for TEM. B) Transverse tentacle sections were viewed at low magnification on the TEM and photographs of both the gastrodermis (Ga) and epidermis (Ep) were taken within each of four quadrants (i-iv). Note: A light micrograph is used here for illustrative purposes. C) Micrographs were then analyzed using ImagePro Plus 7.0 software to determine i) total cytoplasmic area, ii) total area occupied by APSs, as well as iii) total area occupied by symbionts (Sy) for calculation of % APSs. Ga=gastrodermis, Ep=epidermis, gvc=gastrovascular cavity, Mg=mesoglea, Sy=*Symbiodinium*. Number quantities next to APSs signify area occupied by each. Number inside dotted lines (surrounding symbionts) signifies the total area that they occupy. Scale bars = 60 μm (B) and 5μm (C).

Statistical analysis

Differences in % APSs were tested between 0 and 48 h for both stressed and control groups of symbiotic and aposymbiotic anemones and between rapamycin treated anemones and controls after 12 h using paired t-tests. Differences in % APSs were also tested between gastrodermis and epidermis in treatment tissues after 48 h (symbiotic and aposymbiotic) or 12 hr (rapamycin). Comparison of the % APSs

A) between Exp 2 controls at t=0 h and Exp 2 controls at t=48 h,

B) between Exp 1 t=0 h (pre-stress) and control t=0 h for Exp2 and

C) between Exp 1 t=48 h of heat stress and Exp 2 t=48 h of heat stress showed no statistical differences ($p > 0.277$), so the stress treatment results for these two experiments were pooled for further statistical analyses. Since values were in the form of percentages, they were arcsin transformed for statistical analysis; however, results are presented as percentage values for greater clarity.

Significance of the difference in average number of expelled *Symbiodinium* cells/anemone after 48 h between unstressed control and heat stressed treatment anemones was determined using a t-test. All statistical tests were conducted using a significance level of 5% (alpha=0.05) with SAS 9.2 software.

Algal cell counts

In order to quantify symbiont loss resulting from heat-induced bleaching, expelled *Symbiodinium* cells were collected from both control and stressed anemone containers (n=3) after 48 h of treatment. For each anemone the collected algae were centrifuged, and then re-suspended in 250 mL of 0.45 μm MFAW. Cells were then counted with a Neubauer hemacytometer (Perez and Weis, 2006) and the average number of algal cells that were expelled per anemone after 48 h was calculated for controls and heat stress treatment anemones.

Results and Discussion

Autophagy in unstressed and heat-stressed symbiotic anemones

Examination of unstressed (control) symbiotic *A. pallida* gastrodermis (Fig. 23A) and epidermis (Fig. 23D) revealed a consistently healthy cellular appearance, which consists of intact epithelial cells with abundant cytoplasm (Chapter 3); however, as previously reported in Chapter 3, symbiotic tissues exposed to a 48 h heat-stress treatment exhibited numerous APSs within both host gastrodermal (Fig. 23B and C) and epidermal (Fig. 23E and F) cells. Large, dense APSs were commonly observed within degraded cellular regions that exhibited markedly sparse cytoplasm (Fig. 23F). Measurements of % APSs (= [(area occupied by APSs) / (adjusted cytoplasmic area)] X 100]) ranged from a low of 0.711% to a high of 7.511%. Values are given as the mean % area occupied by APSs ± S.D. In symbiotic anemones there were no significant differences in unstressed control gastrodermal tissues ($p=0.777$) between 0 h ($\bar{x}$ = 0.711%±0.360, n=3) and 48 h ($\bar{x}$ = 0.744%±0.168, n=3) or in unstressed control epidermal tissues ($p=0.277$) between 0 h ($\bar{x}$ = 0.609%±0.341, n=3) and 48 h ($\bar{x}$ = 0.868%±0.150, n=3) (Fig. 24). In addition, no significant differences were found between unstressed control gastrodermal tissues ($p=0.304$) at 0 h ($\bar{x}$ = 0.711%±0.360, n=3) as compared to treatment tissues prior to heat stress ($\bar{x}$ = 0.843%±0.192, n=6). Similarly, no differences were found in unstressed control epidermal tissues ($p=0.582$) at 0 h ($\bar{x}$ = 0.609%±0.341, n=3) as compared to treatment epidermal tissues prior to heat stress ($\bar{x}$ = 0.576%±0.199, n=6). A statistically significant increase in % APSs was measured in both treatment gastrodermal tissues ($\bar{x}$ = 7.551%±2.741, n=6, $p=0.002$) and in treatment epidermal tissues ($\bar{x}$ = 5.303%±3.411, n=6, $p=0.004$) between 0 h and 48 h of heat stress (Fig. 24). Numerically, there was a slight difference in the means between the

gastrodermis ($\bar{x}$ = 7.551%±2.741, n=6) and epidermis ($\bar{x}$ = 5.303%±3.411, n=6) after 48 h of heat stress; however, that difference was not statistically significant (p=0.201) (Fig. 24). An overall lightening in the coloration of the treatment anemones was observed throughout the 48 h stress period indicating that the heat stress treatment induced a bleaching response. After 48 h a significant 12-fold increase ($p < 0.0001$) in expelled algae was observed in heat-treated anemones ($\bar{x}$ = 827,213±4946, n=3) as compared to unstressed controls ($\bar{x}$ = 68,880±902.1, n=3).

These results indicate that autophagic activity does increase in both symbiotic (gastrodermal) and non-symbiotic (epidermal) tissue layers during heat stress induced-bleaching, but that no other external environmental effects play a major role in the response. Cell apoptosis (as determined by the criteria of Dunn et al. (2002; 2004) and *in situ* degradation of symbionts as described by Taylor (1973) and Brown et al. (1995) was rarely observed in host and/or symbiont cells after the heat stress treatment. As expected, symbiont degradation was rare in control animals.

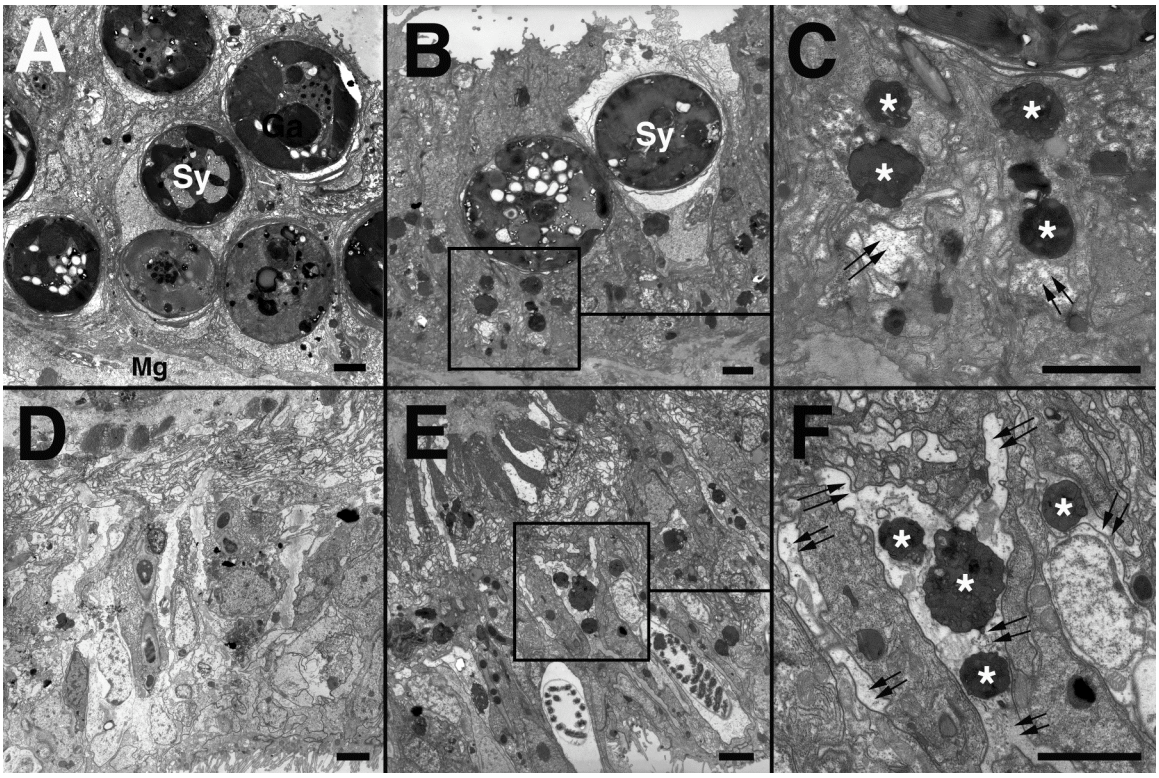

Figure 23: TEM. Transverse sections of symbiotic *Aiptasia pallida* tentacles at mid-tentacle length showing autophagic structures (APSs) in the gastrodermis (A-C) and epidermis (D-F) following heat stress. A) Symbiotic gastrodermal tissues at 0 h (no stress) treatment reveal a healthy ultrastructural appearance (note numerous symbionts = Sy), with few to no visible APSs in the host cytoplasm. B) Host tissues after exposure to 48 h of heat stress display numerous, dense, APSs and associated degraded regions, C) High magnification of boxed region in B showing dense APSs (asterisks) and degraded regions of cytoplasm (double black arrows), D) Epidermal tissue from a symbotic anemone at 0 h (no stress) treatment reveals a healthy appearance and few APSs, E) Host epidermal tissue after 48 h of heat stress treatment showing numerous APSs, F) Higher magnification of boxed region in E showing dense APSs (asterisks) surrounded by degraded cytoplasmic regions (double arrows). Scale bars = 2μm.

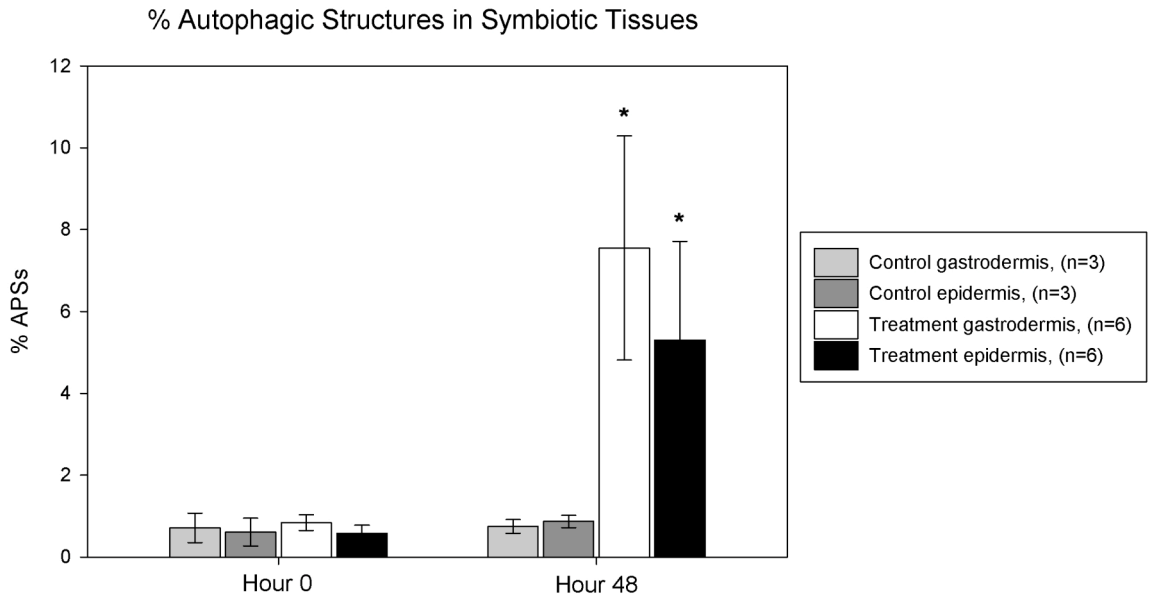

Figure 24: Percent autophagic structures within areas of gastrodermis and epidermis from symbiotic control anemones and within the gastrodermis and epidermis of treatment anemones after 0 and 48 h of control treatment or heat stress. Statistical significance was found in the change in % APSs present in both gastrodermis (p=0.002) and epidermis (p=0.004) of heat stress treatment anemones - designated with asterisks (paired t-test). The error bars represent standard deviation of the mean.

Autophagy in unstressed and heat-stressed aposymbiotic anemones

Unstressed aposymbiotic anemone tissues exhibited a normal overall appearance consisting of what might be described as a low irregular epithelium that was much thinner that that observed in symbiotic anemones. Unstressed aposymbiotic gastrodermal cells exhibited dense cytoplasm that contained few to no degraded regions or visible APSs (Fig. 25A). Alternatively, APSs and highly degraded cellular regions were observed in aposymbiotic gastrodermal tissues subjected to 48 h heat stress treatment (Fig. 25B and C) similar to those of symbiotic tissues (Fig. 23B and C).

Measurements of % APSs in aposymbiotic anemones revealed that there were no significant differences in unstressed control gastrodermal tissues (p=0.729) between 0 h ($\overline{x}$ = 1.514%±0.432, n=3) and 48 h ($\overline{x}$ =1.301%±0.613, n=3) or in unstressed control epidermal tissues

(p=0.291) between 0 h ($\bar{x}$ =0.205 %±0.091, n=3) and 48 h ($\bar{x}$ =0.320%±0.247, n=3). No significant differences were found between unstressed control gastrodermal tissues (p=0.255) at 0 h ($\bar{x}$= 1.514 %±0.432, n=3) and treatment gastrodermal tissues prior to heat stress ($\bar{x}$= 1.15 %±0.079, n=3). Similarly, no differences were found in unstressed control epidermal tissues (p=0.194) ($\bar{x}$=0.205%±0.091, n=3) and treatment epidermal tissues prior to or following heat stress ($\bar{x}$=1.611%±1.099, n=3) (Fig. 26). A statistically significant increase in % APS was seen in aposymbiotic treatment gastrodermal tissues after 48 h of heat stress ($\bar{x}$= 5.946%±0.584, n=3, p=0.004) (Fig. 26). A significant difference in % APSs was found between the gastrodermis ($\bar{x}$= 5.946%±0.584, n=3) and epidermis ($\bar{x}$=1.611%±1.099, n=3) after 48 h of heat stress (p=0.016) (Fig. 26).

Stressed aposymbiotic tissues displayed increased numbers of APSs and degraded regions in the gastrodermis similar to that observed in stressed symbotic anemones. This observation supports our hypothesis that the autophagic response is primarily host-derived.

Biochemical induction of autophagy

In order to confirm the role of autophagy in APS formation and subsequent cellular degradation during heat stress, several symbiotic anemones were exposed to 25μM rapamycin, a known inducer of autophagy (Noda and Ohsumi, 1998), in 1% DMSO for 12 h and % APSs was quantified as above. As noted in Chapter 3, examination of tentacle tissues from rapamycin treated anemones revealed a strikingly similar cellular appearance to those exposed to heat stress, exhibiting numerous APSs and degraded regions of cytoplasm (Fig. 25E and F).

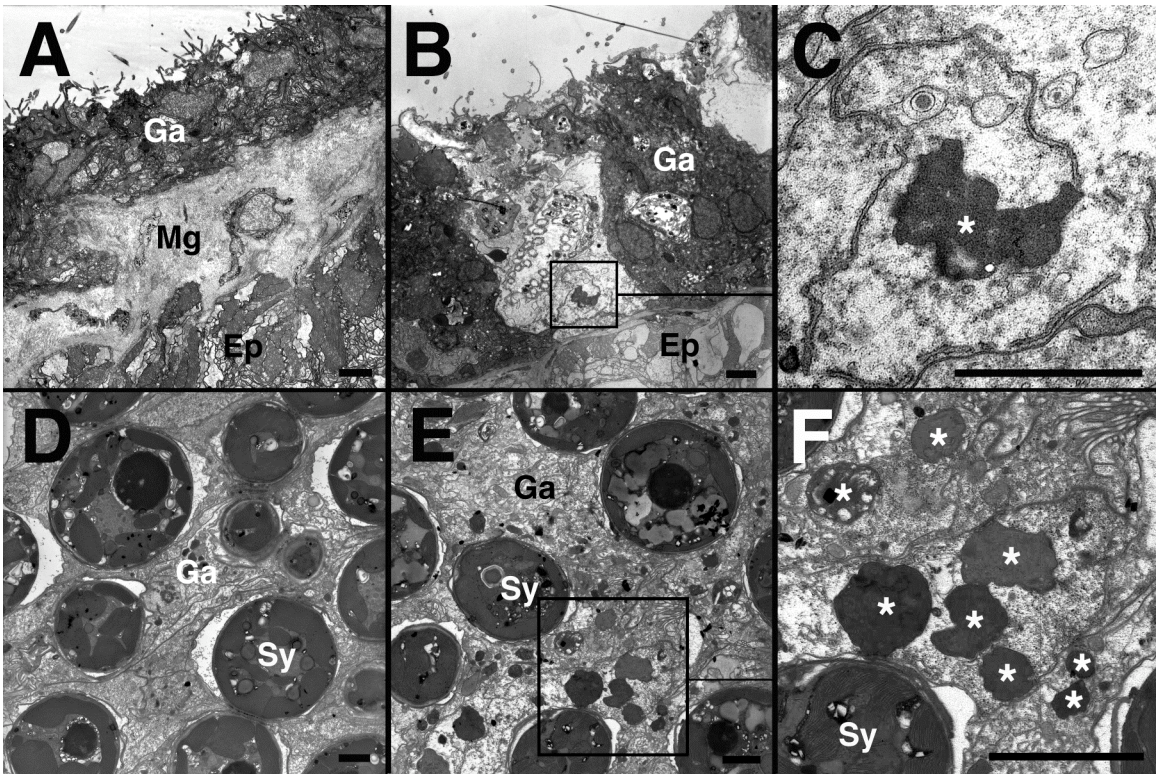

Figure 25: TEM: Transverse sections of *Aiptasia pallida* tentacles at midlength. Autophagic structures (APSs) form in aposymbiotic anemones (A-C) following heat stress and in rapamycin treated symbiotic anemones (D-F). A) Aposymbiotic gastrodermis tissues at 0 h (no stress) treatment reveal healthy ultrastructural appearance with few to no visible autophagic structures. B) Gastrodermal tissues at 48 h (stress treatment) display APSs and associated degraded regions (note degraded nematocyst in gastrodermis), C) Higher magnification of a dense APS (asterisk) D) Control symbiotic gastrodermal tissues exposed to 1% DMSO at 12 h (no stress) exhibit little to no APSs with no cytoplasmic degradation, E) Symbiotic gastrodermal tissues exposed to 12 h of 25 μM rapamycin result in the presence of numerous dark APSs with surrounding degraded cytoplasm, and F) Higher magnification of dense APSs (asterisks) in rapamycin treated gastrodermis. Scale bars = 2μm.

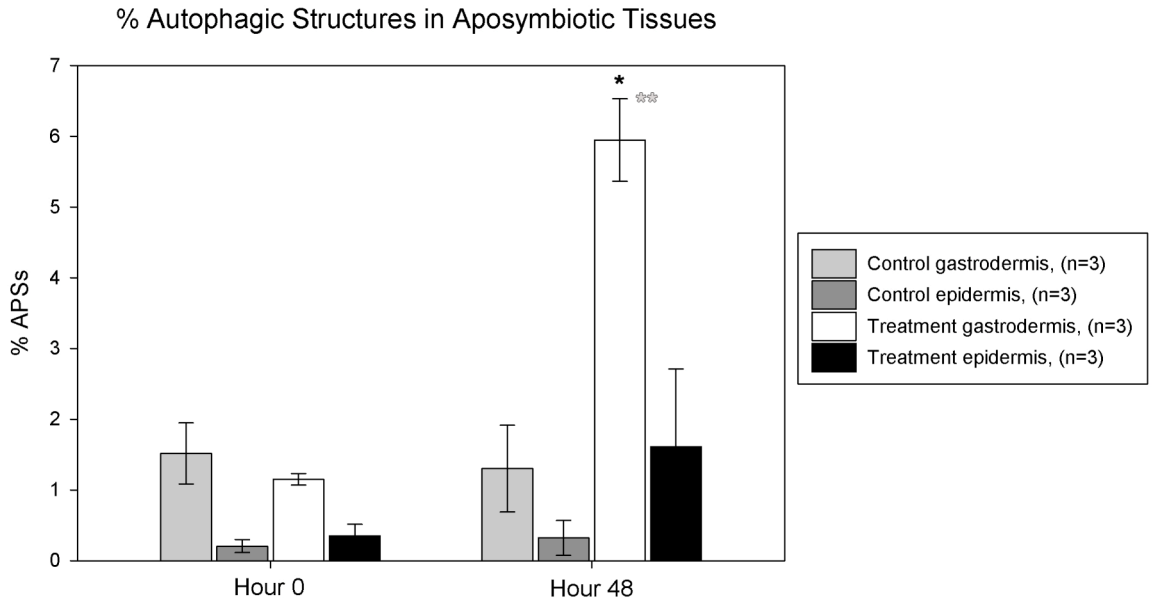

Figure 26: Percent autophagic structures within the gastrodermis and epidermis of aposymbiotic control and treatment anemones after 0 and 48 h. Statistical significance was found in the change in % APSs present in the gastrodermis of treatment anemones - designated with single black asterisk (paired t-test, p = 0.004). A significant difference in %APSs was also found between the gastrodermis and epidermis in treatment anemones after 48 h –designated by double gray asterisks (t-test, p=0.016). The error bars represent standard deviation of the mean.

A statistically significant increase in % APS was measured in treatment gastrodermal tissues incubated in 25µM rapamycin in 1% DMSO ($\bar{x}$ =9.134%±5.524, n=3, p=0.006) as compared to control tissues incubated in 1% DMSO for 12 h ($\bar{x}$ = 1.778%±1.206, n=3) (Fig. 27). A statistically significant increase in the % APS was also measured in treatment epidermal tissues incubated in 25µM rapamycin in 1% DMSO ($\bar{x}$ =3.883%±1.694, n=3, p=0.005) as compared to control tissues incubated in 1% DMSO for 12 h ($\bar{x}$ =1.245 %±0.333, n=3) (Fig. 27). A significant difference in % APSs was found between the gastrodermis ($\bar{x}$ =9.134%±5.524, n=3) and epidermis ($\bar{x}$ =3.883%±1.694, n=3) after 12 h of rapamycin treatment (p=0.010) (Fig. 27).

Since rapamycin has previously been employed to induce autophagy in a variety of taxa (Ohsumi and Mizushima, 2004), including *A. pallida* (Dunn et al., 2007; Chapter 3), these results

provide further evidence that the structures identified here and in heat stressed tissues were autophagic in origin. Similar to what was observed for heat stressed symbiotic anemones, a visible layer of expelled algae was present on the bottom of each treatment anemone container after 12 h of exposure to rapamycin. Rapamycin-treated anemones also exhibited an overall lightening in the coloration of all anemones when compared to DMSO-incubated controls. This finding suggests that autophagy, whether induced biochemically or by heat stress, can initiate a bleaching response.

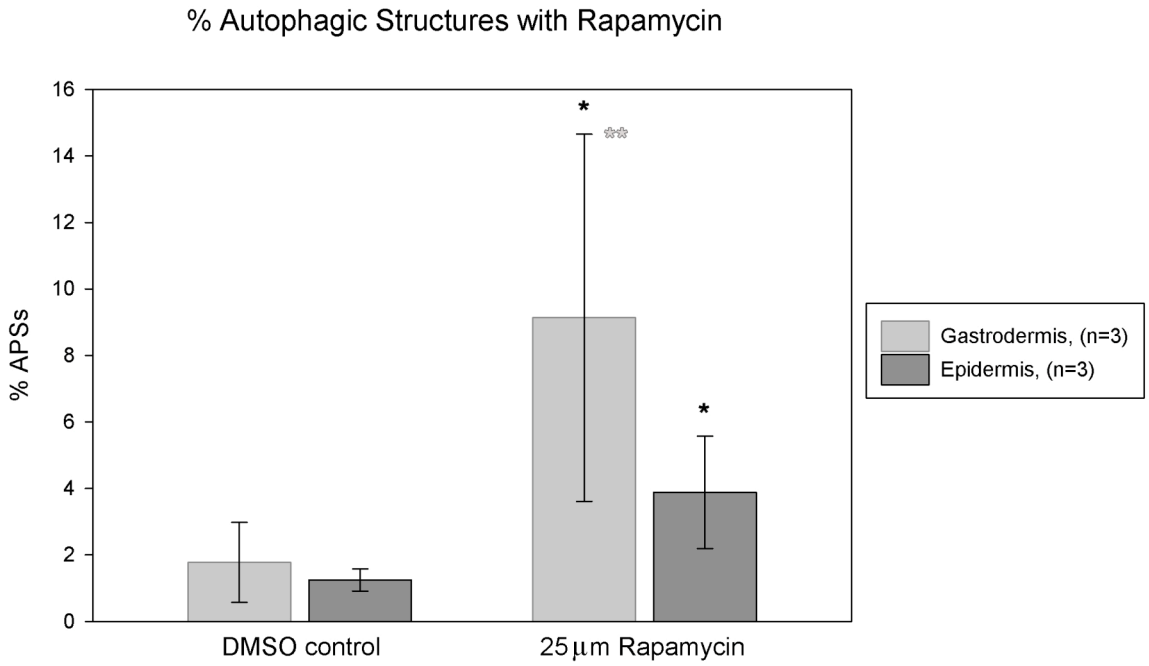

Figure 27: Percent autophagic structures within the gastrodermis and epidermis of symbiotic control (12 h in 1% DMSO) and treatment (12 h in 25 μM rapamycin + 1% DMSO) anemones. Statistical significance was found in the difference in % APSs present in both gastrodermis (p=0.006) and epidermis (p=0.005) of treatment anemones as compared to control anemones-indicated by single black asterisks (paired t-test). A significant difference in % APSs was also found between the gastrodermis and epidermis in treatment anemones after 12 h –designated by double gray asterisks (t-test, p=0.010). The error bars represent standard deviation of the mean.

Conclusions

Autophagy is a highly conserved response pathway that has been identified in a wide variety of taxa (Boya et al., 2005). The autophagic process is tightly regulated by the inhibitory action of the protein kinase, target of rapamycin (TOR), which is controlled through the PI3K/AKT signaling pathway (Levine and Yuan, 2005; Lum et al., 2005). This autophagic pathway regulates a series of developmental stages (described in Chapter 3) that begins with the inclusion of cellular structures/materials within a vacuole, followed by a fusion of that vacuole with a lysosome and degradation of the contents via hydrolytic enzymes. After degradation has occurred, the products are released into the cytoplasm to support biosynthesis of new proteins and other essential materials (Nivon et al., 2009).

In this study, we have performed quantitative measurements on heat stressed symbiotic anemones that verify the autophagic response was widespread and significantly affected both the symbiotic gastrodermal and non-symbiotic epidermal layers. Based on these observations and those made in Chapter 3, we investigated the potential role of the symbionts during the autophagic response by exposing aposymbiotic anemones to an identical heat treatment as symbiotic anemones. Our results demonstrated that aposymbiotic gastrodermal tissues also exhibited a significant increase in autophagic degradative activity after 48 h of heat treatment. These findings indicate that the presence of symbionts is not necessary to initiate an autophagic response to heat stress and thus, that the up-regulation of autophagic activity in stressed anemones is primarily host-derived.

While quantitative changes in autophagic activity were not significant in the epidermis in aposymbiotic heat-stressed anemones, such upregulation of autophagy did occur in the epidermis

of heat stressed symbiotic anemones. This suggests that the presence of symbionts may enhance the autophagic response in host anemones by contributing additional ROS that would increase oxidative stress levels throughout host tissues. Interestingly, the gastrodermis had significantly higher levels of autophagic activity than the epidermis in both the aposymbiotic and rapamycin-treated tissues. This result suggests that there may be physiological differences between gastrodermal and epidermal tissue layers, such as sensitivity to oxidative stress. However, the fact that in heat stressed symbiotic anemones, both the gastrodermis and epidermis exhibited similar levels of autophagic activity suggests that the heat stress response may induce a different autophagic pathway than rapamycin. This variation in stress pathways may also account for the decreased level of autophagic degradation observed in rapamycin treated tissues compared to those heat-stressed.

Autophagy occurs at basal levels in most cells (Ohsumi and Mizushima, 2004) and functions to maintain cell homeostasis by degrading long-lived proteins and/or damaged organelles (Gozuacik and Kimchi, 2007; Levine and Yuan, 2005; Nivon et al. 2009). However, during stressful conditions, autophagy functions primarily to protect cells from significant injury (Swanlund et al., 2008). For example, it is thought that during periods of nutrient deprivation, autophagic activity is upregulated in order to promote cell survival by maintaining mitochondrial ATP energy production through the use of recycled nutrients (Levine and Yuan 2005). Hyperthermic stress conditions can also induce autophagy (Nivon et al., 2009; Oberley et al., 2008; Prasad et al., 2007; Swanlund et al., 2008) in order to clear the cell of damaged organelles and misfolded proteins (Nivon et al., 2009). In addition, autophagy may also function to eliminate cells altogether *via* autophagic cell death (Gozuacik and Kimchi, 2007; Kourtis and Tavernarakis 2009; Xue et al. 2001).

In this current study and in Chapter 3, heat stressed autophagic tissues contained numerous APSs and exhibited varying degrees of cellular degradation. Extensively degraded cells, where organelles and major portions of the cytoplasm were removed, exhibited characteristics of autophagic cell death (Gozuacik and Kimchi, 2007). These cells were frequently observed in both symbiotic and aposymbiotic heat stressed tissues, primarily in the gastrodermis. However, no similar cellular degradation was observed in tissues after exposure to rapamycin, which is known to induce autophagic activity, but not autophagic cell death (Levine and Yuan, 2005). This suggests that the major cytoplasmic degradation observed in many cells of heat stressed symbiotic anemones was an indicator of autophagic cell death events and that this mechanism may be a major contributor to host tissue damage during bleaching events caused by heat stress. Heat stress may upregulate autophagy in an attempt to promote cell survival by recycling nutrients from digestion of damaged organelles and other cytoplasmic constituents. However, if the stress is severe or persists long enough, the damage resulting from autophagy may outweigh positive factors and autophagic cell death may lead to extensive and perhaps irrecoverable tissue damage and eventual host death.

The transition from pro-survival to pro-death pathways is commonly determined by the duration and intensity of the stress conditions (Gozuacik and Kimchi, 2007). Here we provide evidence to confirm that autophagic activity is upregulated during the first 48 h of sub-lethal temperature stress conditions in the absence of significant levels of other cell death mechanisms. It has been shown in other systems that autophagy can occur in the absence of apoptosis or necrosis in response to mild heat stress, but not acute heat shock (Komata et al., 2004). Thus, further investigations are necessary to determine whether it is possible that cell apoptosis and/or

necrosis may additionally occur or replace autophagy after the 48 h stress period examined in our research.

V. Differential gene expression responses to elevated temperature in symbiotic *Aiptasia pallida* anemones using RNA-Seq

Abstract

Coral reefs have dramatically declined over the past few decades as a result of mass mortality bleaching events. Bleaching is as a stress response to elevated temperature and/or light conditions resulting in the loss of intracellular dinoflagellates of the genus *Symbiodinium* from host gastrodermal tissues. This process involves a complex series of events that occur throughout the duration of the bleaching episode and involve cellular interactions between both symbiotic members. However, few studies have investigated the early host stress response when symbiotic breakdown is initiated. In this study, molecular techniques were employed to characterize the host response during the first 48 hours of heat and light stress in *Aiptasia pallida*. Both symbiotic and aposymbiotic anemones were exposed to stress conditions of ~32.5^{o}C at 140 μmol photons $m^{-2}s^{-1}$ irradiance for 12 hours daily followed by 12 hours of darkness at ambient temperature over a 48 h period. Differential gene expression was measured at 0, 3, and 48 hours post stress onset using an RNA-Seq procedure. Results from this investigation indicate that the gene expression profile of *A. pallida* changes during early stages of bleaching, and several key processes were identified that are involved in the host response, including stress response, protein degradation/synthesis, calcium homeostasis, cell-cell interactions, and vesicle trafficking. This study provides a better understanding of the genetic determinants of stress tolerance in a host anthozoan, and offers further insight into the cellular processes that underlie coral bleaching.

Introduction

Coral reefs represent one of the most productive and diverse ecosystems on earth; however, numerous anthropogenic stressors currently threaten their survival (Hoegh-Guldberg et al., 1999, Donner et al., 2007). Coral decline results primarily as a result of the symbiotic breakdown between corals and their intracellular photosynthetic dinoflagellates (=*Symbiodinium*) through a process known as coral bleaching. Although coral bleaching can occur in response to a variety of environmental disturbances, elevated temperatures associated with global climate change are one of is the primary cause of large-scale mass mortality bleaching events (Hughes, 2003; Hoegh-Guldberg et al., 2007).

Symbiotic breakdown is initiated when high levels of reactive oxygen species (ROS) are produced during temperature or light stress (Lesser, 1996; Franklin et al., 2004; Lesser, 2006). ROS production has been shown to occur at high levels in thermally stressed symbionts leading to decreased photosynthetic capability of the symbionts through photoinhibition and subsequent photodamage to photosystem II (PSII) (Warner et al. 1999; Lesser 2006). Alternatively, host cells also independently produce ROS as a result of thermal stress-induced mitochondrial membrane damage (Nii and Muscatine, 1997; Dunn et al., 2012; Chapter 3). When ROS overwhelm the intracellular antioxidant defenses and directly damage cellular structures, bleaching often results. Our current information surrounding the bleaching process has historically been biased towards the response of the algal symbiont (Baird et al., 2008; Weis, 2008). Thus, our current understanding of the responses of corals or other symbiotic cnidarian hosts remains limited (Weis, 2008; Desalvo et al., 2011) despite increasing evidence that suggests that symbiotic dysfunction begins in the host cell (Ainsworth et al., 2008; Dunn et al., 2012; Chapter 3).

Recent advancements in molecular techniques, such as cDNA microarrays and other genetic methods have provided valuable information on how thermal stress impacts a variety of coral hosts (Downs et al., 2000; Edge et al,. 2005; Morgan et al., 2005; Perez and Weis 2006; Richier et al., 2006, 2008; Foret et al., 2007; DeSalvo et al. 2008; Schwarz et al. 2008; Meyer et al., 2011). These studies enable us to address important questions surrounding future bleaching scenarios and develop accurate models of the series of cellular events that occur in the symbiotic host that result in collapse of the symbiosis (Weis, 2008). However, such investigations have been limited by the lack of an experimentally tractable system. The anemone, *Aiptasia pallida,* provides a suitable model system to examine this problem (Weis et al., 2008; Sunagawa et al., 2010; Lehnart et al., 2012). *Aiptasia* maintains a symbiotic relationship with *Symbiodinium* spp. (Sunagawa et al., 2010), and the lack of a calcareous skeleton allows cell biological and microscopical manipulations to be conducted much more easily than in corals. *Aiptasia* also can grow very quickly and are very inexpensive and easy to maintain in the lab. *Aiptasia* spp. maintains a similar relationship with a variety of *Symbiodinium* spp. as do some corals, but can also exist in an aposymbiotic (symbiont-free) state (Weis et al., 2008; Sunagawa et al., 2010; Lenhart et al., 2012). Investigations using the *Aiptasia* model can reveal key cellular events that occur during various stages of the symbiosis, including establishment, maintenance, and breakdown. More recently, significant progress has been made in sequencing technology that has made possible the sequencing and de novo assembly of whole transcriptomes from non-model organisms (Meyer et al., 2009, 2011; Lehnart et al., 2012). Transcriptomic and EST sequences have been made available from a variety of corals (Schwarz et al., 2008; Meyer et al., 2009; 2011; Voolstra et al., 2009) as well as a number of symbiotic anemones, including *A. pallida* (Sunagawa et al., 2009; Lehnart et al., 2012), *Anemonia viridis (*Sabourault et al., 2009),

and *Anthopleura elegantissima* (Richier et al., 2008). These sequence data allow comparative genomics to be assessed among the Scleractinia or Anthozoa, respectively. Furthermore, several cnidarian genomes have recently been completed, and include *Nematostella vectensis* (Putnam et al., 2007), *Hydra magnipapillata* (Chapman et al., 2010), and *Acropora millepora* (Shinzato et al., 2011), enabling genetic analyses to be conducted within members of the phylum. In addition, the transcriptomes of *Symbiodinium spp.* clades A and B have been made public (Bayer et al., 2012), which will allow algal sequences to be distinguished from those of the host.

This study used RNA-Seq to characterize how the gene expression profile of *A. pallida* changes during early stages of bleaching. Several key functional pathways are identified that are involved in the host stress response. In particular, changes in the expression of genes with roles in the stress response, protein degradation/synthesis, calcium homeostasis, cell-cell interaction, and vesicle trafficking were of the most abundant. This study provides a better understanding of the genetic determinants of stress tolerance in a host anthozoan, and offers further insight into the cellular processes that underlie coral bleaching.

Materials and Methods

Culture conditions

Aiptasia pallida harboring symbionts typed as Clade A4 *Symbiodinium* (Santos et al. 2002; Scott Santos, 'personal communication') were collected in the Florida Keys and maintained in artificial seawater (Reef Crystals) at 28-30 ppt salinity. Symbiotic anemones were kept in two 150 gal tanks at 24°C below fluorescent lamps producing 50±5 (± standard deviation) μmol photons $m^{-2}s^{-1}$ irradiance at the level of the anemones. Lights were set on a 12:12 h light/dark regime.

A separate group of anemones, also collected from the Florida Keys, were rendered aposymbiotic by long-term (> 10 years) maintenance in complete darkness in a 150 gal tank at 24°C. The absence of *Symbiodinium* was verified by using PCR nuclear 18S rDNA (Rowan and Powers, 1991) and chloroplast 23S rDNA (Santos et al, 2002). In both cases no PCR product was produced (Scott Santos, 'personal communication'). All anemones were fed freshly hatched *Artemia* larvae three times per week.

Temperature treatments for symbiotic and aposymbiotic anemones

Both symbiotic and aposymbiotic anemones were subjected to the following heat stress treatment previously described in Chapter 3. Both symbiotic (n=6) and aposymbiotic (n=1) medium sized anemones were placed in identical, individual dishes and allowed to acclimate for ~4 days at the ambient room temperature of 24^{o} C under fluorescent light fixtures, each equipped with two 32W bulbs (Phillips F32T8/TL841) producing 50±5 μmol photons $m^{-2}s^{-1}$ irradiance at the level of the anemones. Lights were set on a 12:12 h light/dark regime. Water in these dishes was changed daily and the anemones were fed once during the first 3 days and then held unfed for 48 h prior to the beginning of the experiments. Both symbiotic and aposymbiotic treatment anemones were then transferred in their containers to an incubator at 32.5^{o} C and placed beneath two lamps each equipped with two 20W fluorescent bulbs (GE Ecolux F20T12/G50-ECO) that emitted ~140 μmol photons $m^{-2}s^{-1}$ light intensity at the level of the anemones. The anemones were held in the incubator for 12 h and then removed to a dark, well-ventilated box on the lab bench for 12 h in darkness at 24^{o} C. The incubator and dark box treatments were then repeated over the following 24 h for a total treatment time of 48 h. It took approximately 2.5 h for the 24^{o} C dishes to warm to 32.5^{o} C in the incubator under these conditions. This study primarily focuses

on the effects of heat stress. There was a small difference in light intensity between the anemone culture tanks (50 μmol photons $m^{-2}s^{-1)}$ and the incubator (140 μmol photons $m^{-2}s^{-1}$); however, this is well within the field light intensities (0 to >1000 μmol photons $m^{-2}s^{-1}$) that these symbiotic anemones experience and was not considered to be the primary stressor in our experiments. After exposure to 0, 3, 12, 24, or 48 h of heat stress, approximately ½ of the tentacle crown of symbiotic and whole tentacle crowns of aposymbiotic anemones were excised using forceps and iridectomy scissors and immediately transferred to RNAlater and stored at -20° C.

Preparation of cDNA for Illumina sequencing

Total RNA was extracted from each sample using 1 mL TRIzol and treated with DNAse I to remove residual genomic DNA contamination. cDNA tag libraries were prepared from each RNA sample (n=3 symbiotic and n=1 aposymbiotic for each sampling time) as previously described for the SOLiD System (Meyer et al, 2011), substituting adaptor sequences appropriate for the Illumina HiSeq sequencing platform. Each library was labeled with a sample-specific 6-bp barcode and gel-extracted to isolate the 350-500 bp size fraction.

Sequencing, filtering and mapping

cDNA libraries were pooled for sequencing on a single lane of Illumina HiSeq 2000 (100-bp read length) at Oregon State University's Center for Genome Research and Biocomputing (CGRB). Libraries were initially prepared using custom adaptors that incorporated barcodes ("indices") on both the 5' and 3' end of the construct, so that sample identities were encoded by unique combination of barcodes. Samples were pooled for multiplex sequencing in a single lane on the Illumina HiSeq 2000 (100-bp SE reads) using standard Illumina reagents to sequence the insert and the 3' barcode ("index 1"), but with a custom

sequencing primer for the 5' barcode ("index 2"). Because we found low sequencing efficiency with this custom primer, which prevented demultiplexing of samples based on barcode sequences, we subsequently prepared additional libraries for the 0, 3, and 48 hr samples using new adaptors compatible with standard Illumina TruSeq primers. These new libraries were pooled for multiplex sequencing in a single lane of Illumina HiSeq 2000 SE 100-bp reads at CGRB.

Sequences were processed prior to mapping to remove low-quality and uninformative reads. First, the four non-template bases introduced by reverse transcriptase were trimmed off the raw sequences at the 5' end of each read. Low-quality reads having more than 50 bases with quality scores below 20 were excluded using custom Perl scripts. Any high-quality (HQ) reads matching adaptors used in library preparation (≥15 matching bases) were identified using cross_match (REF) and excluded using custom Perl scripts.

Analysis of tag-based RNA-Seq data requires a reference assembly against which to map the reads, as previously described (Meyer et al, 2011). We initially attempted to analyze these data using a recently published transcriptome assembly for *A. pallida* (Lehnart et al., 2012), but found that redundancy in the assembly led to a substantial loss of data because of ambiguous matches. To address this we constructed a custom transcriptome assembly using sequence data from the published transcriptome (Lehnart et al., 2012), but including only reads derived from aposymbiotic samples. Reads were first filtered to eliminate low-quality reads and reads matching adaptors, as described above. The HQ reads that remained were assembled using Trinity (Grabherr et al, 2011) with minimum kmer coverage = 2. Assembled transcripts were annotated by comparison against UniProt (v2012_06) using BLASTX (e-value threshold = 10^{-4}).

Identification of differentially expressed genes (DEGs)

All calculations and statistical tests were conducted using the R statistical software (version 3.0.0) (R Development Core Team, 2008). We focused our attention on transcripts expressed at ≥2 reads per sample on average, and further excluded any transcripts present in symbiotic samples, but absent in aposymbiotic samples, which might be derived from *Symbiodinium* rather than *Aiptasia*. Read counts were summed across sequencing runs by sample. Expression differences were tested using a negative binomial test implemented in the R package DESeq (version 1.12.0) (Anders & Huber, 2010).

To identify genes differentially expressed in response to the heat stress treatment, we compared expression profiles at the early (3 hour) and late (48 hour) sampling points with initial samples (0 hours). The un-replicated aposymbiotic samples were not used for statistical comparisons, but only used to verify that transcripts were derived from host rather than symbiont. False discovery rate (FDR) was controlled at 5% (Benjamini & Hochberg, 1995).

Results and Discussion

Sequencing, mapping and assembly

Altogether, 115,131,741 raw reads were obtained by sequencing pooled libraries. 82,223,991 HQ reads (71%) remained after quality and adaptor filtering. The gene from which each read originated was identified by mapping HQ reads against an annotated aposymbiotic *Aiptasia* transcriptome. 61,737,036 of these (75% of HQ reads, or 54% of raw reads) were aligned unambiguously against the reference transcriptome.

Response to temperature treatments

Statistical analysis of RNA-Seq counts data (the number of reads mapped to each gene in each sample) revealed large shifts in gene expression resulting from elevated temperature stress. Exposure to 3 h of heat stress induced the differential expression of 293 genes in symbiotic anemones (negative binomial model, FDR = 0.05) (Fig. 28). Of these, 213 genes were upregulated and 80 were downregulated. In later samples (48 h) only 21 genes were differentially expressed, of which 6 were upregulated and 15 were downregulated (Fig. 29). Fold changes ranged from +30.62 to -9.90. 232 of the 293 DEGs identified in 3 h samples (79%) matched known proteins (based on a BLASTX search against UniProt), and 7 of the 21 genes identified in the 48 h timepoint.

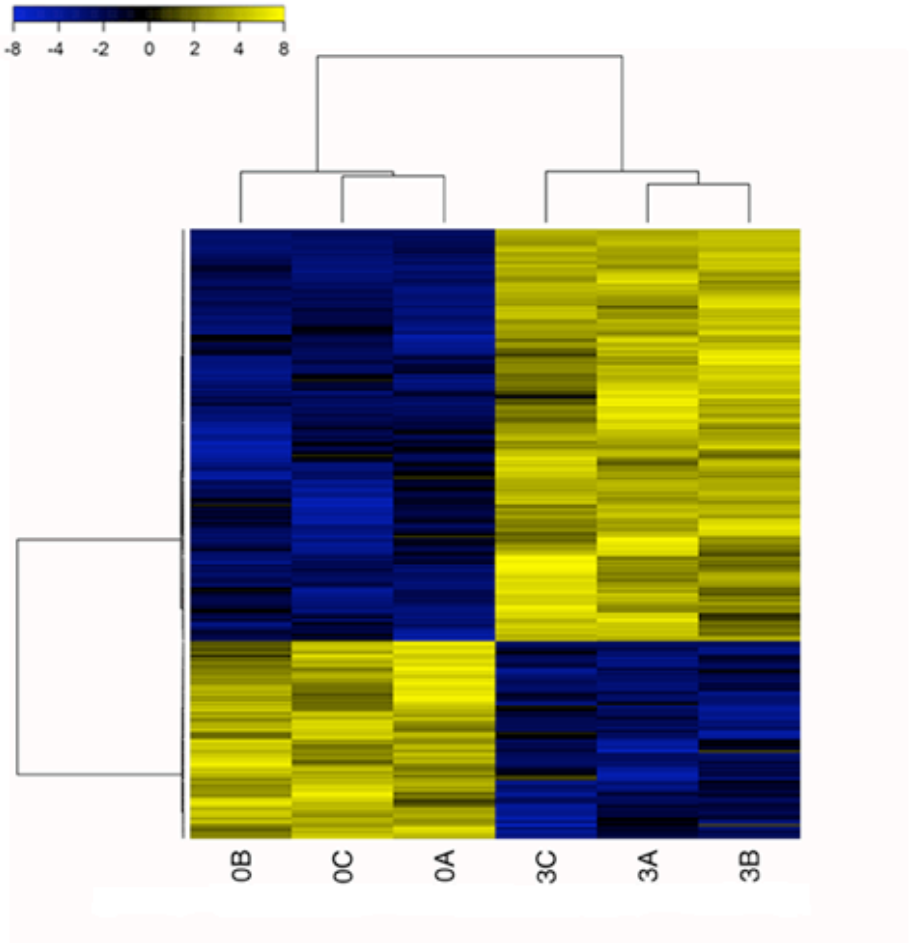

Figure 28. Cluster analysis of differentially expressed genes from control anemones (0A-C, n=3) and anemones exposed to 3 h of thermal stress treatment (3A-C, n=3). Top dendrogram shows distinct clustering of treatment anemones (3A-C) relative to control anemones (0A-C). Side dendrogram shows clustering of genes based on type. Colors represent gene expression patterns; yellow indicates upregulated genes and blue indicates downregulated genes (see color/expression scale in upper left corner).

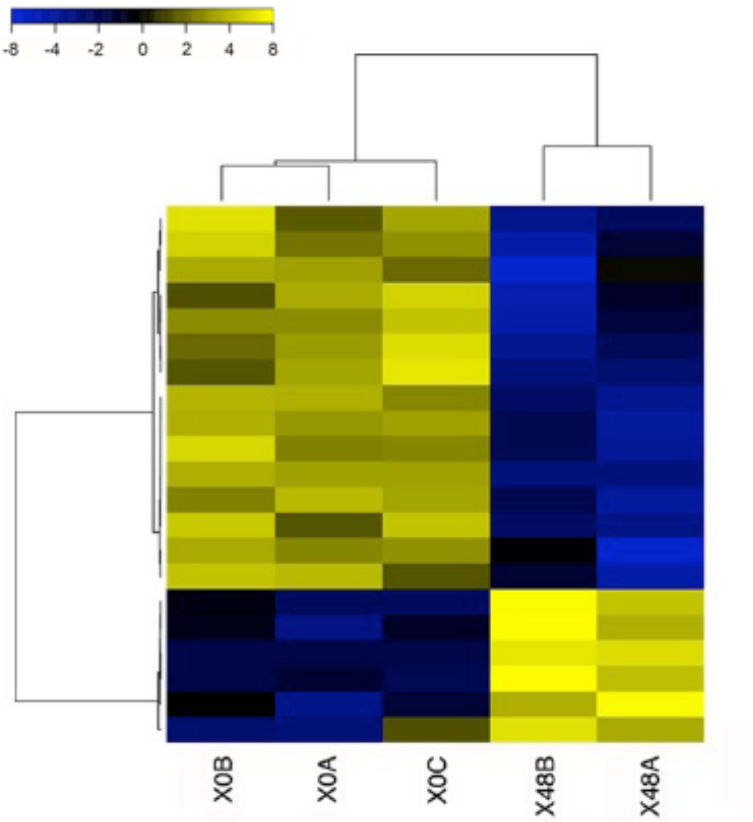

Figure 29. Cluster analysis of differentially expressed genes from control anemones (0A-C, n=3) and anemones exposed to 48 h of thermal stress treatment (48A-B, n=2). Top dendrogram shows distinct clustering of treatment anemones (48A-B) relative to control anemones (0A-C). Side dendrogram shows clustering of genes based on type. Colors represent gene expression patterns; yellow indicates upregulated genes and blue indicates downregulated genes (see color/expression scale in upper left corner).

A subset of the differentially expressed genes (DEGs) produced in this study were categorized into putative functional groups according to GO molecular function or manually defined functions based on literature and database searches (Table 1). After 3 h of thermal stress, the most abundant DEGs were those that had putative functions in the i) general stress response, ii) protein/endosome sorting-assembly, iii) protein degradation, iv) calcium binding/transport, and v) cell adhesion. A majority of these DEGs were upregulated. After 48 h of thermal stress, majority of the annotated DEGs had putative functions involved in i) protein degradation, ii) cell adhesion, and a wide variety of iii) miscellaneous processes that were mostly downregulated. In

both the 3 and 48 h samples many of the DEGs could not be identified based on sequence comparisons (Table 1).

Table 1. Differentially expressed genes after 3 h and 48 h of thermal stress treatment relative to 0 h controls categorized into functional groups.

Gene/Function[1]	Match[2]	Sym 3h FD[3]	P value[3a]	Sym 48h FD[4]	P value[4a]
Stress response					
Heat shock protein 70 (HSP70)	Q5FB18	7.58	<0.0001		
Heat shock protein 90 alpha (HSP90a)	G4W8Y9	7.14	<0.0001		
Hypoxia upregulated protein 1 (hyou1)	F1QUW4	5.85	<0.0001		
Cysteine-rich with EGF-like domain protein 2 (creld2)	Q7SXF6	5.35	<0.0001		
DnaJ homolog subfamily C member 3 (dnajc3)	Q7ZWH5	4.64	<0.0001		
Glucose-regulated protein 94 (GRP94)	A5LGG7	4.29	<0.0001		
Stress-70 protein, mitochondrial (HSPA9)	Q5R511	3.15	<0.0001		
Universal stress protein A-like protein (CLF113016)	H2KVS5	-2.41	0.0002		
Protein degradation/synthesis					
KRR1 small subunit processome component (v1g71320)	A7S7I3	5.71	<0.0001		
Cathepsin L (CATL)	C1BJ28	4.42	<0.0001		
Ubiquitin (UBIQ)	C1BNT5	3.36	<0.0001		
Kelch-like protein 20 (KLHL20)	F1NMM8	2.58	<0.0001		
FAD-dependent oxidoreductase domain-containing protein 2 (FOXRED2)	Q8IWF2			-3.75	0.0018
Cation- dependent mannose- 6- phosphate receptor (MPRD)	B5X109	-3.45	0.0002	-4.04	0.0054
Calcium homeostasis					
Calumenin (CALU)	Q5RDD8	3.63	<0.0001		
Sarco/endoplasmic reticulum calcium ATPase isoform B (SERCA)	B2KKR1	3.08	<0.0001		
Cell-cell interactions					
Galectin-3-binding protein (GW710920)	G5AVF6	2.00	0.0053	2.93	0.0237
Putative cell adhesion protein (Sym32)	Q9NH96	2.84	<0.0001		
Ankyrin repeat protein, putative (TVAG137200)	A2FNS2			-3.44	0.0054
Vesicle trafficking					
RAB26 (rab26)	A0JM47	1.97	<0.0001		
Vesicle-trafficking protein (SEC22B)	Q5ZJW4	1.82	0.0313		
Miscellaneous					
Heme binding protein (MICPUN58704)	C1E6L8	8.99	<0.0001		
Cryptochrome 1 (CRY1)	A2I2P0	5.21	<0.0001		
Wu:fb63a08 protein (wu:fb63a08)	A5D6R8	2.15	0.0020	-3.32	0.0164
Hemagglutinin/amebocyte aggregation factor (HAAF)	B5XEP9			-3.75	0.0018
Krox protein (Krox)	Q9NFK6	-2.04	0.0052	-3.92	0.0212
Cytochrome P450 (cyp46a1)	O97689	-2.56	0.0131		
PAR domain protein 1 (Pdp1)	B0LD02	-6.64	0.0061		
Unknown					
comp20613		30.62	<0.0001		
comp33713				5.11	<0.0001
comp27177		3.03	<0.0001	3.84	0.0009
comp4114		-7.77	<0.0001		
comp15191				-9.90	<0.0001

[1] Genes chosen based on expression values or functional significance and organized into functional groups designated according to Uniprot biological/molecular function or manually defined functions based on literature and database searches.

[2] Match based on Uniprot accession numbers

[3] Fold difference values for symbiotic samples after 3 h relative to 0 h controls

[4] Fold difference values for symbiotic samples after 48 h relative to 0 h controls

[a] p-value (negative binomial model (DESeq), False discovery rate= 0.05) all <0.05

Table 1. Differentially expressed genes after 3 h and 48 h of thermal stress relative to 0 h controls categorized into functional groups that correspond to heatmaps in Figures 28 and 29. Genes represent a subset of the total population of differentially expressed genes chosen based on their high expression values and their functional significance as detected by RNA-Seq. Expression values are shown as fold change for each time point. Putative functional roles are designated according to Uniprot molecular/biological function or manually defined functions based on literature and database searches.

Hierarchical clustering was used to group DEGs with similar expression patterns in the 3 h (Fig. 28) and 48 h (Fig. 29) samples. For both time points, this revealed groups of genes upregulated and downregulated relative to the 0 hr controls. Samples showing similar expression patterns were grouped in the same way, revealing that DEG showed reproducible changes across samples. The majority of DEGs after 3 h were upregulated (73%) relative to 0 hr controls (Fig. 28). Some of these highly upregulated genes were associated with stress response (*HSP70, HSP90a, hyou1*, *creld2, dnajc3, GRP94*), protein degradation/synthesis (*CATL*, *v1g71320, UBIQ*), calcium homeostasis (CALU), cell-cell interactions (*Sym 32*), and vesicle trafficking (*rab26*), while others had miscellaneous (*MICPUN58704*, *CRY1*) and unknown functions (e.g. *comp20613*, with a fold change of 30.62).

A smaller subset of DEGs were downregulated (27%) after 3 h of temperature stress (Fig. 28). Some of these downregulated genes were associated with stress response (*CLF113016*) and others had miscellaneous (*Pdp1*, *cyp46a1*) and unknown functions (e.g. *comp4114*, with a fold change of -7.77).

In contrast to gene expression profiles in the 3 h samples, a majority (71%) of DEGs were downregulated after 48 h of temperature stress (Fig. 29). Some of these highly downregulated genes were associated with protein degradation/synthesis (*MPRD*, *FOXRED2*), cell-cell interactions (*TVAG137200*), and others had miscellaneous (Krox, HAAF, *wu:fb63a08*) and unknown functions (e.g. *comp15191*, with a fold change of -9.90).

A smaller subset (29%) of DEGs were upregulated after 48 h of temperature stress (Fig.

29). Some highly upregulated genes were associated with cell-cell interactions (*GW710920*) and others had unknown functions (*comp33713*, with a fold change of 5.11).

Differential expression across time points

Several genes exhibited differential gene expression after both 3 and 48 h of thermal stress, five of which showed significance ($p < 0.05$) in both timepoints (Table 1). These included 1) *MPRD* (downregulated at 3 and 48h), 2) *GW710920* (upregulated at 3 and 48 h), 3) *Wu:fb63a08* protein (upregulated at 3 h and downregulated at 48 h), 4) *Krox* (downregulated at 3 and 48h), and 5) an unknown protein *comp27177* (upregulated at 3 and 48h).

Some genes exhibited constituitive expression at both 3 and 48 h timepoints (Figs 28 and 29). Notable DEGs included *Sym32* (upregulated 2.84 and 2.66 fold respectively) and *rab26* (upregulated 1.97 and 2.22 fold respectively). In contrast, several genes showed dramatic change in their expression over time, the majority of which were upregulated after 3 h and either remained unchanged or were downregulated after 48 h of thermal stress (Figs 28 and 29). DGEs involved in the putative stress response that exhibited this pattern were *HSP70, HSP90a, hyou1*, and *creld2*, which increased 7.58, 7.14, 5.85, and 5.35 fold, respectively, after 3 h of thermal stress. Upregulation of the genes decreased to 1.09, 1.84, 1.27, 1.36 fold after 48 h. Following the same trend, several DEGs involved in protein degradation, including *v1g71320* and *CATL*, exhibited fold changes of 5.71 and 4.42 fold, respectively, and these values both decreased to 1.73 and 1.82 fold after 48 h. Another notable gene, FOXRED2, was downregulated -3.85 fold after 3 h and upregulated 1.20 fold after 48 h. Some highly expressed miscellaneous DEGs were Heme-binding protein *(MICPUN58704*) (upregulated 8.99 fold after 3 h and downregulated -1.72 fold after 48 of thermal stress) and *Pdp1* (downregulated -6.64 fold after 3 h and

upregulated 1.62 fold after 48 h).

Major functions involved during temperature stress

Stress response

The majority of the genes that were categorized into putative functional groups were associated with the stress response (Table 1). Interestingly, almost all of the DEGs in this group were highly upregulated after 3 h, but remained stable or were downregulated in 48 h samples. This finding supports previous suggestions that the stress response can vary with the length of the thermal treatment in *Aiptasia* spp. (Dunn et al., 2002, 2004; Chapter 3).

The genes involved in this response include the ubiquitous heat shock proteins (HSPs), such as *HSP70, HSP90a*, etc. (Bromage et al., 2009). These proteins act as molecular chaperones that assist in folding newly synthesized proteins in order to maintain tertiary structure (Buckley and Hofmann, 2002). During temperature or light stress conditions, this response maintains proper cell function (Baird et al., 2009). Not surprisingly, RNA-Seq results from this study indicated the upregulation in several HSP genes, including *HSP70, HSP90a, dnajc3* (*HSP40*), and Stress-70 protein (*HSPA9*) in heat stressed *A pallida* after 3 h. These results agree with previous studies documenting the induction of HSPs in response to thermal stress in a variety of cnidarians (Sharp et al., 1994, 1997; Black et al 1995; Fang et al., 1997; Downs et al., 2000, 2002, 2005; Gates and Edmunds, 1999; DeSalvo et al., 2008; Meyer et al., 2011). Other DEGs associated with ER-stress, often caused by mis/unfolded proteins in the lumen of the endoplasmic reticulum (Ron and Walter, 2007), were upregulated in this study after 3 h of thermal stress, which have been previously documented in cnidarians, including hypoxia

upregulated protein 1 (hyoup1) (Aranda et al., 2011) and glucose-related protein 94 (GRP94) (Sharp et al. 1994; Hashimoto et al., 2004).

Protein degradation/synthesis

Numerous genes associated with a protein degradation or synthesis function were differentially expressed after 3 h of thermal stress (Table 1). The most highly upregulated gene in this functional group was *v1g71320*, which encodes the KRR, a small subunit processome component protein. As the name implies, KRR1 proteins appear to be essential components of rRNA maturation and ribosome biogenesis (Gromadka and Rytka, 2000). The remaining five DEGs were involved in the process of protein degradation and included *CATL, UBIQ, KLHL20, FOXRED2, and MPRD* (Table 1). In our analysis, Cathepsin-L (*CATL*) was upregulated after 3 h. Cathepsins are lysosomal cysteine proteases that break down intracellular and endocytosed proteins, particularly those associated with the extracellular matrix (Bromme and Wilson, 2011). Ubiquitin (*UBIQ*) is an important marker of protein degradation and stress in most phyla, including corals and other cnidarians (Downs 2000; Brown 2002; Fauth, 2006). Ubiquitin functions to tag stress-damaged proteins for degradation by proteolytic complexes termed 'proteasomes' (Hershko and Ciechanover, 1998). A measured increase in ubiquitin levels indicates higher levels of protein degradation and turnover (Goff et al., 1988). Kelch-like protein (KLHL20) was also upregulated only after 3 h of thermal stress. KLH20 plays a role in negatively regulating cell death activity by ubiquitinating and degrading death-associated-protein-kinase (DAPK) (Lee et al., 2010).

In contrast, one gene involved with the putative protein degradation function, FAD-dependent oxidoreductase domain-containing protein 2 (FOXRED2) only showed downregulation after 48 h of thermal stress. FOXRED2 is an ER protein that regulates

proteasome activity and may decrease the stress response and cell death when downregulated (Shim et al., 2011). Cation-dependent mannose 6-phosphate receptor (MPRD) was significantly downregulated after both 3 and 48 h of thermal stress. MPRD is involved with lysosome degradative pathway and functions to target lysosomal enzymes to the lysosome (Sleat et al., 2006). This suggests that organelle function may be impaired during thermal stress, which is a known consequence of ROS damage in corals (Richier et al., 2005).

Calcium homeostasis

Two DEGs associated with calcium homeostasis, CALU and SERCA, were upregulated after 3 h of thermal stress (Table 1). Calumenin (CALU) is a Ca^{2+}-binding protein and member of the CREC protein family and has been identified during the heat and/or light stress response in cnidarians (Aranda et al., 2011; Bellantuano et al., 2012; Moya et al., 2012). Bellantuano et al., (2012) found a decrease in expression of calumenin in response to heat stress in corals that had not been pre-conditioned and an increase in pre-conditioned (thermally-tolerant) corals after eight days of thermal stress. Furthermore, Ganot *et al.* (2009) identified calumenin as the most highly upregulated gene of the symbiotic condition in *Anemonia viridis* and suggested that calumenin may play a key role in the cnidarian/dinoflagellate symbiosis. Additionally, these authors proposed that calumenin may be involved in host/dinoflagellate recognition mechanisms through regulation of the anthozoan cell adhesion protein, *Sym32.* The fact that CALU was upregulated during our heat stress study suggests that calcium homeostasis was being disrupted after early stages of thermal stress. This finding lends support to previous studies that have suggested that calcium homeostasis may play an important role in the cnidarian response to heat stress (Fang et al., 1997; Huang et al., 1998; Sandeman, 2006).

Cell-cell interactions

Several genes associated with cell-cell interactions were differentially expressed after varying lengths of thermal stress (Table 1). Galectin-3-binding protein, *GW710920*, was upregulated after 3 and 48 h of thermal stress. Galectin-3 is a carbohydrate-binding protein (Barondes et al., 1994) that has been shown to inhibit apoptosis through cysteine protease pathways (Akahani et al., 1997). Thus, the observed upregulation of *GW710920* throughout the heat stress treatment in our analysis may suggest that apoptosis was being inhibited. This current study used the identical heat stress treatment outlined in Chapter 3, (with only a small increase in irradiance from approximately 50 to 140 μmol photons $m^{-2}s^{-1}$ irradiance) with *Aiptasia pallida,* which resulted in low levels of host/dinoflagellate apoptosis in both experiments.

Another gene, putative cell adhesion protein (*sym32*) was upregulated after 3 h of thermal stress. *sym32* is a fasciclin domain-containing protein that was first described as a 'symbiosis gene' because it was shown that to be highly expressed in the symbiotic state in *Anthopluera elegantissima* (Reynolds et al., 2000). The authors concluded that the *sym32* is involved in regulation of the symbiosis through mediating cell-cell interactions. In a separate investigation, this gene was found to localize to membranes that surround the symbiont within the host cells, further suggesting that it plays an important role in host/dinoflagellate interactions communication and signaling (Schwarz and Weis, 2002). Furthermore, heat with or without UVR stress has been shown to induce the downregulation of both *sym32* and calumenin in *A. viridis* (Moya et al., 2012). Thus, the fact that *sym32* and *CALU* were upregulated after 3 h of heat stress in our analysis further suggests that calumenin plays a role in regulating *sym32*. Additionally, *sym3*2 is likely involved in host-dinoflagellate interactions in *Aiptasia*, which are enhanced during early stages of thermal stress. However, the results of our analysis were in

contrast to those previously reported in *A. viridis* (Moya et al., 2012) since we found a significant upregulation of CALU and sym32 in response to heat stress. This observed upregulation may be due to enhanced host-dinoflagellate signaling resulting from the heat stress response.

Vesicle trafficking

Two genes associated with vesicle trafficking, including *rab26* and *cyp46a,* were upregulated after 3 h of thermal stress (Table 1). Ras-like small GTPases, such as *rab26*, are involved in regulated vesicular secretion in eukaryotic cells (Wagner et al., 1995; Yoshie et al., 2000; Nashida et al., 2006). Previous studies have also shown that dinoflagellates may manipulate host Rab GTPases, preventing lysosomal fusion with host phagosomes that they reside within in order to initiate and maintain the symbiosis (Fitt and Trench 1983; Chen et al. 2003; Chen et al. 2004; Chen et al. 2005). Although it is possible that *rab26* may play a similar role in the cnidarian-dinoflagellate symbiosis, this has not yet been established. Additionally, the vesicle-trafficking protein (*SEC22B*) functions in trafficking between the endoplasmic reticulum and Golgi apparatus (Hay et al., 1997; Liu and Barlowe 2002). It is likely that both rab26 and SEC22B were increased in response to thermal stress, since cells are known to play critical roles in secretion and intracellular transport. Many molecules regulated by this process are known to be involved in the stress response (DeMaio, 2011). These molecules are well positioned to be intercellular signaling molecules, and may act as reporters of stress for other cells and tissues (DeMaio, 2011).

Other heat-stimulated, differentially regulated transcriptional activity

Numerous genes associated with miscellaneous functions were differentially expressed after varying lengths of thermal stress (Table 1). The most highly upregulated gene in this functional groupresponse was by heme-binding protein (*MICPUN58704*), which was

upregulated (8.99 fold) after 3 h of thermal stress. Hemes are prosthetic groups that coordinate redox interactions within multiple intracellular pathways such as in the in electron transport chain and transport of diatomic gases. Many are required for oxygen storage and transport and therefore respiration. They are critical for the support of biosynthetic pathways for almost every form of life (Igarashi and Sun, 2006). Heme production is known to increase in conjunction with elevated xenobiotic detox pathways in cnidarians (Kramarsky-Winter et al., 2009). More recently, heme-binding proteins were shown to be upregulated in response to thermally stressed corals, which may have resulted from iron-induced oxidative injury (Bellantuono et al., 2012).

Another DEG found in our analysis was *cyp46a1*, which was downregulated after 3 h of thermal stress. Cholesterol 24-hydroxylase, *cyp46a1*, is a member of the superfamily of heme-thiolate enzymes (Omura, 2005) that catalyze oxidative transformation leading to activation or inactivation of endogenous and exogenous substrates (Goldstone et al., 2010). *cyp46a1* has been implicated as a critical gene for cholesterol homeostasis and membrane function in human neurons (Russell et al., 2009).

Conclusions

Here we have assembled a reference transcriptome for adult symbiotic *Aiptasia pallida* using an Illumina sequencing platform and characterized major cellular processes that occur as a consequence of thermal stress. Our findings suggest that exposure to a sub-lethal thermal treatment induces differential expression of a variety of cellular activities, including stress response, protein degradation/synthesis, calcium homeostasis, cell-cell interaction, and vesicular trafficking (Table 1). The majority of the genes related to the heat stress response were upregulated after 3 h of thermal treatment and remained stable or downregulated after 48 h of

treatment. Almost all the genes grouped within the stress response functional group followed this trend, as did many genes involved with protein degradation, calcium homeostasis, and vesicle trafficking (Table 1). Previous studies on corals have shown that these processes are affected during thermal stress (Black et al., 1995; Fang et al., 1997; Sharp et al., 1997; Edge et al., 2005; DeSalvo et al., 2008).

In the past 100 years sea surface temperatures have elevated by almost 1^{o}C and are currently increasing at the rate of approximately 1-2^{o}C per century (Hoegh-Guldberg, 1999). Thus, future studies would benefit by evaluating the potential of these differentially expressed genes to serve as potential biomarkers for cnidarian health. In doing so, we may be able to elucidate the cellular and molecular mechanisms that underlie the heat-induced bleaching process that threatens coral reef ecosystems worldwide.

Literature Cited

Abraham, M. C. and S. Shaham. Death without caspases, caspases without death. Trends In Cell Biology. 14(4):184-193.

Ainsworth, T. D., Hoegh-Guldberg, O., Heron, S. F., Skirving, W. J., and W. Leggat. 2008. Early cellular changes are early indicators of pre- bleaching thermal stress in the coral host. Journal of Experimental Biology. 364:63–71.

Ainsworth, T. D. and O. Hoegh-Guldberg. 2008. Cellular processes of bleaching in the Mediterranean coral, *Oculina patagonica*. Coral Reefs. 27:593-597.

Akahani, S., Nangia-Makker, P., Inohara, H., Kim, H. R. C., and A. Raz. 1997. Galectin-3: a novel antiapoptotic molecule with a functional BH1 (NWGR) domain of Bcl-2 family. Cancer Research. 57(23):5272-5276.

Amerongen, H. M., and D. J. Peteya. 1976. The ultrastructure of the muscle system of *Stomphia coccinea.* In: Mackie, G. O. (ed.) Coelenterate Ecology and Behavior. Plenum Publishing Co. New York. pp. 541-547.

Amerongen, H. M., and D. J. Peteya. 1980. Ultrastructural study of two kinds of muscle in sea anemones: the existence of fast and slow muscles. Journal of Morphology 166(2):145-154.

Anders, S. and W. Huber. W. 2010. Differential expression analysis for sequence count data. Genome Biology. 11. R106.

Anderson, P. A. and W. E. Schwab. 1982. Recent advances and model systems in coelenterate neurobiology. Progress in Neurobiology. 19:213-236.

Aranda, M., Banaszak, A. T., Bayer, T., Luyten, J. R., Medina, M. and C. R. Voolstra. 2011. Differential sensitivity of coral larvae to natural levels of ultraviolet radiation during the onset of larval competence. Molecular Ecology, 20(14):2955-2972.

Audesirk, G., and T. Audesirk. 1980. Complex mechanoreceptors in *Tritonia diomedea*. I. Responses to mechanical and chemical stimuli. Journal of Comparative Physiology. 141:101-109.

Baird, A. H., Bhagooli, R., Ralph, P. J. and S. Takahashi. 2009. Coral bleaching: the role of the host. Trends in Ecology and Evolution, 24(1):16-20.

Baker, A.C., 2003. Flexibility and specificity in coral-algal symbiosis: diversity, ecology and biogeography of *Symbiodinium*. Annual Review of Ecological Systematics. 34:661-689.

Barondes, S. H., Castronovo, V., Cooper, D. N. W., Cummings, R. D., Drickamer, K., Fenzi, T., Gin. M. A., Hirabaya.shi, J., Hughes. C., Kasai, K., Leffler, H., Liu, F. T., Lotan, R., Mercurio, A. M., Monsigny, M., Pillai, S.. Poirer, F., Raz, A., Rigby, P. W. J., Rini, J. M., and J. L. Wang. 1994. Galectins: a family of animal 3-galactoside binding lectins. Cell. 76:597-598.

Bayer, T., Aranda, M. Sunagawa, S. Yum, L. K. DeSalvo, M. K., Lindquist, E., Coffroth, M. A., Voolstra, C. R. and M. Medina. 2012. *Symbiodinium* transcriptomes: Genome insights into the dinoflagellate symbionts of reef-building corals. PLoS One 7(4). e35269.

Bellantuono, A. J., Hoegh-Guldberg, O. and M. Rodriguez-Lanetty. 2012. Resistance to thermal stress in corals without changes in symbiont composition. Proceedings of the Royal Society B: Biological Sciences, 279(1731):1100-1107.

Benjamini, Y. and Y. Hochberg. 1995. Controlling the false discovery rate: a practical and powerful approach to multiple testing. Journal of the Royal Statistical Society: Series B (Methodological). 57:289–300.

Black, N. A., Richard V. and A. M. Szmant. 1995:Heat shock protein induction in Montastraea faveolata and Aiptasia pallida exposed to elevated temperatures. The Biological Bulletin. 188(3):234-240.

Boya, P., Gonzalez-Polo, R-A., Casares, N., Perfettini, J-L., Dessen, P., Larochette, N., Metivier, D., Meley, D., Souquere, S., Yoshimori, T., Pierron, G., Codogno, P. and G. Kroemer. 2005. Inhibition of macroautophagy triggers apoptosis. Molecular Cell Biology. 25(3):1025-1040.

Brandt, K. 1881. Über das zusammenleben von thieren und algen. Verhanddlungen der Physiologischen Gesellschaft zu Berlin. 1881-1882: 22-26.

Bromage, E., Carpenter, L, Kaattari, S., and M. Patterson. 2009. Quantification of coral heat shock proteins from individual coral polyps. Marine Ecology Progress Series. 376:123-132.

Brömme, D., and S. Wilson. 2011. Role of cysteine cathepsins in extracellular proteolysis. In: Extracellular matrix degradation. Springer, Berlin Heidelberg. pp. 23-51.

Brown, B. E. 1997. Coral bleaching: causes and consequences. Coral reefs. 16:S129-S138.

Brown, B. E., Downs, C. A., Dunne, R. P., and S. W. Gibb. 2002. Exploring the basis of thermotolerance in the reef coral *Goniastrea aspera*. Marine Ecology Progress Series. 242:119-129.

Brown, B. E., Le Tissier, M. D. A., and J. C. Bythell. 1995. Mechanisms of bleaching deduced from histological studies of reef corals sampled during a natural bleaching event. Marine Biology. 122:655-663.

Brune, B., von Knethen, A. and K. B. Sandau. 1999. Nitric oxide (NO): an effector of apoptosis. Cell Death and Differentiation. 6:969-975.

Brusca, R. C., and G. J. Brusca. 2002. Phylum Cnidaria. In: Invertebrates. No. Ed. 2. Sinauer Associates Incorporated. pp. 226-227.

Buckley, B. A., G. E. Hofmann. 2002. Thermal acclimation changes DNA-binding activity of heat shock factor 1 (HSF1) in the goby *Gillichthys mirabilis*: implications for plasticity in the heat-shock response in natural populations. Journal of Expermental Biology. 205:3231–3240.

Butschli, O. 1887. Protozoa. Bronns Klassen und Ordnungen des Thierreichs. Bd. 1. Abt. 3. Leipzig.

Carrol, D. J. and S. C. Kempf. 1994. Changes occur in the central nervous system of the nudibranch *Berghia verrucicornis* (Mollusca, Opisthobranchia) during metamorphosis. Biological Bulletin. 186:202-212.

Chapman, G., 1953. Studies of the mesoglea of coelenterates. II. Physical properties. Journal of Experimental Biology. 30:440-451.

Chapman, G., 1974. The skeletal system. In: Muscatine, L. and Lenhoff, H. M. (eds) Coelenterate biology: reviews and perspectives. Academic Press, New York. pp. 93-128.

Chapman, J. A., Kirkness, E. F., Simakov, O., Hampson, S. E., Mitros, T., Weinmaier, T., Rattei, T., Balasubramanian, P. G., Borman, J., Busam, D., Disbennett, K., Rfannkock, C., Sumnin, N., Sutton, G. G., Viswanathan, L. D., Walenz, B., Goodstein, D. M., Hllsten, U., Kawahima, T., Prochnick, S. E., Putnam, N. H., Shengquiang, S., Blumberg, B. Dana, C. E., Gee., L. and P. R. Steinmetz. 2010. The dynamic genome of *Hydra*. Nature. 464(7288):592-596.

Chen M., Cheng, Y., Hong, M., and L. Fang. 2004. Molecular cloning of Rab5 (ApRab5) in *Aiptasia pulchella* and its retention in phagosomes harboring live zooxanthellae. Biochemical and Biophysical Research Communications. 324:1024-1033.

Chen, M-C., Hong, M-C., Huang, Y-S., Liu, M-C., Cheng, Y-M. and L-S. Fang. 2005. ApRab11, a cnidarian homologue of the recycling regulatory protein Rab11, is involved in the establishment and maintenance of the *Aiptasia-Symbiodinium* endosymbiosis. Biochemical and Biophysical Research Communications. 338:1607-1616.

Chen, M-C., Cheng, Y-M., Sung, P-J., Kuo C-E and L-S. Fang. 2003. Molecular identification of Rab7 (ApRab7) in *Aiptasia pulchella* and its exclusion from phagosomes harboring zooxanthellae. Biochemical and Biophysical Research Communications. 308:586-595.

Chen, Y. and S. B. Gibson. 2008. Is mitochondrial generation of reactive oxygen species a trigger for autophagy? Autophagy 4(2):246-248.

Chera S, Buzgariu W, Ghila L. and B. Galliot. 2009. Autophagy in *Hydra*: A response to starvation and stress in early animal evolution. Biochimica et biophysica acta.1793(9): 432-1443.

Coles, S. L., and P. L. Jokiel. 1992. Effects of salinity on coral reefs. Pollution in Tropical Aquatic Systems. 147-166.

Cuervo, A. M. (2004). Autophagy: in sickness and in health. Trends in Cell Biology. 14:70-77.

Davis, L. E. Biology of *Hydra*. 1973. Academic Press. New York.

.

Davis LE & Haynes. JF 1968. An ultrastructural examination of the mesoglea of *Hydra*. Zeitschrift für Zellforschung und Mikroskopische Anatomie. 92:149–158.

Davy, S. K., Allemand, D., Weis, V. M. 2012. Cell Biology of Cnidarian-Dinoflagellate Symbiosis 76(2):229-261.

D'elia, C. F., and W. J. Wiebe.1990. Biogeochemical nutrient cycles in coral-reef ecosystems. Ecosystems of the World. 25:49-74.

De Maio, A. 2011. Extracellular heat shock proteins, cellular export vesicles, and the Stress Observation System: A form of communication during injury, infection, and cell damage. Cell Stress and Chaperones. 16(3):235-249.

DeSalvo, M. K., Sunagawa, S., Voolstra, C. R. and M. Medina, M. 2010. Transcriptomic responses to heat stress and bleaching in the elkhorn coral *Acropora palmata*. Marine Ecology Progress Series. 402, 97-113.

Desalvo, M. K., Voolstra, C. R., Sunagawa, S., Schwarz, J. A., Stillman, J. H., Coffroth, M. A. Szmant, A. M. and M. Medina. 2008. Differential gene expression during thermal stress and bleaching in the Caribbean coral *Montastraea faveolata*. Molecular Ecology. 17(17):3952-3971.

Donner, S.D., Knutson, T. R. and M. Oppenheimer. 2007. Model-based assessment of the role of human-induced climate change in the 2005 Caribbean coral bleaching event. Proceedings of the National Academy of Sciences. 104(13):5483-5488.

Douglas, A. E. 2003. Coral bleaching-how and why? Marine Pollution Bulletin. 46:385-392.

Downs, C. A., Dramarsky-Winter, E., Martinez, J., Kushmaro, A., Woodley, C. M., Loya, Y., Ostrander, G. K. 2009. Symbiophagy as a cellular mechanism for coral bleaching. Autophagy 5(2), 211-216.

Downs, C. A., Fauth, J. E., Halas, J. C., Dustan, P., Bemiss, J., and C. M. Woodley. 2002. Oxidative stress and seasonal coral bleaching. Free Radical Biology and Medicine. 33(4):533-543.

Downs, C. A., Fauth, J. E., Robinson, C. E., Curry, R., Lanzendorf, B., Halas, J. C. and C. M. Woodley. 2005. Cellular diagnostics and coral health: declining coral health in the Florida Keys. Marine Pollution Bulletin. 51(5):558-569.

Downs CA, Mueller E, Phillips S, Fauth JE, Woodley CM. 2000. A molecular biomarker system for assessing the health of coral (*Montastraea faveolata*) during heat stress. Marine Biotechnology. 2:533–544

Dunlap, D.L. and Schick, J.M. 1998. Review: Ultravioet radiation-absorbing mycosporine-like amino acids in coral reef organisms: A biochemical and environmental perspective. Journal of Phycology. 34:418-430.

Dunn, S. R., Bythell, J. C., Le Tissier, M. D. A., Burnett, W. J., Thomason, J. C. 2002. Programmed cell death and cell necrosis activity during hyperthermic stress-induced bleaching of the symbiotic sea anemone *Aiptasia sp.* Journal of Experimental Marine Biology and Ecology. 272:29-53.

Dunn, S. R., Pernice, M., Green, K., Hoegh-Guldberg, O., Dove, S. G. 2012. Thermal stress promotes host mitochondrial degradation in symbiotic cnidarians: are the batteries of the reef going to run out? PLoS ONE. 7(7). e39024.

Dunn, S. R., Schnitzler, C. E., Weis, V. M. 2007. Apoptosis and autophagy as mechanisms of dinoflagellate symbiont release during cnidarian bleaching: every which way you lose. Proceedings of the Royal Society of London Series B. Biological Sciences. 274:3079-3085.

Dunn, S. R., Thomason, J. C., Le Tissier, M. D. A., Bythell, J. C. 2004. Heat stress induces different forms of cell death in sea anemones and their endosymbiotic algae depending on temperature and duration. Cell Death and Differentiation. 11:1213-1222.

Dykens, J. A., J. M. Shick, C. Benoit, G. R. Buettner, and G. W. Winston.1992. Oxygen radical production in the sea anemone *Anthopleura elegantissima* and its endosymbiotic algae. Journal of Experimental Biology.168:219-241.

Earnshaw, W. C., L. M. Martins, and S. H. Kaufmann. 1999. Mammalian caspases: structure, activation, substrates, and functions during apoptosis. Annual Review of Biochemistry. 68(1):383-424.

Edge, S. E., Morgan, M. B., Gleason, D. F. and T. W. 2005. Development of a coral cDNA array to examine gene expression profiles in *Montastraea faveolata* exposed to environmental stress. Marine Pollution Bulletin. 51:507-523.

Edinger, A. L. and C. B. Thompson. 2004. Death by design: apoptosis, necrosis and autophagy. Current Opinions in Cellular Biology. 16:663–669.

Fang, L.-S., Huang, S.-P., and K.-L Lin. 1997. High temperature induces the synthesis of heat-

shock proteins and the elevation of intracellular calcium in the coral *Acropora grandis.* Coral Reefs. 16:127-131.

Fang, L-S., Wang, J. T, and K-L. Lin. 1998. The subcellular mechanism of the release of zooxanthellae during coral bleaching. Proceedings of the National Science Council, Republic of China. Part B. Life sciences. 22(4):150-158.

Fauth, J. E. 2006. Final report: Southeast Florida coral biomarker local action study. Florida Department of Environmental Protection. pp. 1-69.

Fautin, D.G. and Mariscal, R.N. 1991. Cnidaria: Anthozoa. In: Harrison, F.W. and Westfall, J.A. (eds) Microscopic Anatomy of Invertebrates, Vol. 2. Placozoa, Porifera, Cnidaria, and Ctenophora. Wiley, NewYork. Pp. 267–358.

Fautin, Daphne G. and Romano, Sandra L. 1997. Cnidaria. Sea anemones, corals, jellyfish, sea pens, hydra. Version 24 April 1997. http://tolweb.org/Cnidaria/2461/1997.04.24 *in* The Tree of Life Web Project, http://tolweb.org/

Fawcett DW 1981. Lysosomes. In: The Cell. W. B. Saunders Company. Philadelphia. pp. 487-514.

Fitt, W. K., Brown, B. E., Warner, M. E., and R. P. Dunne. 2001. Coral bleaching: interpretation of thermal tolerance limits and thermal thresholds in tropical corals. Coral Reefs Report. 20:51-65.

Fitt, W. K. and R. K. Trench. 1983. Endocytosis of the symbiotic dinoflagellate *Symbiodinium microadriaticum* Freudenthal by endodermal cells of the scyphistomae of *Cassiopeia xamachana* and resistance of the algae to host digestion. Journal of Cell Science 64:195-212.

Forêt, S., Kassahn, K. S., Grasso, L. C., Hayward, D. C., Iguchi, A., Ball, E. E. and D. J. Miller. 2007. Genomic and microarray approaches to coral reef conservation biology. Coral Reefs. 26(3):475-486.

Franklin, D.J., Hoegh-Guldberg, O., Jones, R.J., Berges, J.A. 2004. Cell death and degenerationin the symbiotic dinoflagellates of the coral *Stylophora pistillata* during bleaching. Marine Ecology Progress Series. 272:117-130.

Freudenthal, H.D., 1962. *Symbiodinium* gen. nov. and *Symbiodinium microadriaticum* sp. nov., a Zooxanthella: Taxonomy, life cycle, and morphology. Journal of Protozoology. 9:45-52.

Gates, R. D. and P. J. Edmunds. 1999. The physiological mechanisms of acclimatization in tropical reef corals. American Zoologist, 39(1):30-43.

Gates, R. D. and L. M. Muscatine. 1992. Temperature stress causes host cell detachment in symbiotic cnidarians: implications for coral bleaching. Biological Bulletin. 182(3):324-332.

Gauthier, Geraldine F. 1963. Cytological studies on the gastroderm of *Hydra*. Journal of Experimental Zoology 152.1:13-39.

Glider, W. V. 1983. The biology of the association of *Symbiodinium microadriaticum* with *Aiptasia pallida*: an anemone-alga symbiosis. Ph.D. Thesis, University of Nebraska, Lincoln, Nebraska. pp. 102.

Glynn, P. W. 1996. Coral reef bleaching; ecological perspectives. Coral Reefs 12:1-17

Glynn, P. W., Peters, E. C. and L. Muscatine. 1985. Coral tissue microstructure and necrosis: relation to catastrophic coral mortality in Panama. Disease in Aquatic Organisms. 1:29-37.

Goff, S.A., Voellmy, R., and Goldberg, A. L. 1988. Protein breakdown and the heat-shock response. In: Ubiquitin, Rechsteiner, M. (ed.). New York: Plenum Press: 207–238.

Goldberg, W. M. 2002. Gastrodermal structure and feeding responses in the scleractinian *Mycetophyllia reesi*, a coral with novel digestive filaments. Tissue and Cell. 34(4):246-261.

Goldstone, J. V. McArthur, M. G., Kubota, A., Zanette, J., Parente, T., Jönsson, M. E., Nelson, D. R., and J. J. Stegeman. 2010. Identification and developmental expression of the full complement of Cytochrome P450 genes in Zebrafish. BMC Genomics. 11:643.

Goulet, T. L., Cook, C., and D. L. Goulet. 2005. Effect of short-term exposure to elevated temperatures and light levels on photosynthesis of different host–symbiont combinations in the *Aiptasia pallida*/*Symbiodinium* symbiosis. Limnology and Oceanography. 50(5):1490–1498.

Gozuacik, D. and A. Kimchi. 2004. Autophagy as a cell death and tumor suppressor mechanism. Oncogene. 23:2891-2906.

Gozuacik, D., Kimchi, A. 2007. Autophagy and cell death. Current Topics in Developmental Biology. 78:217-45.

Grabherr, M. G., Haas, B. J., Yassour, M., Levin, J. Z., Thompson, D. A., Amit, I., Adiconis, X., Fan, L., Raychowdhury, R., Zeng, Q., Chen, Z., Mauceli, E., Hacohen, N., Gnirke, A., Rhind, N., di Palma, F., Birren, B. W., Nusbaum, C., Lindblad-Toh, K., Friedman, K., and A. Regev. 2011. Full-length transcriptome assembly from RNA-Seq data without a reference genome. Nature Biotechnology 29(7):644-652.

Grimmelikhuijzen, C. J. P. and J. A. Westfall. 1995. The nervous systems of cnidarians. The nervous systems of invertebrates: an evolutionary and comparative approach. Birkhäuser Base l:7-24.

Gromadka, R. and J. Rytka. 2000. The KRR1 gene encodes a protein required for 18S rRNA synthesis and 40S ribosomal subunit assembly in *Saccharomyces cerevisiae*. ACTA Biochemica Polonica-English Edition. 47(4):993-1006.

Hand, A. 1970. Fine structure of Von-Ebners gland of the rat. Journal of Cell Biology. 44:340-353.

Hara, T., Nakamura, K., Matsui, M., Yamamoto, A., Nakahara, Y., Suzuki-Migishima, R. et al. 2006. Suppression of basal autophagy in neural cells causes neurodegenerative disease in mice. Nature. 441:885–889.

Harvell, C. D., Kim, K., Burkholder, J. M., Colwell, R. R., Epstein, P. R., Grimes, D. J., Hoffmann, E. E., Lipp, E. K., Osterhaus, A. D. M. E., Overstreet, R. M., Porter, J. W., Smith, G. W., and G. R. Vasta. 1999. Emerging marine diseases-climate links and anthropogenic factors. Science 285:1505–1510.

Hashimoto, K., Shibuno, T., Murayama-Kayano, E., Tanaka, H. and T. Kayano. 2004. Isolation and characterization of stress-responsive genes from the scleractinian coral *Pocillopora damicornis*. Coral Reefs, 23(4):485-491.

Hay J. C., Chao, D. S., Kuo, C. S., Scheller, R. H. 1997. Protein interactions regulating vesicle transport between the endoplasmic reticulum and Golgi apparatus in mammalian cells. Cell. 89:149–158.

Haynes, J. F. Epithelial-muscle cells. 1973. Biology of *Hydra*. Academic Press, London New York. pp. 233-237.

Haynes, Julian F., and Lowell E. Davis. 1969. The ultrastructure of the zymogen cells in *Hydra viridis*. Zeitschrift für Zellforschung und Mikroskopische Anatomie. 100(2):316-324.

Haynes, Julian F., Allison L. Burnett, and Lowell E. Davis. 1968. Histological and ultrastructural study of the muscular and nervous systems in *Hydra*. I. The muscular system and the mesoglea. Journal of Experimental Zoology 167.3: 283-293.

Hershko, A. and A. Ciechanover. 1998. The ubiquitin system. Annual Review of Biochemistry. 67:425-479.

Hess, A. 1961. The fine structure of cells in *Hydra*. The biology of *Hydra*. 1-43.

Hess, A., Cohen, A., and E. Robson. 1957. Observations on the structure of *Hydra* as seen with the electron and light microscopes. Quarterly Journal of Microscopy Science. 98:315-326.

Hoegh-Guldberg, O. 1999. Climate change, coral bleaching and the future of the world's coral reefs. Marine and Freshwater Research. 50:839-866.

Hoegh-Guldberg O., Mumby, P. J., Hooten, A. J., Steneck, R. S., Greenfield, P., Gomez, E., Harvell, C. D., Sale, P. F., Edwards, A. J., Caldeira, K., Knowlton, N., Eakin, C. M., Iglesias-Prieto, R., Muthiga, N., Bradbury, R. H., Dubi, A., and M. E. Hatziolos. 2007. Coral Reefs under rapid climate change and ocean acidification. Science. 318:1737–1742.

Holtzman, E. 1989. Autophagy and related phenomena, In: Siekevitz. P. (Ed.), Lysosomes. Plenum Press, New York. pp. 243-253.

Huang W. P. and D. J. Klionsky. 2002. Autophagy in yeast: a review of the molecular machinery. Cell Structure and Function. 27:409–420.

Huang, S. P., Lin, K. L., and L. S. Fang. 1998. The involvement of calcium in heat-induced coral bleaching. Zoological Studies-Taipai. 37:89-94.

Hughes, T. P. 2003. Climate change, human impacts, and the resilience of coral reefs. Science. 301:929-933.

Hyman, L.H. 1940. The invertebrates: Protozoa through Ctenophora (I). McGraw-Hill, New York.

Igarashi, K. and Sun, J. 2006. Antioxidants & Redox Signaling. 8(1-2):107-118.
Iglesias-Prieto, R., Matta, J. L., Robins, W. A., & Trench, R. K. 1992. Photosynthetic response to elevated temperature in the symbiotic dinoflagellate *Symbiodinium microadriaticum* in culture. Proceedings of the National Academy of Sciences, 89(21):10302-10305.

James, E. R. and D. R. Green. 2004. Manipulation of apoptosis in the host-parasite interaction. Trends in Parasitology. 20:280-287.

Jing, Y. and X-M. Tang. 1999. The convergent point of the endocytic and autophagic pathways in Leydig cells. Cell Research. 9:243-253.

Kamada Y, Funakoshi T, Shintani T, Nagano K, Ohsumi M, Ohsumi Y. 2000. Tor-mediated induction of autophagy via an Apg1 protein kinase complex. Journal of Cell Biology.150:1507–1513.

Kang, R., Zeh, H. J., Lotze, M. T., and D. Tang. 2011. The Beclin 1 network regulates autophagy and apoptosis. Cell Death and Differentiation. 18:571-580.

Kass-Simon, G., Scappaticci Jr., A.A., 2002. The behavioral and developmental physiology of nematocysts. Canadian Journal of Zoology 80:1772–1794.

Kelekar, A. 2006. Autophagy. Annals of the New York Academy of Sciences. 1066(1):259-271.

Keough, E. M., and R. G. Summers. 1976. An ultrastructural investigation of the striated subumbrellar musculature of the anthomedusan, *Pennaria tiardla*. Journal of Morphology.149:507-526.

Kiffin, R., Bandyopadhyay, U. and A. M. Cuervo. 2006. Oxidative stress and autophagy. Antioxidants and Redox Signaling. 8(1)2:152-162.

Klionsky, D. J., Emr, S. D. 2000. Autophagy as a regulated pathway of cellular degradation.

Science. 290(5497):1717–1721.

Klionsky, D. J., Creg, J. M., Dunn, W. A., Emr, S. D., Sakai, Y., Sandoval, I. V., Sibirny, A., Subramani, S., Thumm, M., Veenhuis, M., and Y. Ohsumi. 2003. A unified nomenclature for yeast autophagy-related genes. Developmental Cell. 5(4):539-545.

Kloepper, T. H., Kienle, C. N. and D. Fasshauer. 2008. SNAREing the basis of multicellularity: consequences of protein family expansion during evolution. Molecular Biology and Evolution 25(9):2055-2068.

Komata, T., Kanzawa, T., Nashimoto, T., Aoki, H., Endo, S., Nameta, M., Takahashi, H., Yamamoto, T., Kondo, S., Tanaka, R. 2004. Mild heat shock induces autophagic growth arrest, but not apoptosis in U251-MG and U87-MG human malignant glioma cells. Journal of Neurooncology. 68:101-111.

Komatsu, M., Waguri, S., Chiba, T., Murata, S., Iwata, J., Tanida, I., Ueno, T., Masato, K., Uchiyama, Y., Kominami, E., and K. Tanaka. 2006. Loss of autophagy in the central nervous system causes neurodegeneration in mice. Nature. 441:880–884.

Kosta A, Roisin-Bouffay C, Luciani MF, Otto GP, Kessin RH, Golstein P. 2004. Autophagy gene disruption reveals a non-vacuolar cell death pathway in *Dictyostelium*. Journal of Biological Chemistry. 279:48404–48409.

Kourtis, N. and N. Tavernarakis. 2009. Autophagy and cell death in model organisms. Cell Death and Differentiation. 16:21-30.

Kov, A. L., Vellai, T. and M. Fritz. 2000. Autophagy in *Caenorhabditis elegans*. Madame Curie Bioscience Database [Internet]. Austin, Tx: Landes Bioscience; 2000 http://www.ncbi.nlm.nih.gov/books/NBK5981/

Kramarsky-Winter, E., Downs, C. A., Downs, A., and Y. Loya. 2009. Cellular responses in the coral *Stylophora pistillata* exposed to eutrophication from fish mariculture. Evolutionary Ecology Research. 11:1-21.

Kushmaro A., Rosenberg, E., Fine, M., and Y. Loya. 1997. Bleaching of the coral *Oculina patagonica* by *Vibrio* AK- 1. Marine Ecology Progress Series. 147:159-165

Lawen, Alfons. 2003. Apoptosis-an introduction. Bioessays. 25(9):888-896.

Lee, Y. R., Yuan, W. C., Ho, H. C., Chen, C. H., Shih, H. M., and R. H. Chen. 2010. The Cullin 3 substrate adaptor KLHL20 mediates DAPK ubiquitination to control interferon responses. The EMBO Journal. 29(10):1748-1761.

Lehnart, E. M., Burriesci, M. S. and J. R. Pringle. 2012. Developing the anemone *Aiptasia* as a tractable model for cnidarian-dinoflagellate symbiosis: the transcriptome of aposymbiotic *A. pallida.* BMC Genomics. 13:271.

Lesser, M.P. and Shick, J.M. 1990. Effects of visible and ultraviolet radiation on the ultrastructure of zooxanthellae (*Symbiodinium* sp.) in culture and *in situ*. Cell and Tissue Research. 261(3):501-508.

Lesser, M. P. 1996. Elevated temperatures and ultraviolet radiation cause oxidative stress and inhibit photosynthesis in symbiotic dinoflagellates. Limnological Oceanography. 41:271-283.

Lesser, M. P. 1997. Oxidative stress causes coral bleaching during exposure to elevated temperatures. Coral Reefs. 16.187-192.

Lesser, M. P. 2004. Experimental coral reef biology. Journal of Experimental Marine Biology and Ecology. 300:217-252.

Lesser, M. P. 2006. Oxidative stress in marine environments: biochemistry and physiological ecology. Annual Review of Physiology. 68:253-278.

Lesser, M. P. 2007. Coral reef bleaching and global climate change: Can corals survive next centuries? Proceedings of the National Academy of Science. 104(13):5259-5260.

Lesser, M. P. and J. H. Farrell. 2004. Exposure to solar radiation increases damage to both host tissues and algal symbionts of corals during thermal stress. Coral Reefs. 23:367–377.

Le Tissier, M. D. and B. E. Brown. 1996. Dynamics of solar bleaching in the intertidal reef coral *Goniastrea aspera* at Ko Phuket, Thailand. Marine Ecology Progress Series. 136:235-244.

Levine B. and D. J. Klionsky. 2004.Development by self-digestion:molecular mechanisms and biological functions of autophagy. Developmental Cell. 6:463-477.

Levine, B. and J. Yuan. 2005. Autophagy ain cell death: an innocent convict? Journal of Clinical Investigation. 115(10):2679-2688.

Liu Y, and C. Barlowe. 2002. Analysis of Sec22p in endoplasmic reticulum/Golgi transport reveals cellular redundancy in SNARE protein function. Molecular and Biological Cell. 13:3314–3324.

Lockshin, R. A. and Z. Zakeri. 2007. Caspase-independent cell death? Oncogene 2004, 23:2766-2773.

Margulls, L., Thorington, G., Berger, B., and J. Stolz. 1978. Endosymbiotic bacteria associated with the intracellular green algae of *Hydra vinidis*. Current Microbiology. 1:227-232.

Mariscal, R.N., and Bigger, C.H. 1976. A comparison of putative sensory receptors associated with nematocysts in the anthozoan and scyphozoan. In Coelenterate ecology and behavior. Edited by G.O. Mackie. Plenum Press, New York. pp. 559–568.

Mariscal, R. N., E. J. Conklin, and C. H. Bigger. 1978. The putative sensory receptors associated with the cnidae of cnidarians. Scanning Electron Microscropy. 2:959-966.

Megill WM, Gosline JM, & Blake RW 2005. The modulus of elasticity of fibrillin-containing elastic fibres in the mesoglea of the hydromedusa *Polyorchis penicillatus*. Journal of Experimental Biology. 208:3819–3834.

Meyer, E., Aglyamova, G. V. and M. V. Matz. 2011. Profiling gene expression responses of coral larvae (*Acropora millepora*) to elevated temperature and settlement inducers using a novel RNA-Seq procedure. Molecular Ecology, 20(17):3599-3616.

Mizushima N. and D. J. Klionsky. 2007. Protein turnover via autophagy: Implications for metabolism. Annual Review of Nutrition. 27: 19–40.

Moya, A., Ganot, P., Furla, P. and C. Sabourault, C. 2012. The transcriptomic response to thermal stress is immediate, transient and potentiated by ultraviolet radiation in the sea anemone *Anemonia viridis*. Molecular Ecology. 21(5):1158-1174.

Muscatine, L. 1990. The role of symbiotic algae in carbon and energy flux in reef corals. In: Dubinsky, Z. (ed), Coral Reefs. Ecosystems of the world. Coral Reefs. Vol. 25. Elsevier, Amsterdam. pp 550.

Muscatine, L., and J. W. Porter. 1977. Reef corals: mutualistic symbioses adapted to nutrient-poor environments. Bioscience. 454-460.

Nashida, T., A. Imai, and H. Shimomura. 2006. Relation of Rab26 to the amylase release from rat parotid acinar cells. Archives of Oral Biology. 51:89–95.

National Oceanic and Atmospheric Administration. Coral Reef Conservation Program. 2012. [Internet]. 2012- http://coralreef.noaa.gov/aboutcorals/values/.

Nii, C. M. and L. Muscatine. 1997. Oxidative stress in the symbiotic sea anemone, Aiptasia pulchella (Carlgren, 1943): contribution of the animal to superocxide ion production at elevated temperature. Biological Bulletin. 192(3):444-456.

Nivon, M., Richet, E., Codogno, P., Arrigo, A-P., Dretz-Remy, C. 2009. Autophagy activation by NFkB is essential for cell survival after heat shock. Autophagy 5(6), 766-783.

Nixon, R. A. 2007. Autophagy, amyloidogenesis and Alzheimer disease. Journal of Cell Science. 120:4081-4091.

Niyogi, K.K. 1999. Photoprotection revisited: genetic and molecular approaches. Annual Review of Plant Physiology. 50:333-359.

Noda, T. and Y. Ohsumi. 1998. Tor, a phosphatidylinositol kinase homologue, controls autophagy in yeast. Journal of Biological Chemistry. 273:3963-3966.

Oberley, T. D., Swanlund, J. M., Zhang, H. J., and K. C. Kregel. 2008. Aging Results in increased autophagy of mitochondria and protein nitration in rat hepatocytes following heat stress. Journal of Histochemical Cytochemistry. 56(6):615-627.

Ohsumi, Y. and N. Mizushima. 2003. Two ubiquitin-like conjugation systems essential of autophagy. Seminars in Cell and Developmental Biology. 15 (2):231-236.

Omura, T. 2005. Heme-thiolate proteins. Biochemical and Biophysical Research Communications. 338:404–409.

Palinscar, E. E., Jones, W. R, Palinscar, J. S., Glowski, M. A., and J. L. Mastro. 1989. Bacterial Aggregates Within the Epidermis of the Sea Anemone *Aiptasia pallida.* Biological Bulletin. 177:130-140.

Parker, G. H., 1919. The elementary nervous system. Lippincott Co, Philadelphia. pp. 215-224.

Perez, S. and V. M. Weis. 2006. Nitric oxide and cnidarian bleaching: an eviction notice mediates the breakdown of the symbiosis. Journal of Experimental Biology. 209:2804-2810.

Porter, J. W. 1972. Predation by *Acanthaster* and its effect on coral species diversity. The American Naturalist. 106(950):487-492.

Prasad, K. V., Taiyab, A., Jothi, D., Srinivas, U. K., and A. S. Streedhar. 2007. Heat shock transcription factors regulate heat induced cell death in a rat histiocytoma. Journal of Biosciences. 32(3):585-593.

Proskuryakov SY, Konoplyannikov AG, Gabai VL. 2003. Necrosis: a specific form of programmed cell death? Exp Cell Res. 283:1-16.

R Development Core Team. 2008. R: A Language and Environment for Statistical Computing. R Foundation for Statistical Computing. Vienna, Austria.

Reynolds, W.S., Schwarz, J.A., and Weis, V.M. 2000. Symbiosis-enhanced gene expression in cnidarian-algal associations: cloning and characterization of a cDNA, sym32, encoding a possible cell adhasion protein. Comparative Biochemistry and Physiology Part A. 126:33-44.

Richardson, K. C., L. Jarett, and F.H. Finke. 1960. Embedding in epoxy resins for ultrathin sectioning in electron microscopy. Stain Technology. 35:313-323.

Richier, S., Furla, P., Plantivaux, A., Merle, P. L. and D. Allemand. 2005. Symbiosis-induced adaptation to oxidative stress. Journal of Experimental Biology. 208:277-285.

Richier, S., Rodriguez-Lanetty, M., Schnitzler, C. E. and V. M. Weis. 2008. Response of the symbiotic cnidarian *Anthopleura elegantissima* transcriptome to temperature and UV increase. Comparative Biochemistry and Physiology Part D: Genomics and Proteomics. 3(4):283-289.

Richier, S., Sabourault, C., Courtiade, J., Zucchini, N., Allemand, D. and P. Furla. 2006. Oxidative stress and apoptotic events during thermal stress in the symbiotic sea anemone, *Anemonia viridis*. FEBS Journal. 273:4186-4198.

Rodriguez-Lanetty, M. Harii, S. and O. Hoegh-Guldberg. 2009. Early molecular responses of coral larvae to hyperthermal stress. Molecular Ecology. 18(24):5101-5114.

Rogers, C. S. 1990. Responses of coral reefs and reef organisms to sedimentation. Marine Ecology Progress Series. Oldendorf. 62(1):185-202.

Ron, D. and P. Waters. 2007. Signal integration in the endoplasmic reticulum unfolded protein response. Nature Reviews Molecular Cell Biology. 8:519-529.

Rose PG, Burnett AL. 1968. An electron microscopic and histochemical study of the secretory cells in *Hydra viridis*. Wilhelm Roux Archive. 161:281–297.

Rost-Roszkowska, M. M., Poprawa, I., Klag, J., Migula, P., Mesjasz-Przybylowicz, J., Przybylowecz, W. 2008. Degeneration of the midgut epithelium in *Epilachna* cf. *nylanderi* (Insecta, Coccinellidae): apoptosis, autophagy, and necrosis. Canadian Journal of Zoology. 86:1179-1188.

Rosic, N. N., Pernice, M., Dunn, S., Dove, S. and O. Hoegh-Guldberg. 2010. Novel cytochrome P450 genes from the symbiotic dinoflagellates of reef-building corals: differential regulation by heat stress. Applied and Environmental Microbiology. 76(9):2823–2829.

Rost-Roszkowska, M. M., Poprawa, I., Klag, J., Migula, P., Mesjasz-Przybylowicz, J. and W. Przybylowecz. 2008. Degeneration of the midgut epithelium in *Epilachna* cf. *nylanderi* (Insecta, Coccinellidae): apoptosis, autophagy, and necrosis. Canadian Journal of Zoology. 86:1179-1188.

Rowan, R. and D. A. Powers. 1991. Molecular identification of symbiotic dinoflagellates (zooxanthellae). Marine Ecology Progress Series. 71:65-73.

Russell D. W., Halford, R. W., Ramirez, D. M., Shah, R. and T. Kotti. 2009. Cholesterol 24-hydroxylase: an enzyme of cholesterol turnover in the brain. Annual Review of Biochemistry. 78:1017-1040.

Sandeman, I. M. 2006. Fragmentation of the gastrodermis and detachment of zooxanthellae in symbiotic cnidarians: a role for hydrogen peroxide and Ca^{2+} in coral bleaching and algal density control. Revista de Biología Tropical. 54:79-96.

Santos, S. R., Taylor, D. J., Coffroth, M. A. 2001. Genetic comparisons of freshly isolated versus cultured symbiotic dinoflagellates: implications for extrapolating to the intact symbiosis. Journal of Phycology. 37:900-912.

Santos, S. R., Taylor, D. J., Kinzie III, R. A., Hidaka, M., Sakai, K., and M. A. Coffroth. 2002.

Molecular phylogeny of symbiotic dinoflagellates inferred from partial chloroplast large subunit (23S)-rDNA sequences. Molecular Phylogenetics and Evolution. 23:97–111.

Sawyer and Muscatine. 2001. Cellular mechanisms underlying temperature-induced bleaching in the tropical sea anemone, *Aiptasia pulchella*. Journal of Experimental Biology. 204(20): 3443-3356.

Scherz-Shouval, Shvets, E., Fass, E., Shorer, H., Gil, L., and Z. Elazar. 2007. Reactive oxygen species are essential for autophagy and specifically regulate the activity of Atg4. The EMBO Journal. 26:1749–1760.

Schwarz, J. A. and V. M. Weis. 2003. Localization of a symbiosis-related protein, Sym32, in the *Anthopleura elegantissima–Symbiodinium muscatinei* association. The Biological Bulletin. 205(3):339-350.

Schwartz, Alan L., et al. 1992. Stress-induced alterations in autophagic pathway: relationship to ubiquitin system. 1992. American Journal of Physiology-Cell Physiology. 262(4):1031-1038.

Scott, R. C., Schuldiner, O., and T. P. Neufeld. 2004. Role and regulation of starvation-induced autophagy in the *Drosophila* fat body. Developmental Cell. 7:167-178.

Seneca, F. O., Forêt, S., Ball, E. E., Smith-Keune, C., Miller, D. J. M. J. van Oppen. 2010. Patterns of gene expression in a scleractinian coral undergoing natural bleaching. Marine Biotechnology. 12(5):594-604.

Seipel, K. and V. Schmid. 2006. Mesodermal anatomies in cnidarian polyps and medusae. Integrative Journal of Developmental Biology. 50:589-599.

Sharp, V. A., Brown, B. A. and D. Miller. 1997. Heat shock protein (Hsp 70) expression in the tropical reef coral *Goniopora djiboutiensis*. Journal of Thermal Biology. 22(1):11-19.

Shick, J. 1991. A Functional Biology of Sea Anemones. Chapman & Hall. New York. pp. 395

Shim, S., Lee, W., Chung, H. and Y. K. Jung. 2011. Amyloid β-induced FOXRED2 mediates neuronal cell death via inhibition of proteasome activity. Cellular and Molecular Life Sciences. 68(12): 2115-2127.

Shinzato, C., Shoguchi, E., Kawashima, T., Hamada, M., Hisata, K., Tanaka, M., Fujie, M., Fujiwara, M., Koyanagi, R., Ikuta, T., Fujiyama, A., Miller, D. J., and N. Satoh. 2011. Using the *Acropora digitifera* genome to understand coral responses to environmental change. Nature. 476(7360):320-323.

Sleat, D. E.,Wang, Y., Sohar, I., Lackland, H., Li, Y. 2006. Identification and validation of mannose 6-phosphate glycoproteins in human plasma reveal a wide range of lysosomal and non-lysosomal proteins. Molecular and Cellular Proteomics 5:1942–1956.

Slautterback, D. B. and D. W. Fawcett. 1959. The development of the cnidoblasts of *Hydra* an electron microscope study of cell differentiation. Journal of Biophysical and Biochemical Cytology. 5(3):441-452.

Slautterback, D. B. 1967. The cnidoblast-musculoepithelial cell complex in the tentacles of *Hydra*. Zeitschrift für Zellforschung und Microscopische Anatomie 79:296-318.

Smith, D.J., Suggett, D.J., Baker, N.R, 2005. Is photoinhibition of zooxanthellae photosynthesis the primary cause of thermal bleaching in corals? Global Change Biology. 11(1):1-11.

Stat, M., Carter, D., Hoegh-Guldberg, O. 2006. The evolutionary history of Symbiodinium and scleractinian hosts- Symbiosis, diversity, and the effect of climate change. Perspectives in Plant Ecology, Evolution and Systematics. 8:23-43.

Steen, R. G., and L. Muscatine. 1987. Low temperature evokes rapid exocytosis of symbiotic algae by a sea anemone. Biological Bulletin. 172:246-263.

Strychar, K. B., Coates, M., Sammarco, P. W., and T. J Piva. 2004. Bleaching as a pathogenic response in scleractinian corals, evidenced by high concentrations of apoptotic and necrotic zooxanthellae. Journal of Experimental Marine Biology and Ecology. 304:99-121.

Strychar, K. B. and P. W. Sammarco. 2009. Exaptation in corals to high seawater temperatures: Low concentrations of apoptotic and necrotic cells in host coral tissue under bleaching conditions. Journal of Experimental Marine Biology and Ecology. 369:31-42.

Sunagawa, S., Wilson, E. C., Thaler, M., Smith, M. L., Caruso, C., Pringle, J. R., Weis, V. M., Medina, M. and J. A. Schwarz. 2009. Generation and analysis of transcriptomic resources for a model system on the rise: the sea anemone *Aiptasia pallida* and its dinoflagellate endosymbiont. BMC Genomics. 10(1):258.

Swanlund, J. M., Kregel, K. C. and T. D. Oberley. 2008. Autophagy following heat stress: the role of aging and protein nitration. Autophagy. 4(7):936-939.

Swanlund, J. M., Kregel, K. C. and T. D. Oberley. 2010. Investigating autophagy: quantitative morphometric analysis using electron microscopy. Autophagy 6(2):270-277.

Szmant, A. M. and N. J. Gassman. 1990. The effects of prolonged bleaching on the tissue biomass and reproduction of the reef coral *Montastrea annularis*. Coral Reefs 8:217-224.

Taylor, D. L. 1968. *In situ* studies on the cytochemistry and ultrastructure of a symbiotic marine dinoflagellate. Journal of Marine Biology Association of UK. 48:359-366.

Taylor, D. L. 1973. The cellular interactions of algal invertebrate symbiosis. Advances in Marine Biology. 11:1-56.

Tchernov, D., Kvitt, H., Haramaty, L., Bibby, T. S., Gorbunov, M. Y., Rosenfeld, H. and P. G.

Falkowski. 2011. Apoptosis and the selective survival of host animals following thermal bleaching in zooanthellate corals. Proceedings of the National Acadamy of Science. 108(24):9905-9909.

Thorington, G., B. Berger, and L. Margulis. 1979. Transmission of symbionts through the sexual cycle of *Hydra viridis* I. Observations on living organisms. Transactions of the American Microscopical Society. 98(3):401-413.

Thunnell, R.; Anderson, D.; Gellar, D.; Miao, Q. (1994) Sea- Surface Temperature Estimates for the Tropical Western Pacific during the Last Glaciation and Their Implications for the Pacific Warm Pool. Quaternery Research. 41:255-264.

Tsujimoto and S. Shimizu. 2005. Another way to die: Autophagic programmed cell death. Cell Death and Differentiation. 12:1528-1534.

Trench, R. K., 1979. The cell biology of plant-animal symbiosis. Annual Reviews in Plant Physiology. 30:485-531.

Tucker, R. P., Shibata, B. and T. N. Blankenship. Ultrastructure of the mesoglea of the sea anemone *Nematostella vectensis* (Edwardsiidae). Invertebrate Biology. 130(1):11-24.

Vader, W. and S. Lönning. 1975. The ultrastructure of the mesenterial filaments of the sea anemone, *Bolocera tuediae*. Sarsia. 58:79-88.

Van Praet, M. and D. Doumenc. 1987. Ordre des Antipathaires. In Grasse, P.-P (ed.)Traite de Zoologie. Cnidaires, Anthozoaires, Vol. III, Fas. 3. Masson, Paris, pp. 189-256.

Wagner, A. C., Strowski, M. Z., Goke, B. and J. A. Williams, J. A. 1995. Molecular cloning of a new member of the Rab protein family, Rab 26, from rat pancreas. Biochemical and biophysical research communications. 207(3):950-956.

Wakefield, T. S. and S. C. Kempf. 2001. Development of host and symbiont specific monoclonal antibodies and confirmation of the origin of the symbiosome membrane in a cnidarian-dinoflagellate symbiosis. Biological Bulletin. 200:127-143

Warner, M. E., Fitt, W., and G. W. Schmidt. 1999. Damage to photosystem II in symbiotic dinoflagellates: A determinant of coral bleaching. Proceedings of the National Academy of Science. 96:8007-8012.

Watson, G. M. 1988. Ultrastructure and cytochemistry of developing nematocysts. In: Hessinger, D. A. and H. M. Lenhoff (eds.) The Biology of Nematocysts. Academic Press. San Diego and other cities. pp. 143-164.

Weber, C. and V. Schmid. 1985. The fibrous system in the extracellular matrix of hydromedusae. Tissue and Cell 17:811–822.

Weis, J. A., Yamataka, S. and P. D. Enos. 1971. Ultrastructural evidence of polarized synapses in the nerve net of *Hydra*. Journal of Cell Biology. 51:318-323.

Weis, V. M. 2008. Cellular mechanisms of coral bleaching. Journal of Experimental Biology. 211:3059-3066.

Weis, V. M., Davy, S. K., Hoegh-Guldberg, O., Rodriguez-Lanetty, M., and J. R. Pringle. 2008. Cell Biology in model systems as the key to understanding corals. Cell Press: Trends in Ecology and Evolution. 23(7):369-376.

Westfall, Jane A. 1970. Ultrastructure of synapses in a primitive coelenterate. Journal of Ultrastructure Research. 32(3):237-246.

Westfall, Jane A. 1973. Ultrastructural evidence for neuromuscular systems in coelenterates. American Zoologist. 13(2):237-246.

Westfall, J. A., Sayyar, K. L. and J. K. Bone. 1997. Ultrastructure of neurons and synapses in the tentacle gastrodermis of the sea anemone *Calliactis parasitica*. Journal of Morphology. 231:217-223.

Westfall, Jane A., Denise D. Landers, and Jennifer D. McCallum. 1998 Different nematocytes have different synapses in the sea anemone *Aiptasia pallida* (Cnidaria, Anthozoa). Journal of Morphology. 238(1):53-62.

Westfall, Jane A., Jennifer D. McCallum, and Ryan W. Carlin. 2001. Neuroglandular synapses in the pharynx of the sea anemone *Aiptasia pallida* (Cnidaria, Anthozoa). Journal of Morphology. 247(2):134-141.

Westfall, J. A. and C. F. Elliot. 2002. Ultrastructure of the tentacle nerve plexus and putative neural pathways in sea anemones. Invertebrate Biology. 121(3):202-211.

Wilkinson, C. R. 1993. Coral reefs are facing widespread extinctions: can we prevent these through sustainable management practices? Proceedings of the 7th International Coral Reef Symposium. Guam, University of Guam. 1:11-21

Wilkinson, C. 2008. Status of Coral Reefs of the World: 2008. Global Coral Reef Monitoring Network Reef and Rainforest Research Centre, Townsville, 304 pp.

Wood, R. L. 1961. The Fine Structure of Intercellular and mesogleal attachments of epithelial cells in *Hydra*. In: Lenhoff, H. M., and W. F. Loomis (eds.) The biology of *Hydra* and of some other coelenterates. Univ of Miami Press. Coral Gables, Florida. pp. 51-67.

Wyllie, A. H., Kerr, J. F. K. and A. R. Currie. 1980. Cell death: The significance of apoptosis. International Review of Cytology. 68:251-306.

Xiong Y, Contento AL, Nguyen PQ, Bassham DC. 2007. Degradation of oxidized proteins by autophagy during oxidative stress in *Arabidopsis*. Plant Physiology. 143:291–299.

Xue, L., Fletcher, G. C., and A. M. Tolkovsky. 2001. Mitochondria are selectively eliminated from eukaryotic cells after blockade of caspases during apoptosis. Current Biology. 11(5):361-365.

Yonge, C. M. and A. G. Nichols. 1931. Studies on the physiology of corals: V. The effect of starvation in light and in darkness on the relationship between corals and zooxanthellae. Scientific Reports from the Great Barrier Reef Expedition. 1:177-211.

Yoshie, S., Imai, A., Nashida, T. and H. Shimomura. 2000. Expression, characterization, and localization of Rab26, a low molecular weight GTPbinding protein, in the rat parotid gland. Histochemistry and Cell Biology. 113:259–263.

Yu, L., Wan, F., Dutta, S., Welsh, S. M., Liu, Z., Freundt, E., Baehrcke, E. and M. Lenardo. 2006. Autophagic programmed cell death by selective catalase degradation. Proceedings from the National Academy of Science. 103(13):4952-4957.

Zhang X., Boot-Handford, R. P., Huxley-Jones, J., Forse, L. N., Mould, A. P, Robertson, D. L., LiLi, Athiyal, M. and M. P. Sarras Jr. 2007. The collagens of *Hydra* provide insight into the evolution of metazoan extracellular matrices. Journal of Biological Chemistry. 282:6792–6802.

Zoccola, D., Tambutté, E., Kulhanek, E., Puverel, S., Scimeca, J. C., Allemand, D., & Tambutté, S. 2004. Molecular cloning and localization of a PMCA P-type calcium ATPase from the coral *Stylophora pistillata*. Biochimica et Biophysica Acta (BBA)-Biomembranes. 1663(1):117-126.

General Conclusions

Mass mortality bleaching events have significantly increased over the last 30 years (1993, 1998, 2005) resulting in a significant decline of coral cover and diversity in many regions of the world. N.O.A.A. (2012) reported that ~90% of Caribbean corals experienced severe bleaching during the 2005 bleaching event, and only ~45% have since recovered. Similar mass mortality episodes are predicted to increase as global climate change results in more frequent high SSTs, endangering the future survival of coral reefs worldwide. Increasing prevalence of bleaching events result primarily from steadily rising SSTs, which represent only one of the major effects of anthropogenic global climate change (N.O.A.A., 2012). Other anthropogenic factors, such as pollution and overharvesting, may significantly exacerbate the weakened condition of corals during warmer seasons and have been linked to numerous disease outbreaks and bleaching events (N.O.A.A., 2012).

Although coral bleaching has been studied for the past few decades, there remains a great deal of "big picture" concepts that currently remain unresolved. In particular, we know very little of how corals immediately respond to elevated SSTs and much speculation remains regarding how symbionts are lost and whether the host and/or symbiont controls the bleaching process (Weis, 2008).

This study provides evidence that elevated autophagic activity results in degradation of host cells and contributes to the eventual loss of the symbiont through a novel cellular bleaching mechanism, 'apical detachment' in the model symbiotic anemone, *Aiptasia pallida*. Results from

this investigation also demonstrated that the anthozoan host is the first member to respond to elevated temperature stress by regulating both host cell and symbiont abundance through autophagy. In addition, ultrastructural observations of a complex entanglement at the mesogleal-gastrodermal cell interface suggest that previous descriptions of the cellular bleaching mechanism termed 'host cell detachment' is an unlikely mechanism for bleaching in *Aiptasia* and is in need of revision. Results from the RNA-Seq analysis revealed the highest levels of differential gene expression in symbiotic *A. pallida* anemones during early stages of a thermal stress treatment, which corroborated our ultrastructural findings. Several key genes and cellular processes were identified that provides a better understanding of the genetic determinants of stress tolerance in a host anthozoan. These findings contribute essential information to our current level of understanding surrounding the bleaching process and will facilitate a better understanding of how the global climate change will affect coral health.